

# NAVAL POSTGRADUATE SCHOOL MONTEREY, CALIFORNIA



## THESIS

**CONVECTIVE HEAT TRANSFER FROM A  
VERTICAL CYLINDER IN A HIGH  
AMPLITUDE RESONANT SOUND FIELD**

by

Mark Bridenstine

September, 1996

Thesis Advisor:

Ashok Gopinath

**Approved for public release; distribution is unlimited.**

19970121 199

DIGITAL QUALITY INSTITUTE 3

## REPORT DOCUMENTATION PAGE

Form Approved OMB No. 0704-0188

Public reporting burden for this collection of information is estimated to average 1 hour per response, including the time for reviewing instruction, searching existing data sources, gathering and maintaining the data needed, and completing and reviewing the collection of information. Send comments regarding this burden estimate or any other aspect of this collection of information, including suggestions for reducing this burden, to Washington Headquarters Services, Directorate for Information Operations and Reports, 1215 Jefferson Davis Highway, Suite 1204, Arlington, VA 22202-4302, and to the Office of Management and Budget, Paperwork Reduction Project (0704-0188) Washington DC 20503.

1. AGENCY USE ONLY <i>(Leave blank)</i>	2. REPORT DATE September 1996	3. REPORT TYPE AND DATES COVERED Master's Thesis	
4. TITLE AND SUBTITLE CONVECTIVE HEAT TRANSFER FROM A VERTICAL CYLINDER IN A HIGH AMPLITUDE RESONANT SOUND FIELD		5. FUNDING NUMBERS	
6. AUTHOR(S) Mark Bridenstine			
7. PERFORMING ORGANIZATION NAME(S) AND ADDRESS(ES) Naval Postgraduate School Monterey CA 93943-5000		8. PERFORMING ORGANIZATION REPORT NUMBER	
9. SPONSORING/MONITORING AGENCY NAME(S) AND ADDRESS(ES)		10. SPONSORING/MONITORING AGENCY REPORT NUMBER	
11. SUPPLEMENTARY NOTES The views expressed in this thesis are those of the author and do not reflect the official policy or position of the Department of Defense or the U.S. Government.			
12a. DISTRIBUTION/AVAILABILITY STATEMENT Approved for public release; distribution is unlimited.		12b. DISTRIBUTION CODE	
13. ABSTRACT <i>(maximum 200 words)</i>  This thesis is part of a continuing study in developing convective heat transfer correlations for a cylinder in a high amplitude zero-mean oscillating flow. The experiment described here utilizes the RTD technique and a steady state heat transfer measurement method with a platinum wire, serving as the test section, positioned across the inner diameter of a cylindrical plexiglass chamber supporting a strong resonant axial acoustic field. Utilizing two different wire diameters of 0.050 mm and 0.127 mm, various pressure ratios, frequencies, and temperature differences, separated flow heat transfer correlations have been developed. This work would find application in the design of heat exchangers for a thermoacoustic engine.			
14. SUBJECT TERMS Thermoacoustic Engines, Heat Exchangers, Oscillatory Flows, Heat Transfer		15. NUMBER OF PAGES 112	
		16. PRICE CODE	
17. SECURITY CLASSIFI- CATION OF REPORT Unclassified	18. SECURITY CLASSIFI- CATION OF THIS PAGE Unclassified	19. SECURITY CLASSIFI- CATION OF ABSTRACT Unclassified	20. LIMITATION OF ABSTRACT UL

NSN 7540-01-280-5500

Standard Form 298 (Rev. 2-89)  
Prescribed by ANSI Std. Z39-18 298-102



Approved for public release; distribution is unlimited.

**CONVECTIVE HEAT TRANSFER FROM A VERTICAL CYLINDER IN A  
HIGH AMPLITUDE RESONANT SOUND FIELD**

Mark Bridenstine  
Lieutenant, United States Navy  
B.S.M.E., University of Notre Dame, 1986

Submitted in partial fulfillment  
of the requirements for the degree of

**MASTER OF SCIENCE IN MECHANICAL ENGINEERING**

from the

**NAVAL POSTGRADUATE SCHOOL**  
**September 1996**

Author:

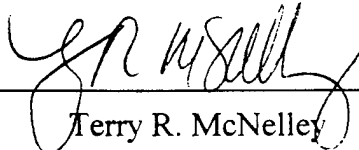


Mark Bridenstine

Approved by:



Ashok Gopinath



Terry R. McNelley

Department of Mechanical Engineering



## **ABSTRACT**

This thesis is part of a continuing study in developing convective heat transfer correlations for a cylinder in a high amplitude zero-mean oscillating flow. The experiment described here utilizes the RTD technique and a steady state heat transfer measurement method with a platinum wire, serving as the test section, positioned across the inner diameter of a cylindrical plexiglass chamber supporting a strong resonant axial acoustic field. Utilizing two different wire diameters of 0.050 mm and 0.127 mm, various pressure ratios, frequencies, and temperature differences, separated flow heat transfer correlations have been developed. This work would find application in the design of heat exchangers for a thermoacoustic engine.



## TABLE OF CONTENTS

I. INTRODUCTION .....	1
II. HISTORICAL.....	3
A. REFRIGERATION .....	3
1. Vapor Refrigeration Cycle .....	3
2. Thermoacoustic Cycle.....	4
B. HEAT TRANSFER.....	6
1. Natural/Forced Convection.....	6
2. Thermoacoustic Streaming .....	8
III. FLUID MECHANICS.....	11
A. RADIAN WAVELENGTH .....	11
B. DISPLACEMENT AMPLITUDE.....	12
C. FREQUENCY PARAMETER.....	14
D. REYNOLDS NUMBER .....	15
E. FLOW SEPARATION .....	16
IV. EXPERIMENT .....	19
A. PURPOSE .....	19
B. EQUIPMENT .....	20
1. Test Cylinder.....	20
2. Acoustic Chamber.....	21
3. Electronics.....	22
C. PROCEDURE .....	25
V. RESULTS AND DISCUSSION .....	31
VI. CONCLUSIONS AND RECOMMENDATIONS .....	39
APPENDIX A: CALIBRATION .....	43
APPENDIX B: SAMPLE CALCULATION .....	49
A. NUSSELT NUMBER .....	49

B. REYNOLDS NUMBER.....	51
APPENDIX C: UNCERTAINTY ANALYSIS .....	53
A. PLATINUM WIRE RESISTANCE.....	53
B. NUSSELT NUMBER .....	55
C. REYNOLDS NUMBER.....	57
APPENDIX D: EXPERIMENTAL DATA .....	61
LIST OF REFERENCES .....	95
INITIAL DISTRIBUTION LIST .....	97

## LIST OF FIGURES

Figure 1. Basic Vapor Refrigeration Cycle .....	3
Figure 2. Basic Thermoacoustic Refrigeration Components .....	5
Figure 3. Vertical Cylinder Natural Convection .....	7
Figure 4. Acoustic Streaming Pattern .....	9
Figure 5. Isothermal "Streaked" Flow .....	17
Figure 6. Acoustic Chamber and Accessories.....	22
Figure 7. Acoustic Electronics Package.....	23
Figure 8. Heat Transfer Electronics Package.....	24
Figure 9. Standing Wave Velocity Profile in a Circular Cylinder .....	26
Figure 10. Nusselt Number versus Reynolds Number (d = 50.8 $\mu\text{m}$ ).....	35
Figure 11. Nusselt Number versus Reynolds Number (d = 127 $\mu\text{m}$ ).....	36
Figure 12. Nusselt Number versus Reynolds Number (both wires) .....	37
Figure 13. Curve Fit for Nusselt Number versus Reynolds Number (d = 50 $\mu\text{m}$ ).....	41
Figure 14. Calibration Chamber.....	44
Figure 15. Platinum Wire Calibration Curve (d = 50.8 $\mu\text{m}$ ).....	46
Figure 16. Platinum Wire Calibration Curve (d = 127 $\mu\text{m}$ ).....	47



## **LIST OF TABLES**

Table 1. Platinum Wire Calibration Data (d = 50.8 $\mu\text{m}$ ) .....	45
Table 2. Platinum Wire Calibration Data (d = 127 $\mu\text{m}$ ) .....	45



## LIST OF SYMBOLS, ACRONYMS, AND/OR ABBREVIATIONS

a	test cylinder radius [m]
A	particle displacement [m]
$\bar{A}$	particle displacement amplitude [m]
$A_s$	surface area [ $\text{m}^2$ ]
c	speed of sound [m/s]
d	diameter of test cylinder [m]
f	frequency [Hz]
h	convective heat transfer coefficient [ $\text{W}/\text{m}^2\text{-K}$ ]
HX	heat exchanger
I	current [Amps]
k	thermal conductivity [ $\text{W}/\text{m}\text{-K}$ ]
KC	Keulegan-Carpenter number
l	length of test cylinder [m]
L	distance from test cylinder to chamber end plate [m]
M	Mach number
Nu	Nusselt number
$P_m$	mean ambient pressure [Pa]
$P_{\text{ref}}$	reference pressure [Pa]
PR	pressure ratio
R	gas constant [ $\text{J}/\text{kg}\text{-K}$ ]
Re	Reynolds number
$R_{\text{PR}}$	precision resistor resistance [ohms]
$R_s$	streaming Reynolds number
$R_w$	wire resistance [ohms]
RMS	root mean square
RTD	resistance temperature detector
SPL	sound pressure level
t	time [s]
$T_c$	cold sink temperature [K]
$T_h$	hot sink temperature [K]
$T_s$	surface temperature [K]
$T_\infty$	ambient temperature [K]
U	velocity [m/s]
$U_0$	velocity amplitude [m/s]
$V_m$	pressure transducer voltage [volts]
$V_0$	voltage [volts]
$V_{\text{PR}}$	precision resistor voltage [volts]
$V_w$	platinum wire voltage [volts]
$\beta$	amplitude ratio

$\chi$	cylinder length scale
$\delta$	boundary layer thickness [m]
$\epsilon$	amplitude parameter
$\gamma$	ratio of specific heats
$\lambda$	wavelength [m]
$\bar{\lambda}$	radian wavelength [m/rad]
$\Lambda$	frequency parameter
$\nu$	kinematic viscosity [m <sup>2</sup> /s]
$\omega$	radian frequency [rad/s]

## I. INTRODUCTION

Pollution free refrigeration is a concept worthy of close inspection in this day and age of an environmentally conscious public. A more far-reaching concern to the masses than the purported global environmental awareness may be the economic impact from a recent international agreement to ban all consumption of chlorofluorocarbons (CFCs) by the turn of the century. This will affect everyone in the industrialized world. Technologies are being investigated to supplant or improve present day refrigerants and/or their associated cycles. Researchers, whose interests come from a broad spectrum including academia, space and the automotive industry, seek to provide an alternative to today's refrigeration technology whereby a CFC-free environment remains.

One method, thermoacoustic refrigeration, blends, in part, the disciplines of convective heat transfer and acoustics. Four real world applications of this technology include the Space ThermoAcoustic Refrigerator (STAR) [Ref. 1], a food refrigerator built in the Republic of South Africa, a cryogenic refrigerator for electronics cooling and a device built by the Ford Motor Company for potential automobile uses. Through continued innovation and experimentation these highly specialized designs may soon become distant relatives of a new age of environmentally safe, mass produced, commercial thermoacoustic refrigeration units.

If theory has been put into practice, why not close the book on laboratory experimentation in this field? At present, thermoacoustic refrigerator technology depends on efficient solid to gas heat transfer from its heat exchangers. Lee and Richardson [Ref. 2] reiterate what has been known for a long time, that is, heat transfer coefficients between gases and solid surfaces are small. If the turbulence intensity of the gas free stream is raised, heat transfer rates will increase. Researchers have found that experiments and analysis involving stationary sound fields rather than real turbulent flow are much simpler. Their experiments have shown that under favorable circumstances the presence of oscillations can cause significant increases in gas heat transfer coefficients.

Today's thermoacoustic refrigerators lack the efficiency of modern day vapor compression cycles. Operating at best at about 50% efficiency of conventional refrigerators, there is much room for improvement especially in heat exchanger design. The intent here is to extend the experimental basis for heat exchanger design in thermoacoustic applications. The fundamental flow regimes and the results from varying characteristic parameters within each have not yet been completely analyzed. The motivation for this work is to develop a better understanding of the relationship between high amplitude resonant sound fields and convective heat transfer rates in a gaseous medium and to develop useful correlations for a portion of the wide parameter regime of interest.

## II. HISTORICAL

### A. REFRIGERATION

#### 1. Vapor Refrigeration Cycle

Vapor compression systems are the most common refrigeration cycles used for both industrial and commercial refrigeration (Figure 1). The working fluid, or refrigerant, in these systems is typically a halogenated hydrocarbon. A measure of efficiency for these cycles, designated the coefficient of performance (COP), comes from the ratio of actual refrigerating effect to the net work required. In theory, the Carnot cycle represents the most efficient cycle. However, several impracticalities arise, therefore, actual systems sacrifice efficiency for a reduction in costs and maintenance.

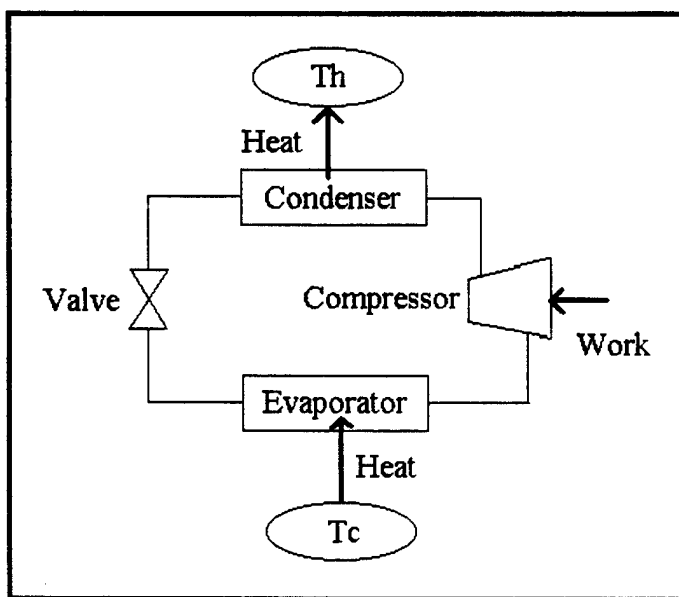


Figure 1. Basic Vapor Refrigeration Cycle

Today's refrigerators grew out of years of theoretical and experimental studies to become efficient, reliable and versatile machines serving numerous applications.

Operating efficiencies on the order of over 90% of Carnot efficiency are not uncommon. Recent international laws requiring an end to the production of environmentally hazardous, ozone-depleting, hydrocarbon refrigerants (i.e., R-11, R-12, R-114) used in many of these systems led to new temporarily acceptable substitutes (i.e., R-134a) and an interest, at least academically, in radically new methods for a future standardized means of refrigeration.

## 2. Thermoacoustic Cycle

Thermoacoustic refrigeration systems can be described in the following very simplistic way. There are six basic system components illustrated in Figure 2. They include the driver or loudspeaker, two heat exchangers, a "stack," and a sound medium (typically a gas) all enclosed within an acoustic chamber. A resonating sound wave, contained within the acoustic chamber, establishes a sinusoidal varying pressure field with antinodes at the chamber ends. Acoustic theory explains the simultaneous formation of sinusoidal displacement and velocity fields 90 degrees out of phase with the pressure field. They are anchored by nodes at the chamber ends. The sound wave remains stationary, however, the gas molecules within the chamber rapidly move back and forth. By precisely positioning the heat exchange elements (i.e., hot heat exchanger, and cold heat exchanger with a "stack" of low thermal conductivity plates in between) away from the pressure and displacement nodes a "bucket brigade" means of heat transfer between gas particles is created along the length of each plate within the stack. If we assume that a half-wavelength sound wave exists within the chamber of Figure 2, the stack cools at the end facing the driver and heats up at the other end. The magnitude of the temperature gradient is directly related to the pressure ratio created in the chamber. As the pressure amplitude increases so does the temperature difference.

Figure 2 also illustrates a simplified version for one cycle of particle oscillation, [Swift Ref. 3]. A gas particle undergoes adiabatic compression when displaced to position A. Following the laws of thermodynamics, an accompanying temperature rise leaves the particle hotter than the plate. Heat is rejected to the plate, from the particle,

which returns to position B while undergoing adiabatic expansion. A temperature decrease accompanying particle expansion lowers its temperature below that of the plate. Heat flows to the particle and “up” the temperature gradient with subsequent compression and displacement of the particle back to position A. A shallow positive temperature gradient forms across the stack from the cold heat exchanger to the hot heat exchanger through adjacent particle heat transfer across the plates as described above.

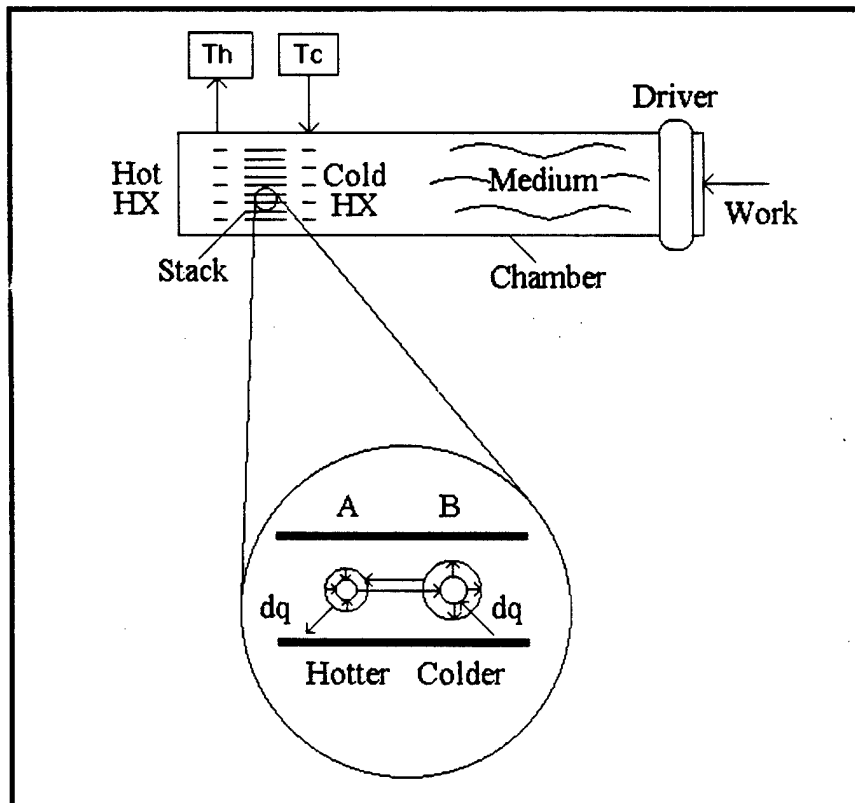


Figure 2. Basic Thermoacoustic Refrigeration Components

In 1993 A. D. Little, Inc., performed a research needs assessment for the Department of Energy [Ref. 4]. They analyzed more than fifteen refrigeration alternatives including substitute refrigerants, improved components and/or alternate cycles. For domestic refrigeration, Little's report concluded that thermoacoustic refrigeration was an

unlikely replacement to vapor compression. Under the categories of priority for research and development, probability of success, and industry involvement, thermoacoustics ranked lowest compared to all other technologies considered. Since that report, however, several corporate sponsored projects, mentioned above in part, affirm the viability of thermoacoustic refrigeration. Steven L. Garrett et al. [Ref. 5] succinctly outline the benefits and predominant technical issues surrounding this technology.

A simple description of the basic flow of heat from one end of the stack to the other, in the presence of an acoustic standing wave, is given above. What has not been considered in great detail is the effect that the same sound wave will have on the heat transfer from the heat exchanger to or from the stack ends. If a gap in physical contact exists between a heat exchanger and the end of the stack, how can we best operate and design the refrigerator to maximize efficient heat transfer across that gap? It is here that significant advances in this technology need to be made both in understanding the theory and incorporating experimental results into design. This study attempts to close the gap between the theory behind thermoacoustic refrigerator heat exchange in a sound field and an efficient heat exchanger design by providing heat transfer correlations in the separated flow regime. It is here that great advances in system efficiency and performance can and need to be made in order to persuade hesitant academics and conservative, potential corporate sponsors of the need for future research, development and investment in this relatively new technology.

## **B. HEAT TRANSFER**

### **1. Natural/Forced Convection**

Generally speaking, there are two distinct modes of convective heat transfer, natural (free) and forced. Each represents a different means by which fluid motion is sustained. The importance of one mode relative to the other is governed by the strength of its respective fluid motion. Forced convection fluid motion, or fluid velocity, is generated by some external forcing condition and, hence, the flow and thermal fields are largely uncoupled. As an example, consider a horizontal cylinder immersed in air.

Assuming that a temperature difference exists between the cylinder and air, a fan used to force air over the cylinder creates the necessary fluid motion for forced convection heat transfer. On the other hand, natural convection fluid motion arises when a body force acts upon a density difference. This density gradient typically results from a temperature difference between the body and the medium. The result is coupled flow and thermal fields, a more difficult problem to solve. Using a vertical cylinder in a quiescent air medium, a temperature difference between the cylinder and air gives way to buoyant forces that create natural convection currents adjacent to the cylinder surface. When the cylinder temperature exceeds that of the air, air adjacent to the cylinder surface is heated. This less dense air rises allowing cooler ambient air to replace it (Figure 3).

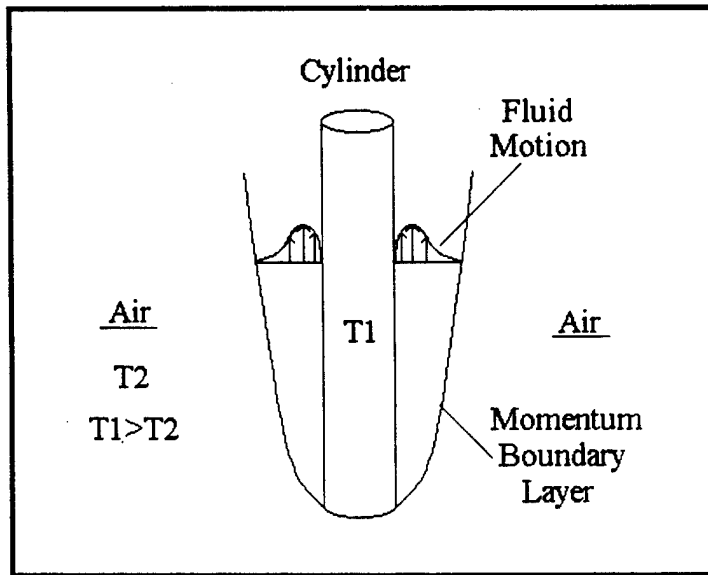


Figure 3. Vertical Cylinder Natural Convection

In all examples of heat transfer, temperature differences give rise to density differences. Therefore, we can say that in the presence of a body force, the effects of natural convection heat transfer are likely to co-exist with forced convection heat transfer. The opposite is not true. The relative importance of these two competing effects is

governed by the ratio of suitably defined Grashof number to Reynolds number (raised to some suitable power). In the limit, as this ratio tends to zero, the buoyancy forces become insignificant. As the ratio tends to infinity, buoyancy forces dominate the forced convection effects. If the two competing effects are comparable in magnitude, mixed or combined convection results.

Analysis of mixed convection flow fields requires knowledge of the two limiting fluid flow cases (i.e., induced buoyant forces and forced convection effects). From Gebhart et al. [Ref. 6], the direction and magnitude of the respective flow fields at any local position along the surface of interest will dictate whether the flow remains attached, separates or reverses. Gebhart et al. present results for differing geometries, surface heating and competing flow field strengths and directions.

## 2. Thermoacoustic Streaming

Early works regarding the effect of sound and vibration on heat transfer, including Lee and Richardson [Ref. 2], Fand and Cheng [Ref. 7], and Fand and Kaye [Ref. 8, 9], were instrumental in introducing a new fluid flow phenomenon called thermoacoustic streaming. All of the above mentioned authors' research utilized a horizontal heated cylinder in air subjected to a horizontal and transverse stationary sound field. The boundary layer velocity fields established for such an arrangement, when not subjected to a sound field, include azimuthal and radial velocities as expected in natural convection. The former give rise to natural convection currents tangential to the cylinder surface while the latter satisfy continuity requirements and are directed toward the cylinder. The magnitude of these tangential currents far outweigh the seemingly insignificant radial currents. When a sound field is introduced, a new boundary layer flow pattern is superimposed upon the natural convection flow. This acoustic streaming pattern, illustrated by Fand [Ref. 10], is presented in Figure 4. What appear to be two distinct flow patterns, inner and outer streaming layers, are shown. The thickness of the inner layer is exaggerated for clarity. The order of magnitude of the streaming velocities depends upon the intensity of the sound field and, for much of the above work,

corresponds to the radial component of the natural convection currents. The outer streaming flow aids the radial flow at the top and bottom of the cylinder but opposes it on the sides. If the basic boundary layer flow pattern around this cylinder is changed, it is reasonable to assume that the heat transfer may also be affected.

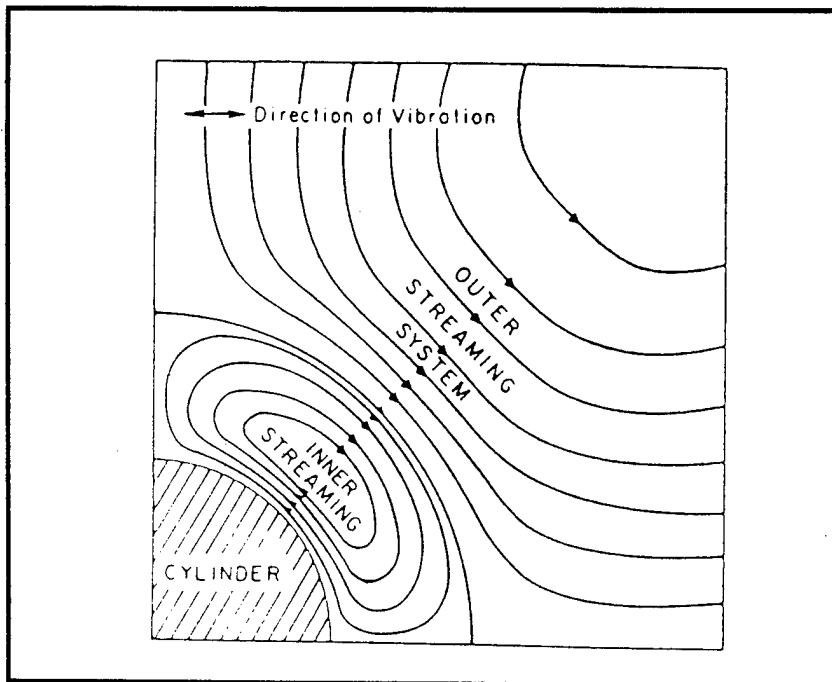


Figure 4. Acoustic Streaming Pattern

In an isothermal experiment this acoustic streaming pattern behavior is well documented. However, when applied to the problem where temperature gradients exist, the streaming pattern deviates from this theory. Several explanations are given in Fand [Ref. 10]. For their specific experiment, Fand and Kaye [Ref. 8] illustrate pictorially the effects of sound on the well known convection flow pattern. Two plumes or vortices form, separate and grow above the cylinder as the sound intensity is increased. The traditional natural convection boundary layer flow is disturbed. Thermoacoustic streaming boundary layer flow, characterized by the two vortices, results. The streaming flows aid heat transfer at the top and bottom but hinder it on the sides. Therefore, a

balance is established whereby the overall heat transfer rate remains unchanged. Lee and Richardson's [Ref. 2] experimental results corroborate this theory noting that sound field intensities below a "critical" sound pressure level (SPL) have no effect on the natural convection heat transfer rate. Once the sound intensity reaches the critical SPL, however, the point of separation for the thermoacoustic vortices has moved down the sides of the cylinder. Streaming velocities separate the boundary layer in the horizontal direction after which the buoyant forces sweep the fluid upwards until the previous area of local reduction in heat transfer is eliminated. The delicate heat transfer balance is compromised yielding an increase in overall heat transfer from the surface. Control of the heat transfer passes from pure natural convection to acoustic streaming.

The above discussion and associated references outline the theory and experimental results regarding attached boundary layer flow for heat transfer from a horizontal cylinder under the influence of a zero-mean oscillating flow. Little data exists concerning the effect such a sound field has on heat transfer from a *vertical* cylinder. More importantly for this research, the theory and experimental data available for *separated flow* heat transfer from a vertical cylinder exposed to a zero-mean oscillating flow is sparse to say the least.

### III. FLUID MECHANICS

To extract meaningful results from experiments conducted by numerous researchers using a variety of physical constants and geometric dimensions, it has become common to present them in a general nondimensional form. This methodology reduces the number of variables and links one researcher's data to another, thereby, enabling the engineer the opportunity to efficiently withdraw relevant conclusions regarding the phenomenon for design purposes. Mapping the results in terms of dimensionless parameters also gives the researcher insight into those areas or boundaries not yet completely analyzed. The important parameters necessary to explain the phenomenon of heat transfer from a cylinder in an zero-mean oscillating flow are presented below. Different fluid flow regimes result. This work attempts to extract heat transfer correlations from experimental data collected within the incompressible, separated flow regime.

#### A. RADIAN WAVELENGTH

Two obvious length scales can be derived from periodic oscillating flow. First, the radian wavelength is defined as

$$\bar{\lambda} = \frac{\lambda}{2\pi} \quad (1)$$

In order to maintain our assumption of incompressibility, the radian wavelength should be larger than the characteristic dimension of the wire, radius,  $a$ . Wire radius is an easily measured quantity as is radian wavelength when presented in the form

$$\bar{\lambda} = \frac{\lambda}{2\pi} = \frac{c/f}{2\pi} = \frac{c}{\omega} \quad (2)$$

The dimensionless parameter that results shall be designated,  $\chi$ . For incompressibility we require

$$\chi = \frac{a}{\lambda} = \frac{a\omega}{c} \ll 1 \quad (3)$$

## B. DISPLACEMENT AMPLITUDE

The fluid particles subjected to a time varying sound field will experience a displacement amplitude,  $\bar{A}$ . This is the second logical acoustic length scale. One can now begin to appreciate the complexity of this problem. In addition to the common characteristic geometric length scale (e.g. wire radius,  $a$ ) found in all bluff body fluid flow experiments, two additional acoustic length scales have been introduced.

In order for flow near the wire surface to remain attached, we expect minimal particle displacement relative to the wire diameter near the wire surface. The amplitude parameter,  $\varepsilon$ , defined as

$$\varepsilon = \frac{\bar{A}}{a} \quad (4)$$

expresses the distance a fluid particle moves relative to the cylinder radius. Its magnitude helps predict the type of flow, separated or attached, along the wire surface. When  $\varepsilon \geq 1$  we anticipate separated flow. For ease of measurement we can expand this equation. Consider a sinusoidal time varying signal. A direct relationship exists between particle amplitude and velocity as seen from the following simple scenario. If particle amplitude is defined by

$$A = \bar{A} \cos(\omega t) \quad (5)$$

then particle velocity follows as

$$U = \frac{d(A)}{dt} \quad (6)$$

Consequently,

$$U = \bar{A}\omega \sin(\omega t) \quad (7)$$

The velocity amplitude,  $U_o$ , where

$$U_o = \bar{A}\omega \quad (8)$$

produces the direct relationship

$$\bar{A} = \frac{U_o}{\omega} \quad (9)$$

One may now measure velocity amplitude along with frequency, or we can carry the scenario one step further. Morse and Ingard [Ref. 11] present a derivation for the relationship between fluid velocity and pressure change for adiabatic compression of a perfect gas as

$$U_o = \frac{c}{\gamma} \frac{P_o}{P_m} \quad (10)$$

Putting all of this together in a form easily measured by experiment, we have

$$\varepsilon = \frac{c}{\alpha\omega} \left[ \frac{P_o}{\gamma P_m} \right] \quad (11)$$

The amplitude parameter by itself is an indication of separated or attached flow. Additionally, when combined with  $\chi$ , the Mach number results as

$$M = \chi \varepsilon = \left( \frac{a\omega}{c} \right) \left( \frac{U_o}{a\omega} \right) = \frac{U_o}{c} \quad (12)$$

We can reinforce the assumption of incompressible flow when  $M \ll 1$ . In much of the literature the amplitude parameter is also expressed as the Keulegan-Carpenter number,

$$KC = \pi \varepsilon \quad (13)$$

another dimensionless parameter.

### C. FREQUENCY PARAMETER

It is important to include the effects of fluid viscosity when discussing velocity and displacement. Recall Stokes' second problem. This addresses the effect an oscillating plate has on an adjacent viscous fluid. A boundary layer thickness (or Stokes layer) of order

$$\delta = \sqrt{\frac{v}{\omega}} \quad (14)$$

dictates how far into the fluid the disturbances created by the oscillating plate can be felt. Solutions to Stokes' second problem show that at a distance greater than approximately  $10\delta$  from the plate surface, the amplitude of fluid particle oscillation has decayed to within one percent of the bulk fluid velocity. For boundary layer flows, this Stokes layer thickness is of the same order of magnitude as the inner streaming layer thickness introduced earlier.

A frequency parameter defined by

$$\Lambda^2 = \left( \frac{a}{\delta} \right)^2 = \frac{a^2 \omega}{\nu} \quad (15)$$

relates the characteristic dimension of the body to the Stokes layer thickness.

It has been shown that for  $\Lambda^2 \gg 1$ , a new, steady, acoustic streaming velocity develops within an outer layer. This steady flow component is of order  $O(\epsilon U_0)$  and appears as an apparent slip velocity on the cylinder surface. It decays to zero within the outer layer. Reynolds stresses linked to the oscillating viscous flow in the Stokes layer are the driving force for this new steady flow. Stuart [Ref. 12] provides a mathematical proof of this. In studies of oscillatory flows, sometimes the parameter

$$\beta = \frac{(2a)^2 f}{\nu} = \frac{2}{\pi} \Lambda^2 \quad (16)$$

is used to characterize the flow.

#### D. REYNOLDS NUMBER

Reynolds number has long been used as a parameter to delineate flow regimes within a given environment. Accurate use of this dimensionless parameter requires the proper definition of velocity and characteristic length. Here, the characteristic length is defined as the cylinder radius,  $a$ . And, in an attempt to find appropriate heat transfer correlations, two slightly different definitions for velocity have been employed. The first comes from the steady, acoustic streaming velocity giving us the streaming Reynolds number as

$$R_s = \frac{(\epsilon U_0) a}{\nu} \quad (17)$$

After some manipulation, the streaming Reynolds number can be related to the acoustic parameters introduced above as

$$R_s = \varepsilon^2 \Lambda^2 \quad (18)$$

The second comes from the fluid particle oscillation velocity resulting in

$$\text{Re}_a = \frac{U_0 a}{\nu}, \quad \text{Re}_d = \frac{U_0 (2a)}{\nu} \quad (19)$$

Again, after some rearranging

$$\text{Re}_a = \varepsilon \Lambda^2, \quad \text{Re}_d = 2 \varepsilon \Lambda^2 = \beta \cdot KC \quad (20)$$

## E. FLOW SEPARATION

Fluid dynamicists (Bearman, Sarpkaya and Williamson to name a few) have long considered the mechanics of flow separation from bluff bodies in an oscillating cross flow. Active areas of research today include: forces induced by the separated flow, a pictorial representation of the wake patterns and numerical solutions that describe the pointwise velocities within these wakes for both two and three dimensional flows. Theoretical hypotheses and experimental results have educated engineers about the effects these flow patterns have on the lift and drag forces imposed upon bodies. The practical application of these studies has dealt mainly with the hydrodynamics of marine structures and vehicles. Extension of these results to heat transfer effects has been minimal.

In 1980 Honji [Ref. 13] presented a paper on his observations of isothermal three-dimensional separated flow from a vertical, oscillating, circular cylinder in water. The resulting photographs of "streaked" flow from various vantage points removed some of

the mystery surrounding the flow instabilities associated with large amplitude oscillations (Figure 5).

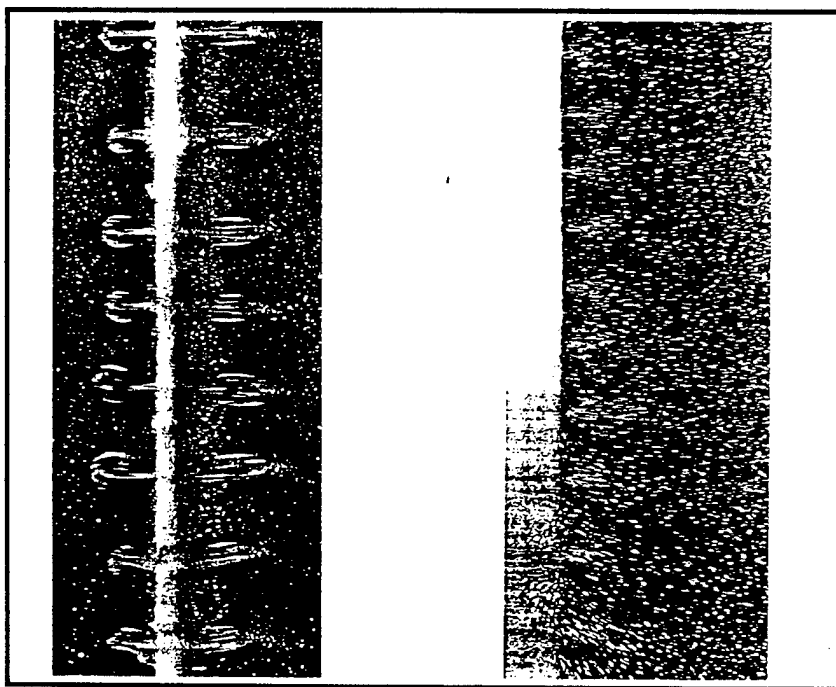


Figure 5. Isothermal "Streaked" Flow

Williamson [Ref. 14] uses several vortex flow regimes, each segregated by Keulegan-Carpenter number, to present pictorially, the formation and movement of vortices, and graphically, the variation in lift and drag forces. He concludes that with an oscillating flow, fluid reversals have a major effect on fluid induced forces. As oscillation amplitude is increased, the frequency per cycle of vortex shedding increases and the angle of vortex departure relative to the incident wave varies, thereby yielding higher induced forces whose oscillations are themselves periodic. Furthermore, the regularity of the vortex pattern appears to break down once a certain amplitude of oscillation is reached, thereby generating a discontinuous and weakened wake pattern. Williamson hypothesizes that three dimensional effects along with destructive vorticity between shed

vortices created in the present half cycle and those created several cycles previous may be the cause.

So, when does flow over a bluff body separate and at what Keulegan-Carpenter number can vortex shedding be observed? Faltinsen [Ref. 15], referencing the works of Bearman, Sarpkaya and Williamson, summarizes the answers to some of these questions. It is commonly agreed upon that once vortices can be seen, separation has occurred. That is not to say, however, that the vortices are necessarily carried away from the vicinity of the body. At very low Keulegan-Carpenter numbers fluid reversal generates mixing of vortices formed in the previous half-cycle with those of the present. The circulation of these are of opposite sense and may cancel each other out. Sarpkaya [Ref. 16] reported separation at a Keulegan-Carpenter number of 1.25. Williamson [Ref. 14] has demonstrated vortex shedding at Keulegan-Carpenter numbers as low as four.

It is clear that significant work has been documented regarding the fluid mechanics associated with flow separation and vortex shedding over a bluff body. It is logically hypothesized here, that similar flow instabilities will arise when temperature gradients, in addition to large amplitude fluid oscillations, are imposed upon a fluid medium near a heated cylinder surface. For this study then, it would seem safe to say that in addition to the previously mentioned requirements for separation, if Keulegan-Carpenter numbers above four are observed, vortex shedding occurs.

## IV. EXPERIMENT

### A. PURPOSE

Not all problems of science can be solved analytically. Many times it is through experiment that the true nature of a scientific phenomenon is best explained and understood. A small sample of the considerable theory and experimental data concerning the effects of sound on attached boundary layer flow heat transfer from a horizontal cylinder has been presented. The research in this area is hardly exhaustive, however, it far outweighs the available material detailing separated flow heat transfer from a vertical cylinder in the presence of a zero-mean oscillating sound field. What is available concerning separated flows in an isothermal environment has also been presented briefly to introduce the relationship between oscillating fluid amplitude and vortex shedding.

Similar geometric, acoustic and fluid mechanics parameters, presented above, are useful in quantifying experimental results in both cases. Such a standardization allows effective comparisons between different experimental works and provides researchers a "map" on which to track the evolution of analyses until a complete understanding is at hand. It is at this point that a confident assessment of the usefulness of thermoacoustics in commercial heat exchanger design can be made.

Analysis of mean external flows over bluff bodies leads one to solve the boundary layer equations. Friction and convective heat transfer correlations developed from these solutions have proven invaluable to modern engineers in their design of new technologies ranging from spacecraft to golf balls. On the other hand, little has been attempted theoretically or experimentally, to analyze the heat transfer behavior from bodies in zero-mean oscillating flow fields. Simple analogies from mean flow behavior are no longer directly applicable.

Fand and Kaye [Ref. 9] describe related work done by Kubanskii in 1952. His experimental arrangement placed the stationary sound field horizontal and parallel, vice transverse, to the axis of a horizontal heated cylinder. He deduced that fluid near the

cylinder surface moved from the antinodes to the nodes at which point the flows meeting from opposite directions collided to form a single stream that moved away perpendicular to the cylinder in a vortex-type or separated flow fashion. These experiments aim to create similar vortex-type flow but from a vertical cylinder subjected to a transverse sound field. The anticipated driving force for these experiments is forced convection rather than the free convection found by Kubanskii.

## B. EQUIPMENT

The approach used here will be similar to that used by Harder [Ref. 17]. Much of the supporting equipment is the same, with the biggest difference coming in the diameter of the test cylinder. A slightly modified acoustic chamber and electric circuit enable the smooth integration of the new test cylinder into the experimental setup.

### 1. Test Cylinder

Recent heat transfer correlations have been developed using small diameter vertical cylinders in a stationary sound field. George Mozerkewich [Ref. 18] conducted transient heat transfer rate analysis on rhenium and titanium wires of diameter ranging from 0.125 to 2 mm. Don Harder [Ref. 17] utilized a 5 mm diameter copper cylinder with an imbedded cartridge heater to develop steady state heat transfer rate solutions. In the present research, a 0.05 mm (and 0.127 mm) diameter platinum wire acts as both the heater and thermometer for steady state heat transfer analysis. One of the more attractive aspects of platinum is its nearly linear temperature-resistance relation. Upon supplying a known current through the approximately 75 mm length of wire, the voltage drop can be measured and from Ohm's Law resistance is easily calculated.

The wire was attached at each end to a copper stud. A small indentation was made on the flat face of each copper stud to allow pooling of the flux and platinum for increased mechanical integrity. The stud was then washed in a nitric acid solution. This provided a "sticky" surface onto which the flux could better adhere. The platinum wire was then soldered at either end to the threaded copper studs. In order to maintain a relatively constant tension in the wire during both calibration and testing, the lower

copper stud remained free to move vertically, thereby, permitting very short extension and contraction movement during temperature changes.

Imposing a temperature versus resistance linear regression model upon the calibration data (App. A), wire temperature is determined for all experimental runs from the calculated resistance. The importance of accurate resistance measurements across the platinum wire cannot be overemphasized. Very low resistance copper and brass circuit connections were used both in calibration and testing. A Kikusui Model PAR 160A regulated DC power supply provided circuit voltage and current control. Voltage and current resolution are approximately 5 mV and 5 mA, respectively.

## 2. Acoustic Chamber

Current development of thermoacoustic refrigerators primarily use either U-shaped or straight circular cross-section housings to support the acoustic driver, heat exchangers and stack. Sound is confined quite well, and standing waves can be easily created in such simple structures. Figure 6 depicts a sketch of the acoustic chamber used in these experiments. Harder [Ref. 17] aptly describes the chamber's physical characteristics prior to a few design changes all of which are described below.

Using approximate dimensions, a 1.8 m plexiglass tube of 9 cm outside diameter and 6 mm wall thickness is capped at one end by a JBL Model 2490H acoustic driver and a moveable end plate at the other. The tube is supported by stanchions at various positions along its length. An Endevco piezoresistive pressure transducer embedded in the moveable endplate provides data for pressure ratio and sound pressure level determination within the chamber. An o-ring seal surrounding this endplate permits its easy movement into and out of the chamber while confining the sound wave. Along the length of the chamber are bored two sets of diagonally opposed 12 mm diameter holes. During testing, the platinum wire assembly is placed at one of these locations while the other is blank-capped except for ambient temperature measurements taken inside the chamber.

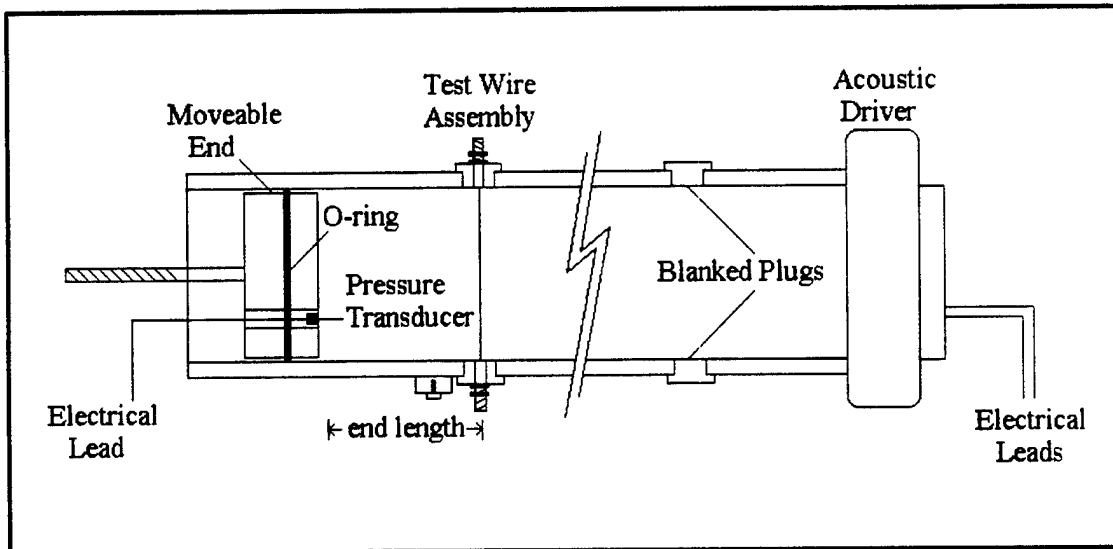


Figure 6. Acoustic Chamber and Accessories

### 3. Electronics

Several pieces of electronics equipment are used to generate the acoustic signal and then to monitor some of its properties. Figure 7 depicts the interconnecting relationships amongst this equipment. Beginning with a Hewlett Packard Model 33120A waveform generator, the desired waveform (sinusoidal), frequency and amplitude are selected. This signal is fed to a Techron Model 7540 power supply amplifier to boost the signal amplitude until a desired pressure ratio or sound pressure level (SPL) is reached. The amplified waveform enters the acoustic chamber via a JBL Model 2490H acoustic driver located at one end of the chamber. A pressure antinode is established at the moveable endplate located at the opposite end of the acoustic chamber. The standing wave pressure signal is sensed by the pressure transducer and amplified 100 times before it is displayed on a Hewlett Packard Model 34401A multimeter as an AC voltage. It is at this point that the pressure ratio and SPL within the chamber can be determined. Simultaneously, the amplified pressure signal is viewed on an oscilloscope to monitor gross waveform regularity. In series with the oscilloscope, a Hewlett Packard Model 3562A dynamic signal analyzer can record the signal frequency and amplitude for all

harmonics. An indication of harmonic interference from the signal analyzer helps determine exactly which frequency-amplitude combinations establish the optimum acoustic conditions in the chamber prior to the steady state heat transfer rate experimental run.

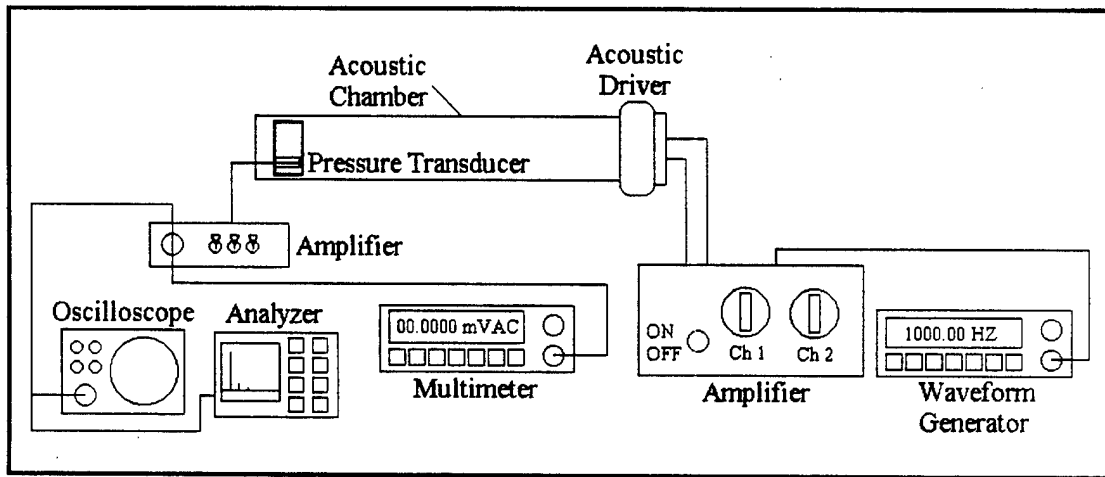


Figure 7. Acoustic Electronics Package

Once the desired acoustic conditions are established, the following additional equipment (Figure 8) is used to establish and monitor the heat transfer characteristics of the experiment. Ambient temperature sensing within the acoustic chamber is performed by manually inserting a T-type thermocouple into the center of the chamber through an upstream, normally capped, hole at the appropriate time. A Keithley Model 740 system scanning thermometer then measures the temperature to an accuracy of  $\pm 0.5^{\circ}\text{C}$ .

The electrical circuit designed to provide the desired temperature versus resistance characteristics for the platinum wire consists of a known fixed resistance and the platinum wire connected in series with a power supply. The resistor is rated at  $98.3\text{ m}\Omega$  with an accuracy of 0.026 % and acts both to minimize the power drawn by the platinum wire and to provide a means for accurate circuit current measurement. A Hewlett Packard Model 3478A digital multimeter connected in parallel across both the resistor

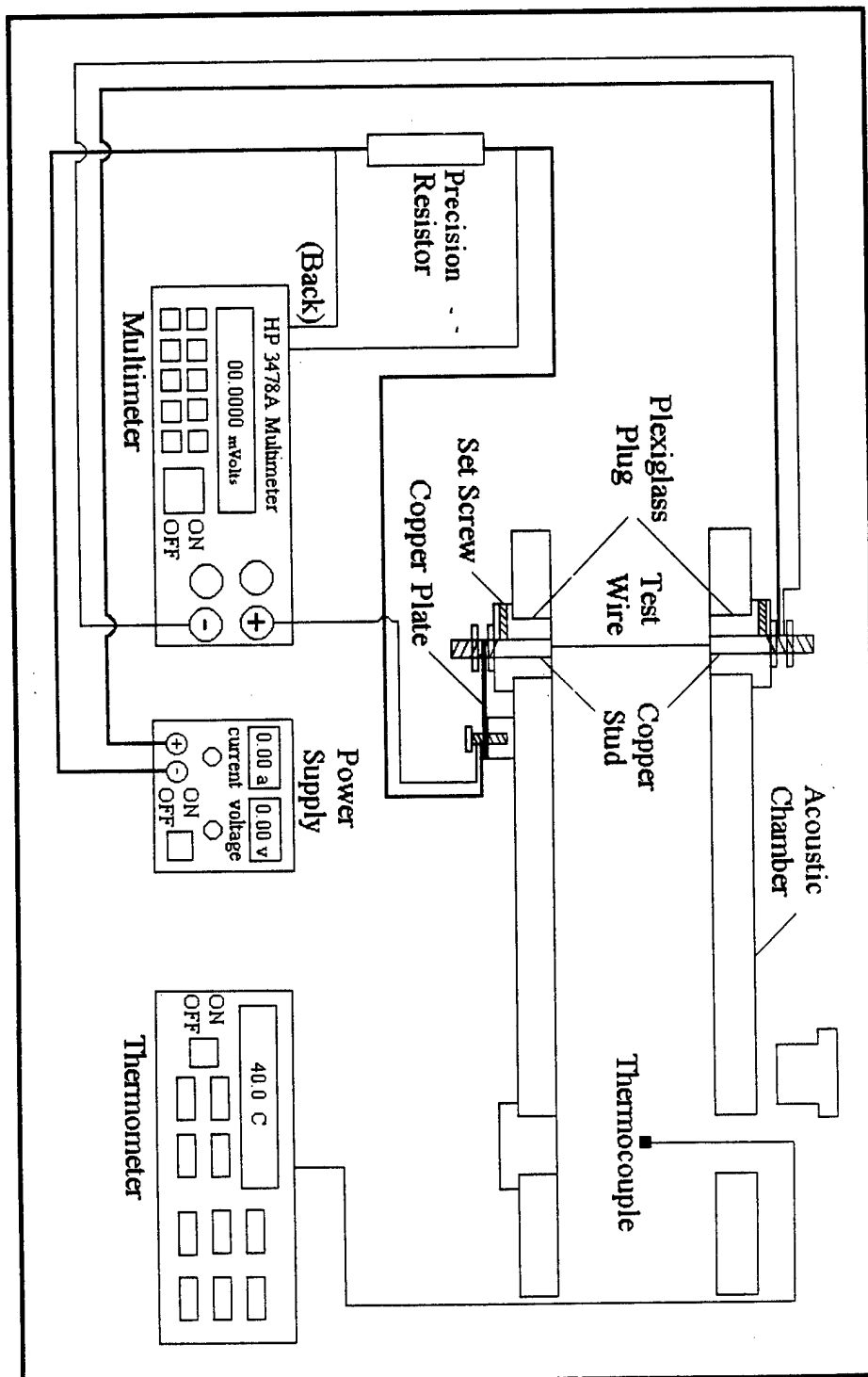


Figure 8. Heat Transfer Electronics Package

and wire accurately measures voltages up to a 5 ½ digit resolution. These measurements are subsequently used to calculate circuit current and wire resistance.

### C. PROCEDURE

Prior to inserting the platinum wire into the acoustic chamber, a series of tests were conducted to identify the resonant frequencies for various chamber end lengths, L. With two sets of diagonally opposed holes bored into the chamber wall, the second set being 50 cm offset from the first (Figure 6), end lengths were incremented by 1 cm from a maximum of 73 cm (123 cm) to a minimum of 42 cm (92 cm) by adjusting the position of the moveable endplate. Sine waves starting at 300 Hz, the lower end of the acoustic driver operating range, were introduced into the chamber. Frequency was raised until a resonant condition existed as evidenced by the wave shape seen on the oscilloscope and peak pressure transducer output as read from a multimeter in root mean square (RMS) volts AC. This resonant conditions occurred at roughly 100 Hz increments up to approximately 1900 Hz, the upper end of the acoustic driver operating range. For each resonant state, the frequency, end length, peak RMS voltage for the fundamental and second harmonic frequencies, and maximum pressure transducer output were recorded. The strength of the second harmonic provided a measure of harmonic interference at the velocity antinode. This information established which frequency and end length combinations to use for actual testing.

The geometry of the experimental setup plays an important role in proper test wire positioning. For a given resonant frequency and end length combination, the standing wave velocity created can be depicted as in Figure 9. Test wire placement at maximum sound velocity (antinode) should produce the greatest heat transfer from the wire. Here a simple analogy to forced convection may be helpful. If instead of an acoustic driver, a fan were placed at one end of the chamber (open-ended at the opposite end in this case), the speed of the fan would effect the heat transfer rate. The higher the fan speed, and therefore air velocity in the vicinity of the wire, the higher would be the

heat transfer rate. Similarly for thermoacoustics, the greater the medium velocity near the wire, the greater the anticipated heat transfer rate.

As is evident from Figure 9 any odd multiple of quarter wavelength (i.e.,  $\lambda/4$ ,  $3\lambda/4$ ,  $5\lambda/4$  etc.) lies at a velocity antinode. From the equation

$$L = \frac{n\lambda}{4}; \quad n = 1, 3, 5, \dots \quad (21)$$

we can determine whether or not a given resonant condition places the test wire at a velocity antinode. Rearranging, we get

$$n = \frac{4L}{c/f}; \quad n = 1, 3, 5, \dots \quad (22)$$

Now, knowing which combinations of resonant frequency and end length were best suited for the fixed geometric conditions, the maximum signal amplitude yielding minimal harmonic interference can be found.

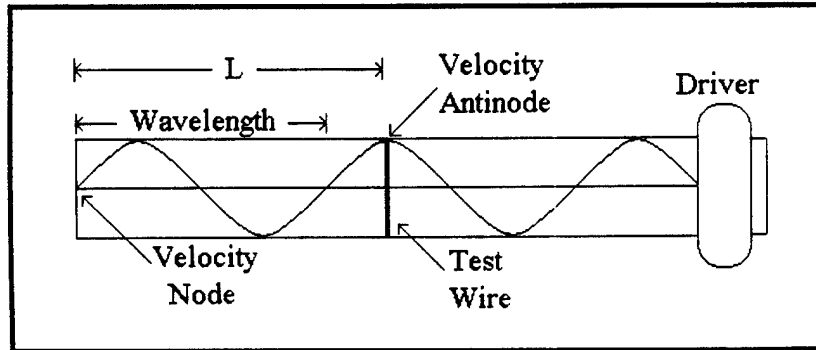


Figure 9. Standing Wave Velocity Profile in a Circular Cylinder

P. D. Richardson [Ref. 19] points out that rather than measuring velocity amplitude with a hot-wire, it is more accurate and convenient to measure pressure

amplitude with a microphone, as done here, since the velocity is directly proportional to the pressure ratio. Recalling that the resonant sound wave pressure is 90 degrees out of phase from the velocity, a pressure antinode exists at the moveable endplate where it is detected by the microphone. The microphone output is amplified 100 times. The signal is then measured by a Hewlett Packard 34401A multimeter as RMS volts AC. The following equation

$$\frac{P_o}{\sqrt{2}} = \frac{\left(\frac{V_o}{\sqrt{2}}\right)}{S} \quad (23)$$

gives the maximum pressure within the chamber. The amplified pressure transducer sensitivity, S, is equal to 0.738 mV/Pa. Solving for pressure, we get

$$P_o = \frac{\left(\frac{V_o}{\sqrt{2}}\right) Volts}{0.522 Volts/kPa} \quad (24)$$

Using 101.35 kPa for mean ambient pressure,  $P_m$ , we can find the pressure ratio from

$$PR = \frac{P_o}{P_m} * 100\% \quad (25)$$

and sound pressure level (SPL) from

$$SPL = 20 \log_{10} \frac{\frac{P_o}{\sqrt{2}}}{P_{ref}} \quad (26)$$

where  $P_{ref}$  is the reference pressure, taken to be 20  $\mu\text{Pa}$  for gases. In order to cover a wide range of fluid particle amplitudes, the pressure ratios used during the experiment varied from 0.9 to 2.9 percent in 0.1 percent increments or up to the point where harmonic interference became greater than approximately ten percent.

Once the optimum acoustic setpoints were found, the calibrated test wire was positioned within the acoustic chamber. Movement of the wire from its calibration chamber to the experimental acoustic chamber required very delicate maneuvering. Any excessive torsional or axial stress exerted on the copper to platinum wire solder joint separated the joint. After the wire was positioned, the complete electrical circuit was established including all measuring instrumentation. At this point, a comprehensive plan was set forth from which repeated experimental data runs could be made with minimal procedural variance between them. The following description details one such experimental data run.

After an initial equipment warm up period, one frequency and end length combination was set. Acoustic signal amplification was adjusted until the desired pressure ratio was obtained. Fine tuning the frequency ensured a resonant condition within the acoustic chamber. The signal characteristics were monitored on both the oscilloscope and frequency analyzer in order to check the level of harmonic interference. Signal amplifier settings were noted and then the signal was secured. After logging an ambient temperature reading within the chamber, a preset source current and voltage were introduced into the circuit. As the wire heated up, the previously marked signal amplifier settings were re-established. Once steady, after approximately 15 seconds, voltage measurements across the series precision resistor and test wire were taken. As soon as these readings were recorded, the power circuit source and signal amplifier were secured. A second ambient temperature reading within the chamber was logged. Differences between initial and final ambient temperature readings could be as high as 0.3 degrees. All of the above readings were then entered into a spreadsheet where acoustic and heat transfer parameters were calculated. Through trial and error the above procedure was

repeated until the correct source current and voltage were found for the desired temperature difference between the ambient and wire surface. Temperature differences of 8, 16, and 24 degrees ( $\pm 0.5$  degrees) were targets for each pressure ratio. At some of the highest pressure ratios for the 127  $\mu\text{m}$  diameter wire, temperature differences of 8, 12, and 16 degrees were used because measured wire voltage fluctuations were unacceptably high at 24 degrees. In addition to three different temperature runs per pressure ratio, each voltage reading within a run was taken in triplicate. Averaging the results from three measurements helped minimize the error for a given parameter within a data run.

The above procedure was used at every pressure ratio and for every frequency and end length combination selected. In addition, nearly the same procedure, minus the sound signal, was followed to determine the heat transfer coefficient for natural convection. The results were compared to those presented by Gebhart et al. [Ref. 6] for natural convection from a semi-infinite thin vertical wire in air to validate the procedure. Our enclosed container geometry does not accurately replicate previous experimental setups, therefore, our results do not match those presented by Gebhart. However, our results were of the same order of magnitude. This offered some validity to our experimental setup and procedure.



## V. RESULTS AND DISCUSSION

This study investigates the heat transfer characteristics of a thin vertical cylinder in an air medium subjected to a high amplitude zero-mean oscillating flow. Two different wire diameters were individually tested, 50  $\mu\text{m}$  and 127  $\mu\text{m}$ . Both wires were exposed to pressure ratios incremented from 0.9 to 2.9 % while ensuring minimal harmonic interference. Additionally, at each pressure ratio setting, data for three separate temperature differences between the ambient and wire surface were taken. In all, nearly 400 data points were collected. Experimental measurements, applicable heat transfer and acoustic parameter calculations and certain parameter uncertainties are presented in a spreadsheet format found in Appendix D.

Use of such thin wires all but guaranteed separated flows in the high amplitude oscillation environment. The calculated values for the amplitude parameter, (i.e., Keulegan-Carpenter number), which were of  $O(10)$ , best corroborated this supposition. An early attempt was made to use a relatively thick 254  $\mu\text{m}$  diameter wire with little success. With this wire, resistance measurements were on the order of 100  $\text{m}\Omega$  with a 1°C temperature change. This corresponded to a 0.6  $\text{m}\Omega$  resistance change. Such small values for resistance generated unacceptably high uncertainties for our measurement technique and available equipment, thereby forcing the use of thinner wires.

The first useful experiments were conducted on a 50  $\mu\text{m}$  diameter wire. Initially, a frequency of 1213 Hz with a corresponding end length of 64 cm was used. This combination most closely placed the maximum velocity at the fixed test wire position. During testing, this combination also showed the least harmonic distortion up to a maximum pressure ratio of 2.9 %. No other combination withstood the distortion requirements at such a high pressure ratio.

Next, the effect of acoustic chamber end length was examined. A frequency near 1213 Hz but with an end length different than 64 cm was desired. The one combination available that offered minimal harmonic distortion was a frequency of 1213 Hz at an end

length of 50 cm. The calculated acoustic and heat transfer parameters from these two data sets were compared and noted to be nearly identical for like pressure ratios and temperature differences. It was concluded that different end lengths for a given frequency, while maintaining a zero-mean oscillating flow within the acoustic chamber, do not alter the resulting heat transfer correlations. In order to gather a more diverse set of data, two additional frequencies and associated end lengths were tested. The results at 1053 Hz ( $L = 58$  cm) and 564 Hz ( $L = 47$  cm) are presented in Appendix D.

Once the 50  $\mu\text{m}$  diameter wire data was organized, a systematic interpretation began. To examine the effects of acoustics on heat transfer, several Nusselt number correlations were investigated using the amplitude and frequency parameters individually and in combination with each other. Nusselt number as a function of Reynolds number, not streaming Reynolds number, provided the best fit to the raw data (Figure 10). From this data, a curve fit yielded the correlation

$$Nu = 0.062 Re^{1.14} \quad (27)$$

Nusselt number errors reached as high as 13 %, while the Reynolds number error was approximately 5 %. Again, the forced convection analogy can be invoked here to help explain these results. Reynolds number is a function of particle velocity for a given cylinder diameter. It has been shown that particle velocity is directly proportional to the pressure ratio, therefore, as the pressure ratio increases so does the Reynolds number. For increasing fluid velocity we expect greater heat transfer and that is precisely what we see in these results.

To extend the range of data and to ensure a suitable Nusselt number correlation had been found, an additional set of data, using the same physical and acoustic parameters as above, was generated for a 127  $\mu\text{m}$  diameter wire. A graph of this data for Nusselt number versus Reynolds number is shown in Figure 11. For this wire, Nusselt number

errors were in the range of 4-15 %, while the Reynolds number error was approximately 2 %.

A graph of the complete set of data from both wires is presented in Figure 12. It was expected that the thicker wire data would fall on top of that for the thinner wire over the common Reynolds numbers, and that the trend of monotonically increasing Nusselt number with Reynolds number would continue into a new higher Reynolds number regime. Neither of these hypotheses were accurately realized. However, within the Reynolds number overlap region for the two wires one can see that even though the data does not strictly overlap, the slopes of the two data sets are comparable.

Obviously, the thicker wire data yielded much more interesting results (Figure 11). A steady increase followed by a peak and subsequent drop in Nusselt number occurs for all three frequencies. As the frequency increases, it appears that the rate at which the Nusselt number drops and the magnitude of the drop also increase. Similarly, for increasing frequency, the drop in Nusselt number occurs at a lower Reynolds number. A discussion of these results follows.

For a given wire diameter (i.e., 127  $\mu\text{m}$ ), increasing frequency corresponds to an increase in  $\beta$ . Physically speaking, the ratio of wire radius,  $a$ , to Stokes layer thickness,  $\delta$ , increases. Similarly stated, the effects of the Stokes fluid oscillations do not extend as far into the bulk fluid. Consequently, one could conclude that the effects of Stokes flow interaction with the shed vortices is reduced. Any mixing effect associated with this interaction fades resulting in a lower heat transfer rate. In Figure 11, three curves are evident, one for each of three frequencies with  $\beta$  of  $O(1)$ . The high frequency ( $\beta$ ) curve sits below the low frequency ( $\beta$ ) curve indicating less heat transfer for a higher frequency as theorized. Furthermore, rather than applying simply a Reynolds number dependence for the heat transfer correlation (Equation 27), we now see a possible  $\beta$  dependence as well. Reviewing Figure 10, the 50.8  $\mu\text{m}$  diameter wire  $\beta$  dependence is not as evident. Here  $\beta$  is of  $O(0.1)$ . Quite possibly,  $\beta$  becomes influential only when of  $O(1)$  or higher.

To explain the sudden Nusselt number drops at high Reynolds number, Williamson's results [Ref. 14] may be helpful. Recalling the work of Williamson, flows yielding high Keulegan-Carpenter numbers evoke separation and varying vortex shedding wake patterns which he groups into KC number regimes. This study includes KC numbers ranging from 14 to 200. If these vortex patterns proceed with some regularity a steady increase in Nusselt number with KC may be expected. However, if between acoustic half-cycles, vortex interference, out of phase vortex shedding along the cylinder length or a loss of regularity in vortex shedding occur, one might expect a disruption in the steady heat transfer from the cylinder. One possible cause, as noted by Williamson, could be an intermittent and random change in the vortex shedding mode (i.e., one side of the cylinder suddenly becoming the preferred side for vortex shedding). Once this change occurs a regularity to the vortex shedding should reappear. Figure 11 gives a limited glimpse at this possibility. The 1213 Hz data shows that a minimum Nusselt number is reached after which an upturn in the curve may be indicative of a return to vortex shedding regularity. The data to support this is far from conclusive, but the hypothesis is in keeping with Williamson's results regarding lift force coefficient fluctuations.

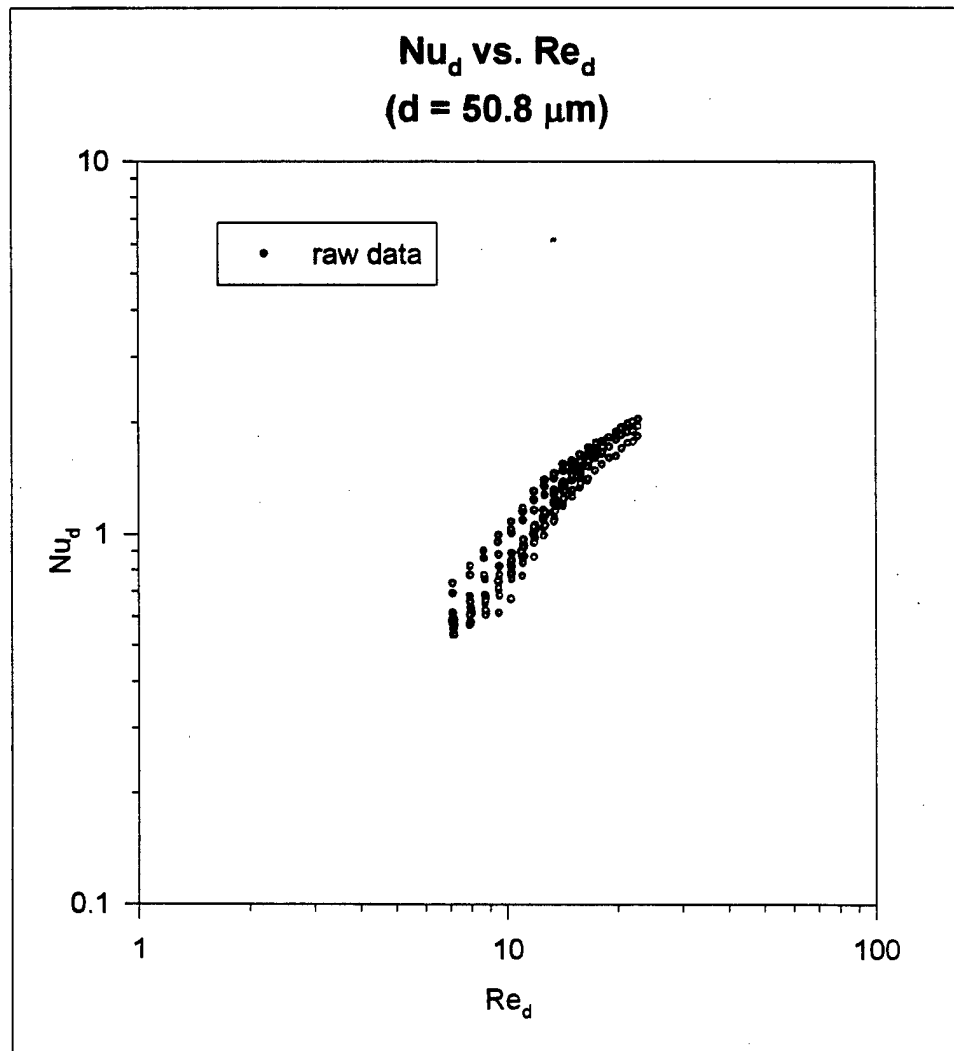


Figure 10. Nusselt Number versus Reynolds Number ( $d = 50.8 \mu\text{m}$ )

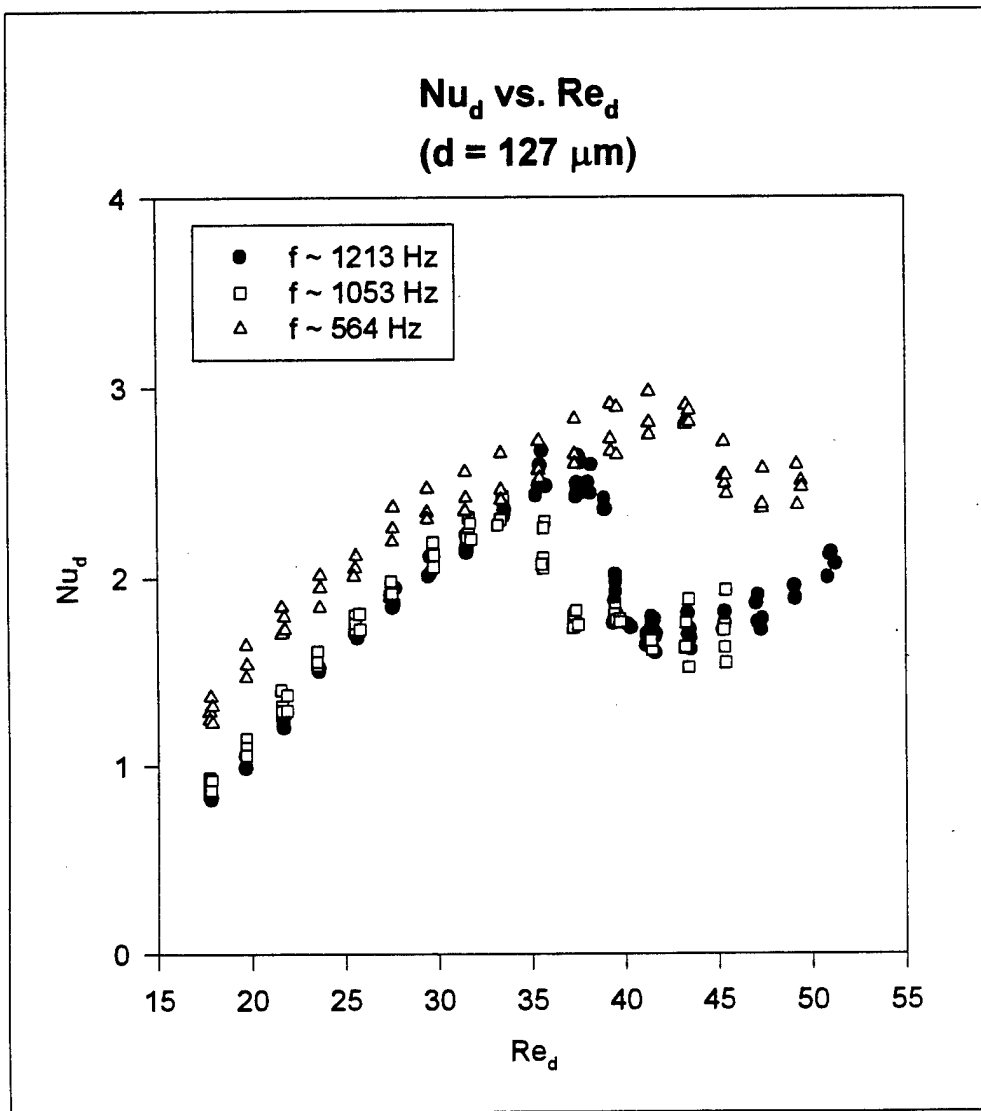


Figure 11. Nusselt Number versus Reynolds Number ( $d = 127 \mu\text{m}$ )

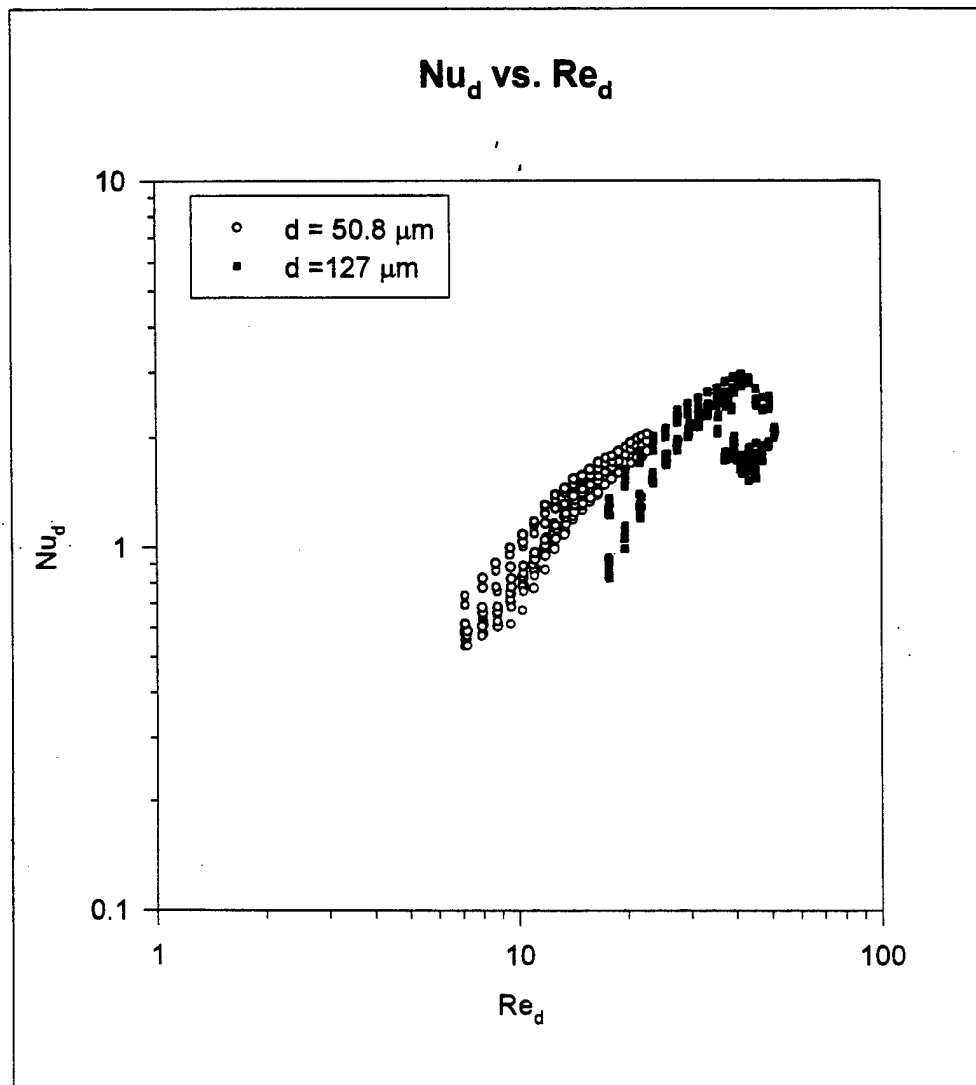


Figure 12. Nusselt Number versus Reynolds Number (both wires)



## VI. CONCLUSIONS AND RECOMMENDATIONS

The motivation for this study was two-fold. First was the desire to gain an understanding of the underlying fluid mechanics for oscillating flow over a bluff body. Second was the need to develop useful heat transfer correlations for high amplitude oscillating flow over a vertical cylinder for application in the design of more efficient thermoacoustic engines. The experiments performed utilized a varying set of acoustic parameters for two different cylinder diameters. Two regimes of varying heat transfer mechanisms are discussed.

Conventional studies of oscillating flow over bluff bodies deal with large  $\beta$  values for varying Keulegan-Carpenter numbers. This study has experimented with very low  $\beta$  and, subsequently, two regimes of differing heat transfer mechanisms have been identified.

For  $\beta$  of  $O(0.1)$  and over a wide range of moderate to high KC numbers (35 to 200), Equation (27) provides a good curve fit to the data and a correlation for the Nusselt number as a function of Reynolds number (Figure 13). In this case, the oscillating Stokes flow interacts with vortex shedding for a combined mechanism of heat transfer. What has not been considered in these experiments is the effect of Prandtl number. Generally speaking, Nusselt number is a function of both Reynolds number and Prandtl number for forced flow over a cylinder. This is an area for expanded research.

For  $\beta$  of  $O(1)$  and over a wide range of moderate to high KC numbers (14 to 86), no definitive correlation has been developed. An introduction to vortex shedding and its effect on heat transfer in this regime has been discussed, but additional data would help solidify these results. In particular, doubling the diameter of the test cylinder, while maintaining KC high enough for vortex shedding, would generate a set of data by which several hypothesis presented above could be validated. Would a thicker wire, and therefore a larger  $\beta$ , generate curves with similar slope but lower heat transfer? If a peak and sudden drop in Nusselt number occurred, would it be at a lower Reynolds number as

the trend from these results indicates? The answers to these questions and validation of the results for  $\beta$  of  $O(1)$  will come from future research.

Once a confident explanation of the mechanisms that control heat transfer for low  $\beta$  values has been found, expanded research should include arrays of cylinders. Analysis of two or more cylinders of variable separation distance arranged as either aligned with the sound wave, staggered or side-by-side is a logical next step to developing heat transfer correlations for operational heat exchangers. A removable section of the acoustic chamber would facilitate test platform interchangeability, make calibration easier and minimize handling of these delicate structures. And finally, use of an automated data acquisition system would provide more uniformity in data taking and speed up the entire testing process.

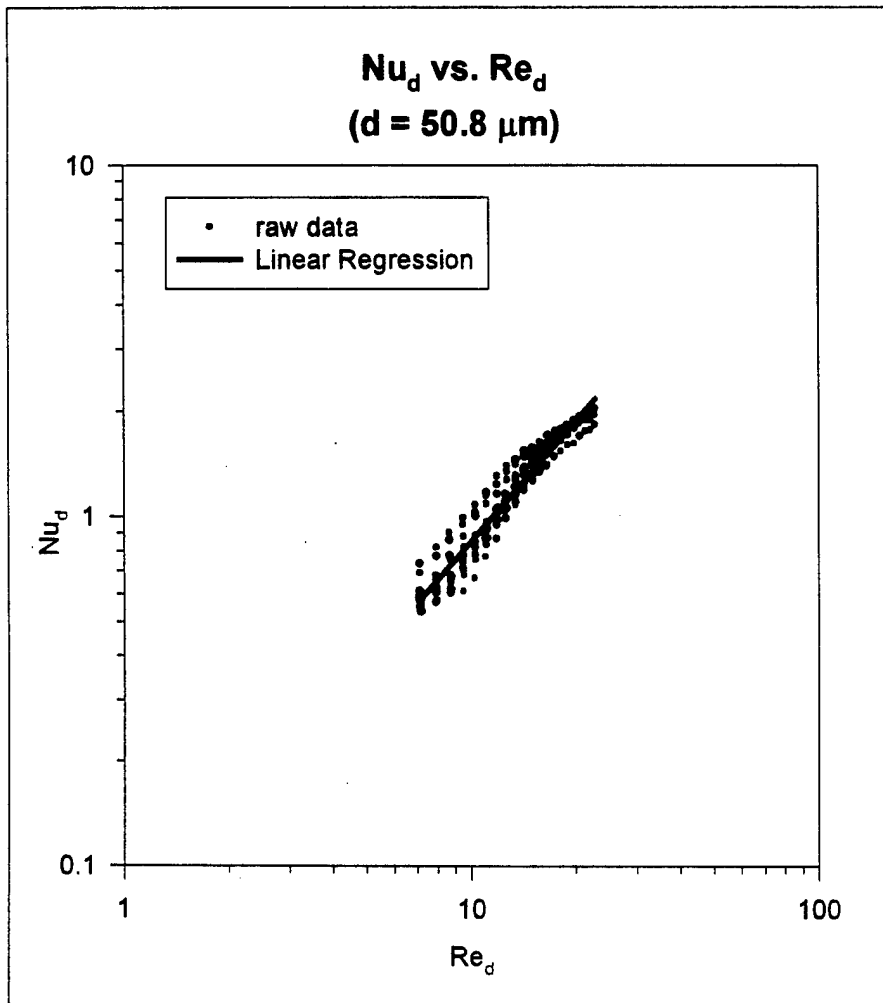


Figure 13. Curve Fit for Nusselt Number versus Reynolds Number ( $d = 50 \mu\text{m}$ )



## APPENDIX A: CALIBRATION

One of the most basic measurements required in order to effectively develop heat transfer correlations is temperature. The two temperature measurements of concern here are of the ambient air within the acoustic chamber and the surface of the platinum wire. Thermoresistive elements, like a platinum wire, provide a nearly linear temperature-resistance relation. A preliminary step to the experimentation was to determine this relation through calibration. Ambient air temperature measurements were made with a calibrated T-type thermocouple.

The platinum wire was mounted in a calibration chamber cut from the same plexiglass tube stock used to make the acoustic chamber. All connectors, electric circuitry and equipment were identical to those used throughout experimentation. Once assembled, as in Figure 14, the calibration chamber, along with a T-type thermocouple, was immersed in a Rosemont Engineering Model 913A ethyl glycol bath. An associated Rosemont Engineering Model 920A commutating bridge provided the reference temperature as measured by a precision temperature probe. A four wire bridge electrical circuit was used to keep the lead resistance as low as possible relative to the platinum wire resistance [Ref. 20].

Numerous resistance versus temperature measurements were taken between 20°C and 50°C, the experimental temperature range of interest. Tables 1 and 2 show the measured wire resistance and associated precision temperature values for the two wire diameters. Column T1 gives the calculated temperature resulting from the linear regression equations. The error is simply the percent difference between the measured and calculated temperatures. Figures 15 and 16 show the statistical linear regression curves superimposed upon the raw data. The following two equations were used throughout the data reduction phase of the experiment for the 50.8  $\mu\text{m}$  and 127  $\mu\text{m}$  diameter wires cases, respectively

$$\text{Temperature } (\text{°C}) = 59.8156 * \text{Resistance } (\Omega) - 224.2799 \quad (\text{A.1})$$

$$\text{Temperature } (\text{°C}) = 436.112 * \text{Resistance } (\Omega) - 261.8139 \quad (\text{A.2})$$

Finally, a calibration data run was made for the 127  $\mu\text{m}$  diameter wire using the actual electric circuit employed in the experiment. Assuming a very high forced convection heat transfer coefficient within the ethyl glycol bath, and applying a low power to the platinum wire, temperature differences between the wire surface and the fluid are assumed insignificant. Voltage measurements were made and wire resistances were calculated. Wire resistance was plotted against the precision temperature to generate an independent calibration curve as seen in Figure 16. The results from these two different calibration techniques were compared and showed a small change in slope and intercept of the calibration curve. The four wire bridge calibration results from both platinum wires were used in all experimental calculations in order to maintain some measure of consistency.

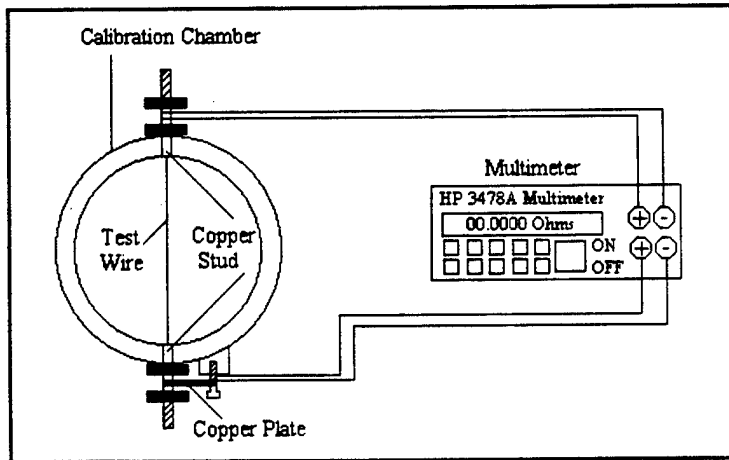


Figure 14. Calibration Chamber

Finally, calibration of the T-type thermocouple, using the same Rosemont Engineering calibration equipment, yielded results within 0.1°C of the reference temperature.

R(w)	T	T1	error
(W)	(C)	(C)	(%)
4.0859	19.87	20.12	1.246
4.1081	21.25	21.45	0.926
4.1395	23.27	23.33	0.243
4.1752	25.56	25.46	0.384
4.2166	28.12	27.94	0.649
4.2465	29.94	29.73	0.716
4.2879	32.29	32.20	0.269
4.3241	34.44	34.37	0.207
4.3810	37.86	37.77	0.232
4.4443	41.37	41.56	0.454
4.5041	44.93	45.14	0.455
4.5631	48.54	48.66	0.256
4.6272	52.2	52.50	0.569
4.5486	47.98	47.80	0.382
4.5100	45.89	45.49	0.883

Table 1. Platinum Wire Calibration Data (d = 50.8  $\mu\text{m}$ )

R(w)	T	T1	error
( $\Omega$ )	(C)	(C)	(%)
0.6439	19.36	19.00	1.902
0.6493	21.50	21.35	0.685
0.6542	23.52	23.49	0.125
0.6592	25.55	25.67	0.472
0.6639	27.60	27.72	0.436
0.6691	29.93	29.99	0.196
0.6746	32.28	32.39	0.331
0.6796	34.39	34.57	0.514
0.6849	36.79	36.88	0.242
0.6900	38.94	39.10	0.418
0.6953	41.37	41.41	0.108
0.7006	43.61	43.73	0.266
0.7060	46.03	46.08	0.111
0.7116	48.61	48.52	0.178
0.7160	50.78	50.44	0.669
0.7040	45.29	45.21	0.179
0.6931	40.55	40.46	0.234
0.6823	35.72	35.75	0.071
0.6710	30.81	30.82	0.024
0.6614	26.58	26.63	0.190

Table 2. Platinum Wire Calibration Data (d = 127  $\mu\text{m}$ )

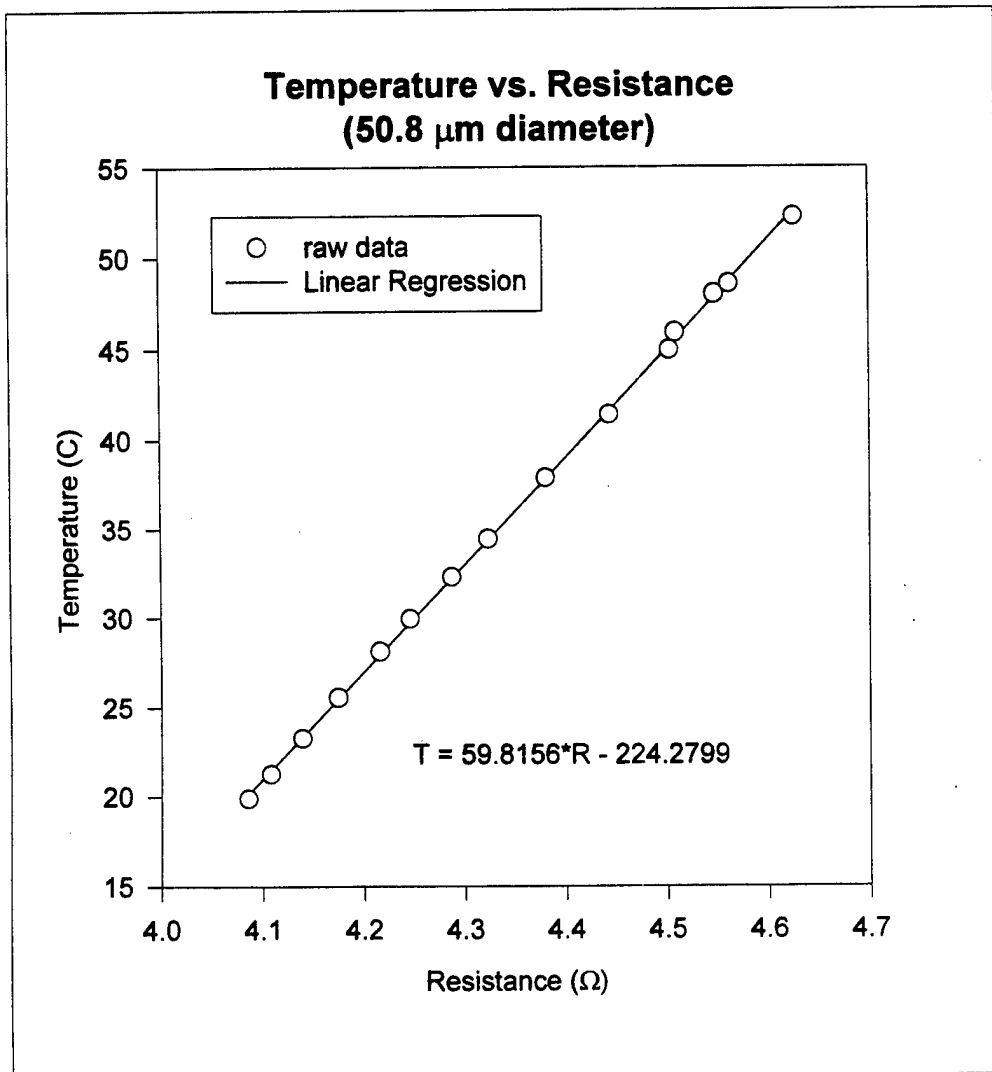


Figure 15. Platinum Wire Calibration Curve ( $d = 50.8 \mu\text{m}$ )

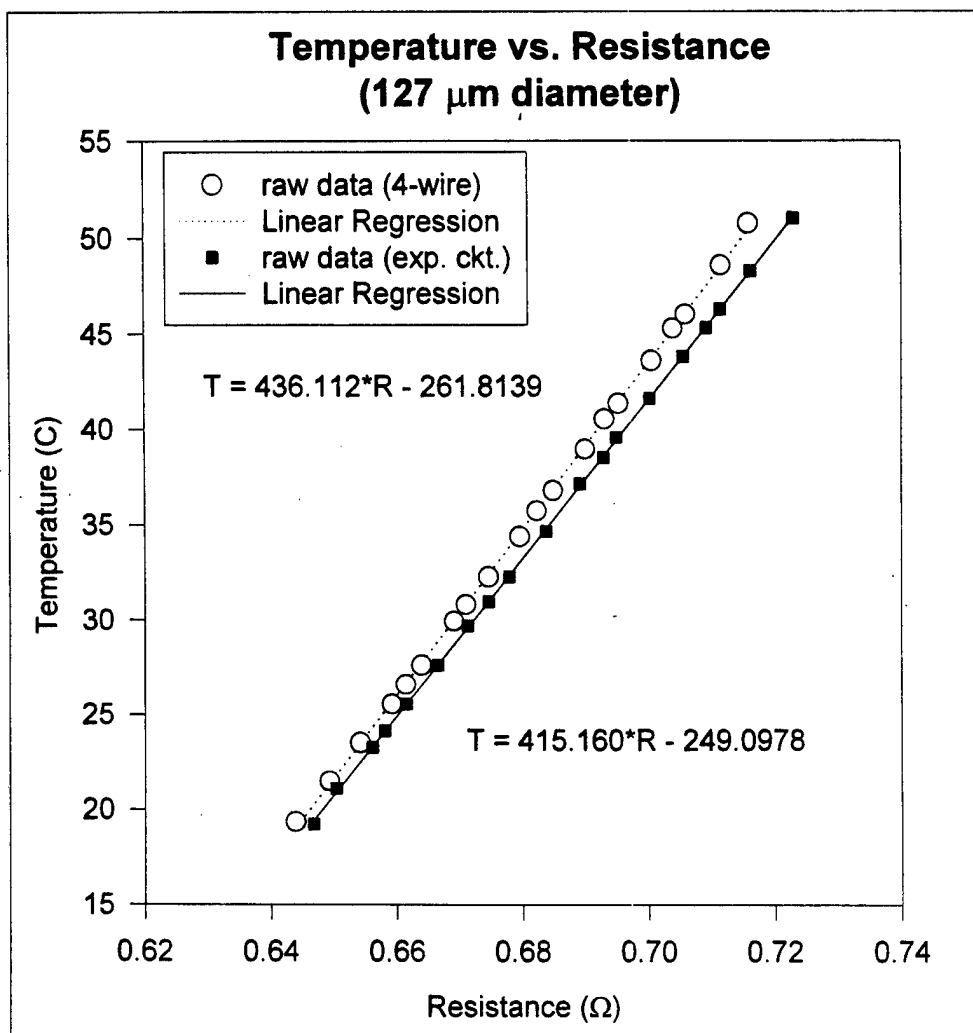


Figure 16. Platinum Wire Calibration Curve ( $d = 127 \mu\text{m}$ )



## APPENDIX B: SAMPLE CALCULATION

The following sample calculations use data collected during an experimental run at  $f \sim 1213$  Hz ( $L = 64$  cm), pressure ratio  $\sim 1.0\%$  and  $\Delta T \sim 24^\circ\text{C}$  for the  $50.8 \mu\text{m}$  diameter platinum wire. The measure values and the properties for air (at 300K) are

$$\begin{array}{ll}
 T_\infty = 25.3^\circ\text{C} & \gamma = \frac{c_p}{c_v} = 1.4 \\
 f = 1218\text{Hz} & R = 287 \frac{\text{m}^2}{\text{s}^2\text{K}} \\
 V_w = 653.18\text{mV} & k = 0.026 \frac{\text{W}}{\text{mK}} \\
 V_{PR} = 14.0310\text{mV} & \nu = 159 \times 10^{-5} \frac{\text{m}^2}{\text{s}} \\
 V_m = 0.533\text{V} & P_m = 101.35\text{kPa}
 \end{array}$$

where  $V_m$  is defined as the measured pressure transducer output voltage (RMS) and  $P_m$  is the mean ambient air pressure.

### A. NUSSELT NUMBER

The Nusselt number equation is

$$Nu = \frac{hd}{k} \quad (\text{B.1})$$

where

$$h = \frac{\text{Power}}{A_s(T_s - T_\infty)} \quad (\text{B.2})$$

Substituting,

$$Nu = \frac{\text{Power}}{A_s(T_s - T_\infty)} \left( \frac{d}{k} \right) \quad (\text{B.3})$$

The wire surface temperature,  $T_s$ , is calculated using the equation found from the wire calibration as described in Appendix A.

$$T_s = 59.8156R_w - 224.2799 \quad (B.4)$$

and

$$R_w = \frac{V_w}{I} = V_w \left( \frac{R_{PR}}{V_{PR}} \right) = \frac{(653.18mV)(98.3m\Omega)}{(14.0310mV)} \quad (B.5)$$

$$R_w = 4576.12m\Omega$$

Therefore,

$$T_s = 49.4^\circ C$$

Power is found from

$$Power = \frac{V_w^2}{R_w} = \frac{(653.18mV)^2 \left( \frac{1V}{100mV} \right)^2}{(4576.12m\Omega) \left( \frac{1\Omega}{1000m\Omega} \right)} \quad (B.6)$$

$$Power = 0.093W$$

Substituting into the Nusselt number equation,

$$Nu = \frac{(0.093W)2(2.54 \times 10^{-5} m)}{(1.20 \times 10^{-5} m^2)(49.4 - 25.3)(K)(0.026 W/mK)}$$

where

$$A_s = \pi dl = 2\pi(2.54 \times 10^{-5} m)(7.53 \times 10^{-2} m) \quad (B.7)$$

$$A_s = 1.20 \times 10^{-5} m^2$$

Finally,

$$Nu = 0.628$$

## B. REYNOLDS NUMBER

The Reynolds number equation is

$$Re_d = \frac{U_0(2a)}{\nu} = 2\epsilon\Lambda^2 \quad (B.8)$$

where

$$U_0 = \frac{c}{\gamma} \left( \frac{P_0}{P_m} \right) \quad (B.9)$$

$$c = \sqrt{\gamma R(T_\infty + 273.15)} \quad (B.10)$$

and

$$P_0 = \frac{V_m}{0.522} \quad (B.11)$$

Making the above substitutions into the Reynolds number equation, we get

$$Re_d = \frac{2aV_m}{0.522\nu P_m} \sqrt{\frac{R}{\gamma}} \sqrt{(T_\infty + 273.15)} \quad (B.12)$$

$$Re_d = \frac{2(2.54 \times 10^{-5} m)(0.533V)}{(0.522V/kPa)(1.59 \times 10^{-5} m^2/s)(101.35 kPa)} \sqrt{\frac{287 m^2/s^2 K}{1.4}} \sqrt{(25.3 + 273.15)(K)}$$

Finally,

$$Re_d = 7.96$$



## APPENDIX C: UNCERTAINTY ANALYSIS

### A. PLATINUM WIRE RESISTANCE

The equation for platinum wire resistance is

$$R_w = \frac{V_w}{I} \quad (C.1)$$

where

$$I = \frac{V_{PR}}{R_{PR}} \quad (C.2)$$

therefore,

$$R_w = V_w \left( \frac{R_{PR}}{V_{PR}} \right) \quad (C.3)$$

The uncertainty becomes

$$u_{R,wire} = \sqrt{\left( \frac{\partial R_w}{\partial V_w} u_{V,wire} \right)^2 + \left( \frac{\partial R_w}{\partial R_{PR}} u_{R,PR} \right)^2 + \left( \frac{\partial R_w}{\partial V_{PR}} u_{V,PR} \right)^2} \quad (C.4)$$

$$u_{R,wire} = \sqrt{\left( \frac{R_{PR}}{V_{PR}} u_{V,wire} \right)^2 + \left( \frac{V_w}{V_{PR}} u_{R,PR} \right)^2 + \left( \frac{-V_w R_{PR}}{V_{PR}^2} u_{V,PR} \right)^2} \quad (C.5)$$

$$\frac{u_{R,wire}}{R_w} = \sqrt{\left( \frac{u_{V,wire}}{V_w} \right)^2 + \left( \frac{u_{R,PR}}{R_{PR}} \right)^2 + \left( \frac{-u_{V,PR}}{V_{PR}} \right)^2} \quad (C.6)$$

$R_{PR} = 0.0983\Omega$

Resistance, Precision Resistor

$u_{R,PR} = 0.026\%$

Uncertainty in Resistance, Precision Resistor

$V_w$  = measured quantity

Voltage, Platinum Wire

$u_{V,wire} = (\% \text{ reading} + \# \text{ counts})$

Uncertainty in Voltage, Platinum Wire

$V_{PR}$  = measure quantity

Voltage, Precision Resistor

$u_{V,PR}$  = (% reading + # counts)

Uncertainty in Voltage, Precision Resistor

The measured quantity uncertainty equations vary depending upon the Hewlett Packard HP 3478A digital multimeter range and resolution for each specific data sample. The following is an example of a data run for  $f \sim 1213$  Hz ( $L = 64$  cm), pressure ratio  $\sim 1.0$  % and  $\Delta T \sim 24^\circ\text{C}$  using the  $50.8 \mu\text{m}$  diameter wire.

$$R_{PR} = 0.0983\Omega$$

$$V_w = 653.18\text{mV}$$

$$u_{R,PR} = 0.026\%$$

$$V_{PR} = 14.0310\text{mV}$$

$$u_{V,wire} = \left( \frac{0.006\%}{100} \right) 653.18\text{mV} + 1\text{count} \left( \frac{100 \times 10^{-6} V}{\text{count}} \right) \left( \frac{1000\text{mV}}{V} \right)$$

$$u_{V,wire} = 0.13919\text{mV}$$

$$u_{V,PR} = \left( \frac{0.035\%}{100} \right) 14.030\text{mV} + 40\text{counts} \left( \frac{100 \times 10^{-9} V}{\text{count}} \right) \left( \frac{1000\text{mV}}{V} \right)$$

$$u_{V,PR} = 0.00891\text{mV}$$

The platinum wire resistance uncertainty is

$$\frac{u_{R,wire}}{R_w} = \sqrt{\left( \frac{0.13919}{653.18} \right)^2 + \left( \frac{0.026}{100} \right)^2 + \left( \frac{-0.00891}{14.030} \right)^2}$$

$$\frac{u_{R,wire}}{R_w} = 7.186 \times 10^{-4} \quad \text{or} \quad 0.07186 \%$$

The calculated platinum wire resistance is

$$R_w = 4576.12 \text{ m}\Omega$$

therefore,

$$u_{R,wire} = 3.29 \text{ m}\Omega$$

## B. NUSSELT NUMBER

The Nusselt number equation is

$$Nu = \frac{hd}{k} \quad (\text{C.7})$$

where

$$h = \frac{Power}{A_s(T_s - T_\infty)} = \frac{\left( \frac{V_w^2}{R_w} \right)}{A_s(T_s - T_\infty)} \quad (\text{C.8})$$

therefore,

$$Nu = \frac{\left( \frac{V_w^2}{R_w} \right)}{d l \pi(T_s - T_\infty)} \left( \frac{d}{k} \right) = \frac{V_w^2}{R_w l k \pi(T_s - T_\infty)} \quad (\text{C.9})$$

From the calibration data the surface temperature of the wire can be written as

$$T_s = A R_w + B \quad (\text{C.10})$$

where  $A$  and  $B$  represent the slope and y-intercept, respectively, from the linear regression model used for the wire calibration. Substituting, the Nusselt number becomes,

$$Nu = \frac{V_w^2}{l k \pi R_w (AR_w + B - T_\infty)} \quad (C.11)$$

and the uncertainty becomes,

$$u_{Nu} = \sqrt{\left(\frac{\partial Nu}{\partial V_w} u_{V,wire}\right)^2 + \left(\frac{\partial Nu}{\partial R_w} u_{R,wire}\right)^2 + \left(\frac{\partial Nu}{\partial T_\infty} u_{T_\infty}\right)^2 + \left(\frac{\partial Nu}{\partial l} u_l\right)^2} \quad (C.12)$$

$$\frac{u_{Nu}}{Nu} = \sqrt{\left(\frac{2}{V_w} u_{V,wire}\right)^2 + \left(\frac{(T_\infty - B - 2AR_w)}{R_w(AR_w + B - T_\infty)} u_{R,wire}\right)^2 + \left(\frac{u_{T_\infty}}{(AR_w + B - T_\infty)}\right)^2 + \left(\frac{-u_l}{l}\right)^2}$$

The following continues from the previous example where  $f \sim 1213$  Hz, pressure ratio  $\sim 1.0\%$  and  $\Delta T \sim 24^\circ\text{C}$ .

$$A = 59.8156^\circ\text{C} / \Omega \quad V_w = 653.18\text{mV}$$

$$B = -224.2799^\circ\text{C} \quad u_{V,wire} = 0.13919\text{mV}$$

$$T_\infty = 25.3^\circ\text{C} \quad l = 0.0753\text{m}$$

$$u_{T_\infty} = 0.5^\circ\text{C} \quad u_l = 3\%$$

$$R_w = 4576.12\text{m}\Omega$$

$$u_{R,wire} = 3.29\text{m}\Omega$$

The Nusselt number uncertainty is

$$\frac{u_{Nu}}{Nu} = \sqrt{(4.26 \times 10^{-4})^2 + (-8.90 \times 10^{-3})^2 + (2.08 \times 10^{-2})^2 + (3.00 \times 10^{-2})^2}$$

$$\frac{u_{Nu}}{Nu} = 3.75 \times 10^{-2} \quad \text{or} \quad 3.75 \%$$

The calculated Nusselt number is

$$Nu = 0.628$$

therefore,

$$u_{Nu} = 0.0236$$

## C. REYNOLDS NUMBER

The Reynolds number equation is

$$Re_d = \frac{(2a)U_0}{\nu} = 2 \frac{a}{\nu} \left( \frac{c}{\gamma} \frac{P_0}{P_m} \right) \quad (C.13)$$

where

$$c = \sqrt{\gamma R(T_\infty + 273.15)} \quad (C.14)$$

$$P_0 = \frac{\left( \frac{V_0}{\sqrt{2}} \right)}{0.522} \quad (C.15)$$

and

$$\frac{V_0}{\sqrt{2}} = \text{microphone output (RMS)}$$

Substituting,

$$Re_d = \sqrt{\frac{R}{\gamma}} \left( \frac{1}{\nu} \right) \left( \frac{1}{0.522 P_m} \right) (2a) \left( \frac{V_0}{\sqrt{2}} \right) \sqrt{(T_\infty + 273.15)} \quad (C.16)$$

Let

$$V_0' = \frac{V_0}{\sqrt{2}} \text{ Volts}, \quad \text{and} \quad T_\infty' = (T_\infty + 273.15)K \quad (\text{C.17})$$

The uncertainty becomes

$$u_{\text{Re}} = \sqrt{\left( \frac{\partial \text{Re}_d}{\partial a} u_a \right)^2 + \left( \frac{\partial \text{Re}_d}{\partial V_0'} u_{V_0'} \right)^2 + \left( \frac{\partial \text{Re}_d}{\partial T_\infty'} u_{T_\infty'} \right)^2} \quad (\text{C.18})$$

$$\frac{u_{\text{Re}}}{\text{Re}_d} = \sqrt{\left( \frac{u_a}{a} \right)^2 + \left( \frac{u_{V_0'}}{V_0'} \right)^2 + \left( \frac{u_{T_\infty'}}{2T_\infty} \right)^2} \quad (\text{C.19})$$

The following continues from the previous example where  $f \sim 1213$  Hz, pressure ratio  $\sim 1.0\%$  and  $\Delta T \sim 24^\circ\text{C}$ .

$$a = 2.54 \times 10^{-5} \text{ m} \quad T_\infty' = (25.3 + 273.15)K$$

$$u_a = 5\% \quad u_{T_\infty'} = 0.5K$$

$$V_0' = 0.533V$$

$$u_{V_0'} = 2.3 \times 10^{-3}V + \left( \frac{0.06\%}{100} \right) 0.533V + \left( \frac{0.03\%}{100} \right) 1V$$

$$u_{V_0'} = 2.920 \times 10^{-3}V$$

The Reynolds number uncertainty is

$$\frac{u_{\text{Re}}}{\text{Re}_d} = \sqrt{\left(\frac{5}{100}\right)^2 + \left(\frac{2.920 \times 10^{-3}}{0.533}\right)^2 + \left(\frac{0.5}{2(298.55)}\right)^2}$$

$$\frac{u_{\text{Re}}}{\text{Re}_d} = 0.0503 \quad \text{or} \quad 5.03\%$$

The calculated Reynolds number is

$$\text{Re}_d = 7.96$$

therefore,

$$u_{\text{Re}} = 0.400$$



## **APPENDIX D: EXPERIMENTAL DATA**

This appendix includes a representative sample of experimentally measured quantities, calculated parameters and uncertainties for the two platinum wire diameters used. Due to space constraints, some constants used in the spreadsheets for calculations have been omitted. The 50.8  $\mu\text{m}$  diameter wire data is reported first followed by the 127  $\mu\text{m}$  diameter wire.



Electromagnetic Information									
$f = 1213 \text{ Hz}$	3.48E-4	2.60E-4	-8.6E-4	0.096	6.97E-4	-0.031	-0.030	0.061	7.44E-4
$L = 64 \text{ cm}$	3.48E-4	2.60E-4	-8.6E-4	0.096	6.97E-4	-0.031	-0.030	0.061	7.44E-4
PR ~ 0.9 %	3.48E-4	2.60E-4	-8.6E-4	0.096	6.96E-4	-0.031	-0.030	0.061	7.51E-4
				0.096	6.96E-4	-0.031	-0.030	0.061	7.51E-4
					0.096	-0.031	-0.030	0.061	7.51E-4
						0.096	-0.031	0.061	7.51E-4
							0.096	-0.031	7.49E-4
								0.096	7.49E-4
									7.49E-4
2.55E-4	2.60E-4	-7.0E-4	5.11E-4	-0.014	-0.030	0.030	4.47E-4	0.050	-8.4E-4
2.55E-4	2.60E-4	-7.0E-4	5.11E-4	-0.014	-0.030	0.030	4.49E-4	0.050	-8.4E-4
2.55E-4	2.60E-4	-7.0E-4	5.11E-4	-0.014	-0.030	0.030	4.51E-4	0.050	-8.4E-4
				0.079	5.11E-4	-0.014	-0.030	0.031	4.49E-4
					0.079	-0.014	-0.030	0.031	4.49E-4
						0.079	-0.014	0.031	4.49E-4
							0.079	-0.014	4.49E-4
								0.079	4.49E-4
									4.49E-4
2.19E-4	2.60E-4	-6.5E-4	4.38E-4	-0.009	-0.030	0.021	3.78E-4	0.050	-8.4E-4
2.19E-4	2.60E-4	-6.5E-4	4.38E-4	-0.009	-0.030	0.021	3.79E-4	0.050	-8.4E-4
2.19E-4	2.60E-4	-6.5E-4	4.38E-4	-0.009	-0.030	0.021	3.79E-4	0.050	-8.4E-4
				0.073	4.38E-4	-0.009	-0.030	0.021	3.79E-4
					0.073	-0.009	-0.030	0.021	3.79E-4
						0.073	-0.009	0.021	3.79E-4
							0.073	-0.009	3.79E-4
								0.073	3.79E-4
									3.79E-4
PR ~ 1.1 %	3.30E-4	2.60E-4	-8.2E-4	0.092	6.59E-4	-0.030	-0.030	0.061	7.44E-4
3.30E-4	2.60E-4	-8.2E-4	0.092	6.59E-4	-0.030	-0.030	0.060	7.29E-4	0.050
3.30E-4	2.60E-4	-8.2E-4	0.092	6.59E-4	-0.030	0.059	7.22E-4	0.050	-8.4E-4
				0.092	6.59E-4	-0.030	0.059	7.22E-4	0.050
					0.092	-0.030	0.059	7.22E-4	0.050
						0.092	-0.030	0.059	7.22E-4
							0.092	-0.030	7.22E-4
								0.092	7.22E-4
									7.22E-4
2.43E-4	2.60E-4	-6.8E-4	4.86E-4	-0.013	-0.030	0.030	4.50E-4	0.050	-8.4E-4
2.43E-4	2.60E-4	-6.8E-4	4.86E-4	-0.013	-0.030	0.030	4.51E-4	0.050	-8.4E-4
2.43E-4	2.60E-4	-6.8E-4	4.86E-4	-0.013	-0.030	0.031	4.52E-4	0.050	-8.4E-4
				0.077	4.86E-4	-0.014	-0.030	0.031	4.52E-4
					0.077	-0.014	-0.030	0.031	4.52E-4
						0.077	-0.014	0.031	4.52E-4
							0.077	-0.014	4.52E-4
								0.077	4.52E-4
									4.52E-4
2.08E-4	2.60E-4	-6.3E-4	4.071	4.17E-4	-0.009	-0.030	0.021	3.76E-4	0.050
2.08E-4	2.60E-4	-6.3E-4	4.071	4.17E-4	-0.009	-0.030	0.021	3.77E-4	0.050
2.08E-4	2.60E-4	-6.3E-4	4.071	4.17E-4	-0.009	-0.030	0.021	3.77E-4	0.050
				0.071	4.071	-0.009	-0.030	0.021	3.77E-4
					0.071	-0.009	-0.030	0.021	3.77E-4
						0.071	-0.009	0.021	3.77E-4
							0.071	-0.009	3.77E-4
								0.071	3.77E-4
									3.77E-4
PR ~ 1.3 %	3.00E-4	2.60E-4	-7.7E-4	0.087	5.99E-4	-0.027	-0.030	0.059	7.19E-4
3.00E-4	2.60E-4	-7.7E-4	0.087	5.99E-4	-0.028	-0.030	0.060	7.27E-4	0.050
3.00E-4	2.60E-4	-7.7E-4	0.087	5.99E-4	-0.028	-0.030	0.060	7.27E-4	0.050
				0.087	5.99E-4	-0.028	-0.030	0.060	7.27E-4
					0.087	-0.028	-0.030	0.060	7.27E-4
						0.087	-0.028	0.060	7.27E-4
							0.087	-0.028	7.27E-4
								0.087	7.27E-4
									7.27E-4
2.28E-4	2.60E-4	-6.5E-4	0.074	4.56E-4	-0.013	-0.030	0.031	4.53E-4	0.050
2.28E-4	2.60E-4	-6.5E-4	0.074	4.56E-4	-0.013	-0.030	0.031	4.54E-4	0.050
2.28E-4	2.60E-4	-6.5E-4	0.074	4.56E-4	-0.013	-0.030	0.031	4.54E-4	0.050
				0.074	4.56E-4	-0.013	-0.030	0.031	4.54E-4
					0.074	-0.013	-0.030	0.031	4.54E-4
						0.074	-0.013	0.031	4.54E-4
							0.074	-0.013	4.54E-4
								0.074	4.54E-4
									4.54E-4
2.28E-4	2.60E-4	-6.5E-4	0.074	4.56E-4	-0.013	-0.030	0.031	4.53E-4	0.050
2.28E-4	2.60E-4	-6.5E-4	0.074	4.56E-4	-0.013	-0.030	0.031	4.54E-4	0.050
2.28E-4	2.60E-4	-6.5E-4	0.074	4.56E-4	-0.013	-0.030	0.031	4.54E-4	0.050
				0.074	4.56E-4	-0.013	-0.030	0.031	4.54E-4
					0.074	-0.013	-0.030	0.031	4.54E-4
						0.074	-0.013	0.031	4.54E-4
							0.074	-0.013	4.54E-4
								0.074	4.54E-4
PR ~ 1.5 %	2.76E-4	2.60E-4	-7.3E-4	0.082	5.52E-4	-0.026	-0.030	0.060	7.23E-4
2.76E-4	2.60E-4	-7.3E-4	0.082	5.52E-4	-0.027	-0.030	0.061	7.29E-4	0.050
2.76E-4	2.60E-4	-7.3E-4	0.082	5.52E-4	-0.027	-0.030	0.061	7.30E-4	0.050
				0.082	5.52E-4	-0.027	-0.030	0.061	7.27E-4
					0.082	-0.027	-0.030	0.061	7.27E-4
						0.082	-0.027	0.061	7.27E-4
							0.082	-0.027	7.27E-4
								0.082	7.27E-4
2.11E-4	2.60E-4	-6.2E-4	0.071	4.21E-4	-0.013	-0.030	0.032	4.57E-4	0.050
2.11E-4	2.60E-4	-6.2E-4	0.071	4.21E-4	-0.013	-0.030	0.032	4.57E-4	0.050
2.11E-4	2.60E-4	-6.2E-4	0.071	4.21E-4	-0.013	-0.030	0.032	4.57E-4	0.050
				0.071	4.21E-4	-0.013	-0.030	0.032	4.57E-4
					0.071	-0.013	-0.030	0.032	4.57E-4
						0.071	-0.013	0.032	4.57E-4
							0.071	-0.013	4.57E-4
								0.071	4.57E-4
1.76E-4	2.60E-4	-5.2E-4	0.068	3.53E-4	-0.031	-0.030	0.020	4.78E-4	0.050
1.76E-4	2.60E-4	-5.2E-4	0.068	3.53E-4	-0.031	-0.030	0.020	4.78E-4	0.050
1.76E-4	2.60E-4	-5.2E-4	0.068	3.53E-4	-0.031	-0.030	0.020	4.78E-4	0.050
				0.068	3.53E-4	-0.031	-0.030	0.020	4.78E-4
					0.068	-0.031	-0.030	0.020	4.78E-4
						0.068	-0.031	0.020	4.78E-4
							0.068	-0.031	4.78E-4
								0.068	4.78E-4



Experiment ID		Run ID		Run Type		Run Order		Run Status		Run Duration		Run Start		Run End		Run Interval		
Run Type	Run ID	Run Type	Run ID	Run Type	Run ID	Run Type	Run ID	Run Type	Run ID	Run Type	Run ID	Run Type	Run ID	Run Type	Run ID	Run Type	Run ID	
PR - 1.123 Hz	2.72E-4	2.60E-4	7.2E-4	0.081	5.43E-4	-0.027	-0.030	0.065	7.62	0.050	-8.5E-4	3.47E-3	5.01					
L = 64 cm	2.72E-4	2.60E-4	7.2E-4	0.081	5.43E-4	-0.027	-0.030	0.064	7.62	0.050	-8.5E-4	3.47E-3	5.01					
PR - 1.17 %	2.72E-4	2.60E-4	7.2E-4	0.081	5.43E-4	-0.027	-0.030	0.064	7.62	0.050	-8.5E-4	3.47E-3	5.01					
1.97E-4	2.60E-4	2.8E-3	0.282	3.95E-4	-0.049	-0.030	0.031	6.52	0.050	-8.5E-4	3.48E-3	5.01						
1.97E-4	2.60E-4	2.8E-3	0.282	3.95E-4	-0.049	-0.030	0.031	6.52	0.050	-8.5E-4	3.48E-3	5.01						
1.97E-4	2.60E-4	2.8E-3	0.282	3.95E-4	-0.049	-0.030	0.031	6.52	0.050	-8.5E-4	3.48E-3	5.01						
PR - 1.19 %	2.51E-4	2.60E-4	6.8E-4	0.077	5.01E-4	-0.025	-0.030	0.061	7.22	0.050	-8.5E-4	3.17E-3	5.01					
2.51E-4	2.60E-4	6.8E-4	0.077	5.01E-4	-0.024	-0.030	0.060	7.15	0.050	-8.5E-4	3.17E-3	5.01						
1.87E-4	2.60E-4	2.66E-3	0.285	3.75E-4	-0.046	-0.030	0.031	6.29	0.050	-8.4E-4	3.17E-3	5.01						
1.87E-4	2.60E-4	2.66E-3	0.285	3.75E-4	-0.046	-0.030	0.031	6.29	0.050	-8.4E-4	3.17E-3	5.01						
1.87E-4	2.60E-4	2.66E-3	0.285	3.75E-4	-0.045	-0.030	0.031	6.25	0.050	-8.4E-4	3.17E-3	5.01						
1.61E-4	2.60E-4	2.2E-3	0.224	3.22E-4	-0.028	-0.030	0.021	4.60	0.050	-8.4E-4	3.17E-3	5.01						
1.61E-4	2.60E-4	2.2E-3	0.223	3.22E-4	-0.028	-0.030	0.021	4.61	0.050	-8.4E-4	3.17E-3	5.01						
1.61E-4	2.60E-4	2.2E-3	0.224	3.22E-4	-0.028	-0.030	0.021	4.58	0.050	-8.5E-4	3.17E-3	5.01						
PR - 2.1 %	2.44E-4	2.60E-4	3.55E-3	0.356	4.87E-4	-0.116	-0.030	0.062	13.49	0.050	-8.4E-4	3.17E-3	5.01					
2.44E-4	2.60E-4	3.55E-3	0.356	4.87E-4	-0.115	-0.030	0.061	13.34	0.050	-8.4E-4	3.17E-3	5.01						
2.44E-4	2.60E-4	3.55E-3	0.355	4.87E-4	-0.116	-0.030	0.062	13.48	0.050	-8.4E-4	3.17E-3	5.01						
1.84E-4	2.60E-4	2.6E-3	0.258	3.67E-4	-0.045	-0.030	0.032	6.30	0.050	-8.4E-4	2.94E-3	5.01						
1.84E-4	2.60E-4	2.6E-3	0.258	3.67E-4	-0.046	-0.030	0.032	6.31	0.050	-8.4E-4	2.94E-3	5.01						
1.84E-4	2.60E-4	2.6E-3	0.258	3.67E-4	-0.045	-0.030	0.031	6.27	0.050	-8.4E-4	2.94E-3	5.01						
7.92E-5	2.60E-4	2.1E-3	0.214	1.56E-4	-0.026	-0.030	0.021	4.49	0.050	-8.4E-4	2.94E-3	5.01						
7.92E-5	2.60E-4	2.1E-3	0.214	1.56E-4	-0.026	-0.030	0.021	4.47	0.050	-8.4E-4	2.94E-3	5.01						
7.92E-5	2.60E-4	2.1E-3	0.213	1.56E-4	-0.026	-0.030	0.021	4.49	0.050	-8.4E-4	2.94E-3	5.01						
1.78E-4	2.60E-4	2.5E-3	0.333	4.61E-4	-0.103	-0.030	0.058	12.20	0.050	-8.4E-4	2.73E-3	5.01						
1.78E-4	2.60E-4	2.5E-3	0.333	4.61E-4	-0.104	-0.030	0.059	12.34	0.050	-8.4E-4	2.73E-3	5.01						
1.78E-4	2.60E-4	2.5E-3	0.333	4.61E-4	-0.104	-0.030	0.059	12.34	0.050	-8.4E-4	2.73E-3	5.01						
7.85E-5	2.60E-4	2.1E-3	0.208	1.57E-4	-0.026	-0.030	0.021	4.49	0.050	-8.4E-4	2.73E-3	5.01						
7.85E-5	2.60E-4	2.1E-3	0.208	1.57E-4	-0.026	-0.030	0.021	4.50	0.050	-8.4E-4	2.73E-3	5.01						
7.85E-5	2.60E-4	2.1E-3	0.208	1.57E-4	-0.026	-0.030	0.021	4.49	0.050	-8.4E-4	2.73E-3	5.01						

Experiment Information	PR Volts (mV)	Wire Volts (mV)	Wires (mA)	V <sub>in</sub> (V)	V <sub>out</sub> (V)	F <sub>in</sub> (Hz)	F <sub>out</sub> (Hz)	h (W/m <sup>2</sup> )	R <sub>in</sub> (Ω)	R <sub>out</sub> (Ω)	h <sub>in</sub> (W/m <sup>2</sup> )	h <sub>out</sub> (W/m <sup>2</sup> )	K <sub>C</sub>	A <sub>AV</sub> (A/V)	B <sub>AV</sub> (A/V)	C <sub>AV</sub> (A/V)	G(D)	R <sub>1</sub> (Ω)	R <sub>2</sub> (Ω)	R <sub>3</sub> (Ω)	R <sub>4</sub> (Ω)	SP (dB)	Power (W)		
f = 1213 Hz	13.61	592.79	4281.50	31.82	8.12	150	630	1215	1.330	317	841.0	317	19.8	1.64	0.001	31.98	100.5	0.31	0.20	1.39E-9	569.2	2.51	159	0.082	
L = 6 cm	23.6	13.61	592.79	4281.50	31.82	8.22	1215	1.330	317	830.8	317	19.8	1.62	0.001	31.98	100.5	0.31	0.20	1.41E-9	569.0	2.51	159	0.082		
PR = 2.5 %	23.5	13.61	592.79	4281.50	31.92	8.32	1215	1.330	317	820.6	317	19.8	1.60	0.001	31.97	100.4	0.31	0.20	1.42E-9	568.8	2.51	159	0.082		
23.7	19.57	877.68	4408.58	39.42	15.72	210	920	1215	1.331	317	924.8	317	19.8	1.81	0.001	32.01	100.6	0.31	0.20	2.68E-9	570.1	2.52	159	0.175	
23.6	19.56	877.68	4410.84	39.56	15.96	1215	1.331	317	910.7	317	19.8	1.80	0.001	32.00	100.5	0.31	0.20	2.72E-9	569.9	2.52	159	0.175			
23.6	19.57	877.69	4408.63	39.43	15.83	1215	1.331	317	918.8	317	19.8	1.79	0.001	32.00	100.5	0.31	0.20	2.70E-9	570.0	2.52	159	0.175			
23.7	24.32	1125.60	4549.61	47.36	24.16	250	1170	1215	1.331	317	959.2	317	19.8	1.87	0.001	32.01	100.6	0.31	0.20	4.11E-9	570.1	2.52	159	0.278	
23.8	24.32	1125.61	4549.65	47.86	24.06	1215	1.331	317	963.1	317	19.8	1.88	0.001	32.01	100.6	0.31	0.20	4.09E-9	570.3	2.52	159	0.278			
23.8	24.32	1125.60	4549.61	47.86	24.06	1215	1.331	317	963.2	317	19.8	1.88	0.001	32.01	100.6	0.31	0.20	4.09E-9	570.3	2.52	159	0.278			
PR = 2.7 %	23.3	14.17	616.59	4277.40	31.58	8.28	150	650	1215	1.431	366	893.7	366	21.3	1.75	0.001	34.39	108.0	0.31	0.20	1.06E-9	657.9	2.70	160	0.089
23.4	14.17	616.59	4277.40	31.58	8.18	1215	1.431	366	904.7	366	21.3	1.77	0.001	34.39	108.1	0.31	0.20	1.05E-9	658.2	2.70	160	0.089			
23.4	14.17	616.59	4277.40	31.58	8.18	1215	1.431	366	904.7	366	21.3	1.77	0.001	34.39	108.1	0.31	0.20	1.05E-9	658.2	2.70	160	0.089			
23.4	20.21	905.93	4406.38	39.29	15.89	210	950	1215	1.433	367	975.4	367	21.3	1.91	0.001	34.44	108.2	0.31	0.20	2.02E-9	660.0	2.71	160	0.186	
23.3	20.20	905.95	4408.66	39.43	16.13	1215	1.433	367	960.6	367	21.3	1.88	0.001	34.44	108.2	0.31	0.20	2.05E-9	659.8	2.71	160	0.186			
23.3	20.21	905.93	4406.38	39.29	16.09	1215	1.433	367	963.2	367	21.3	1.88	0.001	34.43	108.2	0.31	0.20	2.05E-9	659.5	2.71	160	0.186			
23.4	24.98	1154.50	4540.52	47.31	24.13	23.91	260	1200	1215	1.435	368	1021.1	368	21.4	2.00	0.001	34.44	108.4	0.31	0.20	3.02E-9	661.9	2.71	160	0.293
23.3	24.98	1154.52	4542.42	47.43	24.13	1215	1.435	368	1011.7	368	21.4	1.98	0.001	34.46	108.3	0.31	0.20	3.06E-9	661.6	2.71	160	0.293			
23.2	24.98	1154.51	4540.56	47.32	24.12	1215	1.435	368	1012.5	368	21.4	1.98	0.001	34.46	108.3	0.31	0.20	3.04E-9	661.3	2.71	160	0.293			
23.4	24.98	1154.52	4542.42	47.43	24.13	1215	1.435	368	1012.5	368	21.4	1.98	0.001	34.46	108.3	0.31	0.20	3.06E-9	661.3	2.71	160	0.293			
23.4	24.98	1154.51	4540.56	47.32	24.12	1215	1.435	368	1015.1	368	21.4	1.98	0.001	34.46	108.3	0.31	0.20	3.04E-9	661.6	2.71	160	0.293			
23.4	24.98	1154.50	4540.52	47.31	24.13	1215	1.435	368	1017.7	368	21.4	1.98	0.001	34.46	108.3	0.31	0.20	3.04E-9	661.6	2.71	160	0.293			
23.4	24.98	1154.52	4542.42	47.43	24.13	1215	1.435	368	1018.3	368	21.4	1.98	0.001	34.46	108.3	0.31	0.20	3.04E-9	661.6	2.71	160	0.293			
23.4	24.98	1154.51	4540.56	47.32	24.12	1215	1.435	368	1019.9	368	21.4	1.98	0.001	34.46	108.3	0.31	0.20	3.04E-9	661.6	2.71	160	0.293			
23.4	24.98	1154.52	4542.42	47.43	24.13	1215	1.435	368	1021.5	368	21.4	1.98	0.001	34.46	108.3	0.31	0.20	3.04E-9	661.6	2.71	160	0.293			
23.4	24.98	1154.51	4540.56	47.32	24.12	1215	1.435	368	1023.1	368	21.4	1.98	0.001	34.46	108.3	0.31	0.20	3.04E-9	661.6	2.71	160	0.293			
23.4	24.98	1154.52	4542.42	47.43	24.13	1215	1.435	368	1024.7	368	21.4	1.98	0.001	34.46	108.3	0.31	0.20	3.04E-9	661.6	2.71	160	0.293			
23.4	24.98	1154.51	4540.56	47.32	24.12	1215	1.435	368	1026.3	368	21.4	1.98	0.001	34.46	108.3	0.31	0.20	3.04E-9	661.6	2.71	160	0.293			
23.4	24.98	1154.52	4542.42	47.43	24.13	1215	1.435	368	1027.9	368	21.4	1.98	0.001	34.46	108.3	0.31	0.20	3.04E-9	661.6	2.71	160	0.293			
23.4	24.98	1154.51	4540.56	47.32	24.12	1215	1.435	368	1029.5	368	21.4	1.98	0.001	34.46	108.3	0.31	0.20	3.04E-9	661.6	2.71	160	0.293			
23.4	24.98	1154.52	4542.42	47.43	24.13	1215	1.435	368	1031.1	368	21.4	1.98	0.001	34.46	108.3	0.31	0.20	3.04E-9	661.6	2.71	160	0.293			
23.4	24.98	1154.51	4540.56	47.32	24.12	1215	1.435	368	1032.7	368	21.4	1.98	0.001	34.46	108.3	0.31	0.20	3.04E-9	661.6	2.71	160	0.293			
23.4	24.98	1154.52	4542.42	47.43	24.13	1215	1.435	368	1034.3	368	21.4	1.98	0.001	34.46	108.3	0.31	0.20	3.04E-9	661.6	2.71	160	0.293			
23.4	24.98	1154.51	4540.56	47.32	24.12	1215	1.435	368	1035.9	368	21.4	1.98	0.001	34.46	108.3	0.31	0.20	3.04E-9	661.6	2.71	160	0.293			
23.4	24.98	1154.52	4542.42	47.43	24.13	1215	1.435	368	1037.5	368	21.4	1.98	0.001	34.46	108.3	0.31	0.20	3.04E-9	661.6	2.71	160	0.293			
23.4	24.98	1154.51	4540.56	47.32	24.12	1215	1.435	368	1039.1	368	21.4	1.98	0.001	34.46	108.3	0.31	0.20	3.04E-9	661.6	2.71	160	0.293			
23.4	24.98	1154.52	4542.42	47.43	24.13	1215	1.435	368	1040.7	368	21.4	1.98	0.001	34.46	108.3	0.31	0.20	3.04E-9	661.6	2.71	160	0.293			
23.4	24.98	1154.51	4540.56	47.32	24.12	1215	1.435	368	1042.3	368	21.4	1.98	0.001	34.46	108.3	0.31	0.20	3.04E-9	661.6	2.71	160	0.293			
23.4	24.98	1154.52	4542.42	47.43	24.13	1215	1.435	368	1043.9	368	21.4	1.98	0.001	34.46	108.3	0.31	0.20	3.04E-9	661.6	2.71	160	0.293			
23.4	24.98	1154.51	4540.56	47.32	24.12	1215	1.435	368	1045.5	368	21.4	1.98	0.001	34.46	108.3	0.31	0.20	3.04E-9	661.6	2.71	160	0.293			
23.4	24.98	1154.52	4542.42	47.43	24.13	1215	1.435	368	1047.1	368	21.4	1.98	0.001	34.46	108.3	0.31	0.20	3.04E-9	661.6	2.71	160	0.293			
23.4	24.98	1154.51	4540.56	47.32	24.12	1215	1.435	368	1048.7	368	21.4	1.98	0.001	34.46	108.3	0.31	0.20	3.04E-9	661.6	2.71	160	0.293			
23.4	24.98	1154.52	4542.42	47.43	24.13	1215	1.435	368	1050.3	368	21.4	1.98	0.001	34.46	108.3	0.31	0.20	3.04E-9	661.6	2.71	160	0.293			
23.4	24.98	1154.51	4540.56	47.32	24.12	1215	1.435</																		

Number	Model	PR	PR ~ 16 %	PR ~ 25 %	PR ~ 27.6 %	PR ~ 29 %
1 - 1213 Hz	2.29E-4	2.60E-4	-3.3E-3	0.331	4.57E-4	-0.108
L = 64 cm	2.29E-4	2.60E-4	-3.3E-3	0.331	4.57E-4	-0.106
PR - 2.5 %	2.29E-4	2.60E-4	-3.3E-3	0.331	4.57E-4	-0.105
1.74E-4	2.60E-4	2.4E-3	0.241	3.48E-4	-0.043	-0.030
1.74E-4	2.60E-4	2.4E-3	0.242	3.48E-4	-0.042	-0.030
1.74E-4	2.60E-4	2.4E-3	0.241	3.48E-4	-0.043	-0.030
0.241						
7.78E-5	2.60E-4	2.0E-3	0.201	1.56E-4	-0.025	-0.030
7.78E-5	2.60E-4	2.0E-3	0.201	1.56E-4	-0.025	-0.030
7.78E-5	2.60E-4	2.0E-3	0.201	1.56E-4	-0.025	-0.030
0.201						
PR ~ 2.7 %	2.22E-4	2.60E-4	-3.2E-3	0.319	4.44E-4	-0.102
2.22E-4	2.60E-4	3.2E-3	0.319	4.44E-4	-0.102	-0.030
2.22E-4	2.60E-4	3.2E-3	0.319	4.44E-4	-0.103	-0.030
0.319						
1.70E-4	2.60E-4	2.3E-3	0.235	3.41E-4	-0.041	-0.030
1.70E-4	2.60E-4	2.3E-3	0.235	3.41E-4	-0.041	-0.030
1.70E-4	2.60E-4	2.3E-3	0.235	3.41E-4	-0.041	-0.030
0.235						
7.73E-5	2.60E-4	2.0E-3	0.197	1.55E-4	-0.024	-0.030
7.73E-5	2.60E-4	2.0E-3	0.197	1.55E-4	-0.024	-0.030
7.73E-5	2.60E-4	2.0E-3	0.197	1.55E-4	-0.024	-0.030
0.197						
PR ~ 29 %	2.20E-4	2.60E-4	-3.1E-3	0.316	4.40E-4	-0.102
2.20E-4	2.60E-4	-3.1E-3	0.316	4.40E-4	-0.104	-0.030
2.20E-4	2.60E-4	-3.1E-3	0.316	4.40E-4	-0.104	-0.030
0.316						
1.69E-4	2.60E-4	2.3E-3	0.233	3.38E-4	-0.041	-0.030
1.69E-4	2.60E-4	2.3E-3	0.233	3.38E-4	-0.041	-0.030
1.69E-4	2.60E-4	2.3E-3	0.233	3.38E-4	-0.041	-0.030
0.233						
7.71E-5	2.60E-4	-1.9E-3	0.195	1.54E-4	-0.024	-0.030
7.71E-5	2.60E-4	-1.9E-3	0.195	1.54E-4	-0.024	-0.030
7.71E-5	2.60E-4	-1.9E-3	0.195	1.54E-4	-0.024	-0.030
0.195						

Experiment Information	PR Yield (%)	We Vol (mL)	We Vol (mL)	Out Vol (mL)	Vol (mL)	Fist Vol (mL)	Mic Vol (mL)	Re Vol (mL)	H Vol (mL)	Mic Vol (mL)	Re Vol (mL)	H Vol (mL)	Con Vol (mL)	Re Vol (mL)	H Vol (mL)	KC Vol (mL)	AV Vol (mL)	X Vol (mL)	KC Vol (mL)	AV Vol (mL)	X Vol (mL)	G(D) Vol (mL)	R <sub>95%</sub> Vol (mL)	R <sub>99%</sub> Vol (mL)	R <sub>99.9%</sub> Vol (mL)	PR % Vol (mL)	PR % Vol (mL)	PR % Vol (mL)	
1 - 1.213 Hz	24.1	7.737	331.56	4288.76	32.25	8.15	50	366	1213	0.476	41	27.1	41	0.53	0.001	11.52	36.2	0.31	0.20	8.30E-8	73.7	0.90	150	0.027					
L = 50 cm	24.2	7.737	331.56	4288.63	32.25	8.05	50	366	1213	0.476	41	274.7	41	0.54	0.001	11.52	36.2	0.31	0.20	8.19E-8	73.8	0.90	150	0.027					
PR = 0.9 %	24.3	7.737	331.56	4288.76	32.25	7.95	50	366	1213	0.476	41	277.9	41	0.54	0.001	11.53	36.2	0.31	0.20	8.08E-8	73.8	0.90	150	0.027					
...	24.2	11.033	495.97	4418.91	40.04	15.84	120	550	1213	0.479	41	292.4	41	0.57	0.001	11.55	36.3	0.31	0.20	1.60E-7	74.1	0.91	150	0.056					
...	24.2	11.033	495.96	4418.82	40.03	15.83	120	550	1213	0.479	41	292.5	41	0.57	0.001	11.55	36.3	0.31	0.20	1.60E-7	74.1	0.91	150	0.056					
...	24.2	11.033	495.97	4418.91	40.04	15.84	120	550	1213	0.479	41	292.4	41	0.57	0.001	11.55	36.3	0.31	0.20	1.60E-7	74.1	0.91	150	0.056					
...	24.2	13.531	627.21	4556.55	48.27	24.07	140	660	1213	0.478	41	298.4	41	0.58	0.001	11.52	36.2	0.31	0.20	2.49E-7	73.8	0.90	150	0.086					
...	24.3	13.531	627.20	4556.48	48.27	23.97	140	660	1213	0.478	41	299.7	41	0.59	0.001	11.53	36.2	0.31	0.20	2.49E-7	73.8	0.90	150	0.086					
...	24.4	13.531	627.20	4556.48	48.27	23.87	140	660	1213	0.478	41	298.7	41	0.59	0.001	11.53	36.2	0.31	0.20	2.49E-7	73.8	0.90	150	0.086					
PR ~ 1.1 %	24.3	8.3119	363.27	4292.52	32.48	8.18	90	380	1214	0.586	62	312.8	62	0.61	0.001	14.12	44.4	0.31	0.20	3.69E-8	110.7	1.11	152	0.031					
...	24.2	8.320	363.26	4291.88	32.44	8.24	90	380	1214	0.586	62	310.4	62	0.61	0.001	14.12	44.3	0.31	0.20	3.72E-8	110.7	1.11	152	0.031					
...	24.1	8.319	363.26	4292.40	32.47	8.37	90	380	1214	0.586	62	305.5	62	0.60	0.001	14.11	44.3	0.31	0.20	3.78E-8	110.6	1.11	152	0.031					
...	24.4	11.801	531.06	4423.54	40.32	15.92	130	560	1214	0.584	61	333.3	61	0.65	0.001	14.07	44.2	0.31	0.20	7.29E-8	110.0	1.10	152	0.064					
...	24.4	11.800	531.04	4423.83	40.33	15.93	130	560	1214	0.584	61	332.9	61	0.65	0.001	14.07	44.2	0.31	0.20	7.27E-8	110.0	1.10	152	0.064					
...	24.4	11.801	531.05	4423.54	40.32	15.92	130	560	1214	0.584	61	333.2	61	0.65	0.001	14.07	44.2	0.31	0.20	7.29E-8	110.0	1.10	152	0.064					
...	24.5	14.410	668.88	4561.37	48.56	24.06	150	700	1214	0.585	62	339.0	61	0.66	0.001	14.10	44.3	0.31	0.20	1.09E-7	110.5	1.11	152	0.098					
...	24.5	14.400	668.65	4564.46	48.75	24.25	150	700	1214	0.585	62	336.2	61	0.66	0.001	14.10	44.3	0.31	0.20	1.09E-7	110.5	1.11	152	0.098					
...	24.5	14.410	668.65	4561.30	48.56	24.06	150	700	1214	0.585	62	338.1	61	0.66	0.001	14.10	44.3	0.31	0.20	1.09E-7	110.5	1.11	152	0.098					
...	24.5	14.400	668.65	4561.30	48.56	24.06	150	700	1214	0.585	62	338.1	61	0.66	0.001	14.10	44.3	0.31	0.20	1.09E-7	110.5	1.11	152	0.098					
...	24.5	14.410	668.65	4561.37	48.56	24.25	150	700	1214	0.585	62	338.1	61	0.66	0.001	14.10	44.3	0.31	0.20	1.09E-7	110.5	1.11	152	0.098					
PR ~ 1.3 %	21.0	8.645	372.21	4232.30	28.88	7.98	90	400	1207	0.691	85	345.8	85	10.2	0.68	0.001	16.65	52.3	0.31	0.20	1.88E-8	153.6	1.31	153	0.033				
...	20.9	8.645	372.20	4232.19	28.87	7.97	90	400	1207	0.691	85	341.7	85	10.2	0.67	0.001	16.65	52.3	0.31	0.20	1.90E-8	153.5	1.31	153	0.033				
...	20.9	8.644	372.20	4232.68	28.90	8.00	90	400	1207	0.691	85	340.4	85	10.2	0.67	0.001	16.65	52.3	0.31	0.20	1.91E-8	153.5	1.31	153	0.033				
...	21.1	13.09	581.65	4367.93	36.99	15.89	140	620	1207	0.691	85	405.6	85	10.2	0.79	0.001	16.65	52.3	0.31	0.20	3.78E-8	153.7	1.31	153	0.077				
...	20.9	13.08	581.64	4371.19	37.19	16.29	140	620	1207	0.691	85	395.5	85	10.2	0.77	0.001	16.65	52.3	0.31	0.20	3.88E-8	153.5	1.31	153	0.077				
...	20.8	13.09	581.63	4367.78	36.98	16.18	140	620	1207	0.691	85	398.3	85	10.2	0.78	0.001	16.64	52.3	0.31	0.20	3.88E-8	153.5	1.31	153	0.077				
...	21.0	16.13	738.40	4499.98	44.89	23.89	170	780	1207	0.691	85	422.0	85	10.2	0.82	0.001	16.65	52.3	0.31	0.20	5.69E-8	153.6	1.31	153	0.121				
...	21.1	16.13	738.39	4499.92	44.89	23.79	170	780	1207	0.691	85	423.9	85	10.2	0.83	0.001	16.65	52.3	0.31	0.20	5.68E-8	153.7	1.31	153	0.121				
...	21.1	16.14	738.41	4497.26	44.73	23.63	170	780	1207	0.691	85	424.3	85	10.2	0.83	0.001	16.65	52.3	0.31	0.20	5.68E-8	153.7	1.31	153	0.121				

Parameter		Value		Value		Value		Value		Value	
$f \sim 1213$ Hz	3.56E-4	2.60E-4	-8.7E-4	0.097	7.12E-4	-0.032	-0.030	0.051	7.52	0.050	-8.4E-4
$L = 50$ cm	3.56E-4	2.60E-4	-8.7E-4	0.097	7.13E-4	-0.032	-0.030	0.062	7.61	0.050	-8.4E-4
PR = 0.9 %	3.56E-4	2.60E-4	-8.7E-4	0.097	7.12E-4	-0.032	-0.030	0.063	7.68	0.050	-8.4E-4
									7.60		
2.62E-4	2.60E-4	-7.1E-4	0.080	5.23E-4	-0.014	-0.030	0.032	4.58	0.050	-8.4E-4	6.03E-3
2.62E-4	2.60E-4	-7.1E-4	0.080	5.23E-4	-0.014	-0.030	0.032	4.58	0.050	-8.4E-4	6.03E-3
								4.58			
2.19E-4	2.60E-4	-6.5E-4	0.073	4.39E-4	-0.009	-0.030	0.021	3.76	0.050	-8.4E-4	6.04E-3
2.19E-4	2.60E-4	-6.5E-4	0.073	4.39E-4	-0.009	-0.030	0.021	3.76	0.050	-8.4E-4	6.04E-3
								3.76			
PR = 1.1 %	3.35E-4	2.60E-4	-8.3E-4	0.093	6.71E-4	-0.030	-0.030	0.061	7.45	0.050	-8.4E-4
	3.35E-4	2.60E-4	-8.3E-4	0.093	6.71E-4	-0.030	-0.030	0.061	7.40	0.050	-8.4E-4
	3.35E-4	2.60E-4	-8.3E-4	0.093	6.71E-4	-0.030	-0.030	0.060	7.31	0.050	-8.4E-4
								7.39			
2.48E-4	2.60E-4	-6.9E-4	0.018	4.97E-4	-0.014	-0.030	0.031	4.55	0.050	-8.4E-4	5.05E-3
2.48E-4	2.60E-4	-6.9E-4	0.078	4.97E-4	-0.014	-0.030	0.031	4.55	0.050	-8.4E-4	5.05E-3
								4.55			
2.10E-4	2.60E-4	-3.1E-3	0.314	4.19E-4	-0.039	-0.030	0.021	5.33	0.050	-8.4E-4	5.04E-3
2.10E-4	2.60E-4	-3.1E-3	0.315	4.19E-4	-0.039	-0.030	0.021	5.30	0.050	-8.4E-4	5.04E-3
								5.32			
3.29E-4	2.60E-4	-8.1E-4	0.091	6.57E-4	-0.030	-0.030	0.063	7.65	0.050	-8.5E-4	4.36E-3
3.29E-4	2.60E-4	-8.1E-4	0.091	6.57E-4	-0.030	-0.030	0.063	7.57	0.050	-8.5E-4	4.36E-3
								7.55	0.050	-8.5E-4	4.36E-3
								7.59			
PR = 1.3 %	3.29E-4	2.60E-4	-8.1E-4	0.091	6.57E-4	-0.030	-0.030	0.063	7.39	0.050	-8.5E-4
	3.29E-4	2.60E-4	-8.1E-4	0.091	6.57E-4	-0.030	-0.030	0.063	7.25	0.050	-8.5E-4
	3.29E-4	2.60E-4	-8.1E-4	0.091	6.57E-4	-0.030	-0.030	0.063	7.28	0.050	-8.5E-4
								7.31			
2.32E-4	2.60E-4	-3.4E-3	0.312	4.64E-4	-0.060	-0.030	0.021	5.06	0.050	-8.5E-4	4.36E-3
2.32E-4	2.60E-4	-3.4E-3	0.343	4.64E-4	-0.058	-0.030	0.031	5.07	0.050	-8.5E-4	4.36E-3
								5.07			
2.32E-4	2.60E-4	-3.4E-3	0.342	4.64E-4	-0.059	-0.030	0.031	5.09	0.050	-8.5E-4	4.36E-3
								5.07			
1.95E-4	2.60E-4	-2.8E-3	0.285	3.91E-4	-0.035	-0.030	0.021	5.07	0.050	-8.5E-4	4.36E-3
1.95E-4	2.60E-4	-2.8E-3	0.285	3.91E-4	-0.035	-0.030	0.021	5.09	0.050	-8.5E-4	4.36E-3
								5.07			



1-1213 Hz		2.92E-4		2.60E-4		-4.4E-3		0.437		5.83E-4		-0.142		-0.030		0.062		15.77		0.050		-8.5E-4		3.86E-3		5.02	
L = 50 cm		2.92E-4		2.60E-4		-4.4E-3		0.437		5.83E-4		-0.136		-0.030		0.059		15.18		0.050		-8.5E-4		3.86E-3		5.02	
PR = 15 %		2.92E-4		2.60E-4		-4.4E-3		0.437		5.83E-4		-0.139		-0.030		0.061		15.42		0.050		-8.5E-4		3.86E-3		5.02	
																		15.46								5.02	
																		15.46								5.02	
																		15.46								5.02	
																		15.46								5.02	
																		15.46								5.02	
																		15.46								5.02	
																		15.46								5.02	
																		15.46								5.02	
																		15.46								5.02	
																		15.46								5.02	
																		15.46								5.02	
																		15.46								5.02	
																		15.46								5.02	
																		15.46								5.02	
																		15.46								5.02	
																		15.46								5.02	
																		15.46								5.02	
																		15.46								5.02	
																		15.46								5.02	
																		15.46								5.02	
																		15.46								5.02	
																		15.46								5.02	
																		15.46								5.02	
																		15.46								5.02	
																		15.46								5.02	
																		15.46								5.02	
																		15.46								5.02	
																		15.46								5.02	
																		15.46								5.02	
																		15.46								5.02	

Experiment Number	Ta (°C)	PR Vol (mV)	Wire Vol (mV)	Wire Res (mΩ)	I <sub>3</sub> (mA)	I <sub>5</sub> (mA)	I <sub>6</sub> (mA)	Cur (mA)	Vol (mV)	Freq (Hz)	m <sub>0</sub> (mV)	Re (mΩ)	N (mΩ)	Coil (mΩ)	X (mA)	S (mA)	KC (mA)	AA (mA)	R (mA)	R <sub>0</sub> (mA)	R <sub>0</sub> (mA)	GrD (mA)	R <sub>1</sub> (mA)	R <sub>2</sub> (mA)	S1 (dB)	PR % (mA)	S2 (dB)	PR % (mA)
PR ~ 1.053 Hz	24.5	7.8050	341.10	4295.43	32.65	8.15	80	370	1052	0.483	48	276.4	48	0.54	4.9E-4	13.43	42.2	0.27	0.17	6.0E-8	92.7	0.91	150	0.027				
L = 58 cm	24.4	7.8050	341.10	4295.43	32.65	8.25			1052	0.483	48	273.1	48	0.53	4.9E-4	13.43	42.2	0.21	0.17	6.1E-8	92.6	0.91	150	0.027				
PR ~ 0.9 %	24.4	7.8052	341.09	4295.19	32.64	8.24			1052	0.483	48	273.5	48	0.53	4.9E-4	13.43	42.2	0.27	0.17	6.1E-8	92.6	0.91	150	0.027				
24.5	11.0536	497.60	4425.17	40.41	15.91	120	530	1052	0.482	48	292.6	48	0.57	4.9E-4	13.40	42.1	0.27	0.17	1.1E-7	92.3	0.91	150	0.056					
24.4	11.0535	497.69	4425.12	40.41	16.01			1052	0.482	48	290.8	48	0.57	4.9E-4	13.40	42.1	0.27	0.17	1.2E-7	92.2	0.91	150	0.056					
24.4	11.0536	497.60	4425.17	40.41				1052	0.482	48	300.7	48	0.57	4.9E-4	13.40	42.1	0.27	0.17	1.2E-7	92.3	0.91	150	0.056					
24.5	13.5320	627.57	4558.83	48.41	23.91	150	660	1052	0.482	48	300.7	48	0.57	4.9E-4	13.40	42.1	0.27	0.17	1.7E-7	92.3	0.91	150	0.086					
24.5	13.5321	627.57	4558.80	48.41	23.91			1052	0.482	48	300.7	48	0.57	4.9E-4	13.40	42.1	0.27	0.17	1.7E-7	92.3	0.91	150	0.086					
24.5	13.5323	627.58	4558.80	48.41	23.91			1052	0.482	48	300.7	48	0.57	4.9E-4	13.40	42.1	0.27	0.17	1.7E-7	92.3	0.91	150	0.086					
PR ~ 1.1 %	24.5	8.3406	364.31	4293.66	32.55	8.05	90	390	1052	0.584	71	319.6	70	0.62	4.9E-4	16.24	51.0	0.27	0.17	2.7E-8	135.5	1.10	152	0.031				
	24.5	8.3409	364.32	4293.62	32.55	8.05			1052	0.584	71	319.7	70	0.62	4.9E-4	16.24	51.0	0.27	0.17	2.7E-8	135.5	1.10	152	0.031				
	24.5	8.3406	364.32	4293.77	32.55	8.05			1052	0.584	71	319.3	70	0.62	4.9E-4	16.24	51.0	0.27	0.17	2.8E-8	135.5	1.10	152	0.031				
24.5	12.1129	545.39	4426.01	40.46	15.96	130	580	1052	0.584	71	350.3	70	0.68	4.9E-4	16.24	51.0	0.27	0.17	2.7E-8	135.5	1.10	152	0.067					
24.5	12.1129	545.39	4426.01	40.46	15.96			1052	0.584	71	350.3	70	0.68	4.9E-4	16.24	51.0	0.27	0.17	2.7E-8	135.5	1.10	152	0.067					
24.5	12.1130	545.39	4425.98	40.46	15.96			1052	0.584	71	350.3	70	0.68	4.9E-4	16.24	51.0	0.27	0.17	2.7E-8	135.5	1.10	152	0.067					
24.5	15.4256	716.18	4563.87	48.71	24.21	160	750	1052	0.584	71	386.3	70	0.76	4.9E-4	16.24	51.0	0.27	0.17	8.4E-8	135.5	1.10	152	0.112					
24.5	15.4259	716.18	4563.79	48.71	24.21			1052	0.584	71	386.2	70	0.76	4.9E-4	16.24	51.0	0.27	0.17	8.4E-8	135.5	1.10	152	0.112					
24.5	15.4254	716.18	4563.93	48.71	24.21			1052	0.584	71	386.3	70	0.76	4.9E-4	16.24	51.0	0.27	0.17	8.4E-8	135.5	1.10	152	0.112					
PR ~ 1.3 %	24.4	9.2480	403.90	4293.18	32.52	8.12	100	430	1052	0.681	99	389.4	98	10.3	0.76	4.9E-4	19.21	60.4	0.27	0.17	1.4E-8	189.6	1.31	153	0.038			
	24.3	9.2479	403.89	4293.12	32.52	8.22			1052	0.681	99	384.8	98	10.3	0.75	4.9E-4	19.21	60.4	0.27	0.17	1.4E-8	189.4	1.31	153	0.038			
	24.3	9.2481	403.89	4293.03	32.51	8.21			1052	0.681	99	385.1	98	10.3	0.75	4.9E-4	19.21	60.4	0.27	0.17	1.4E-8	189.5	1.31	153	0.038			
24.4	13.8610	613.00	4430.40	40.73	16.33	150	650	1052	0.690	99	432.3	98	10.3	0.84	4.9E-4	19.19	60.3	0.27	0.17	2.9E-8	189.0	1.30	153	0.085				
24.5	13.6016	613.01	4430.28	40.72	16.22			1052	0.690	99	435.2	98	10.3	0.85	4.9E-4	19.19	60.3	0.27	0.17	2.8E-8	189.1	1.30	153	0.085				
24.5	13.5613	613.01	4430.38	40.73	16.23			1052	0.690	99	435.0	98	10.3	0.85	4.9E-4	19.19	60.3	0.27	0.17	2.8E-8	189.1	1.30	153	0.085				
24.4	16.6228	771.13	4558.70	48.40	24.00	180	810	1052	0.691	99	452.2	98	10.3	0.88	4.9E-4	19.21	60.4	0.27	0.17	4.2E-8	189.6	1.31	153	0.130				
24.4	16.6322	771.12	4557.55	48.33	23.93			1052	0.691	99	453.6	98	10.3	0.89	4.9E-4	19.21	60.4	0.27	0.17	4.2E-8	189.6	1.31	153	0.130				
24.4	16.6332	771.12	4557.27	48.32	23.92			1052	0.691	99	454.0	98	10.3	0.89	4.9E-4	19.21	60.4	0.27	0.17	4.2E-8	189.6	1.31	153	0.130				
24.4	10.135	441.75	4284.56	32.00	7.80	110	470	1051	0.798	131	485.7	130	11.9	0.95	4.9E-4	22.15	69.6	0.27	0.17	7.8E-9	252.1	1.50	155	0.046				
24.2	10.134	441.75	4284.98	32.03	7.83			1051	0.796	131	484.1	130	11.9	0.95	4.9E-4	22.15	69.6	0.27	0.17	7.8E-9	252.1	1.50	155	0.046				
24.2	10.134	441.76	4285.08	32.03	7.83			1051	0.796	131	483.7	130	11.9	0.95	4.9E-4	22.15	69.6	0.27	0.17	7.8E-9	252.1	1.50	155	0.046				
24.2	14.865	659.46	4420.38	40.13	15.93	160	700	1051	0.796	131	514.0	130	11.9	1.00	4.9E-4	22.15	69.6	0.27	0.17	7.8E-9	252.1	1.50	155	0.098				
24.3	14.871	659.44	4418.44	40.01	15.71			1051	0.796	131	521.3	131	11.9	1.02	4.9E-4	22.15	69.6	0.27	0.17	1.58E-8	252.2	1.50	155	0.098				
24.3	14.668	659.43	4419.28	40.06	15.76			1051	0.796	131	519.5	131	11.9	1.01	4.9E-4	22.15	69.6	0.27	0.17	1.58E-8	252.2	1.50	155	0.098				
24.3	17.98	83.32	4550.59	47.92	23.62	190	870	1051	0.794	131	535.2	130	11.8	1.05	4.9E-4	22.09	69.4	0.27	0.17	2.39E-8	251.1	1.50	155	0.152				
24.4	17.95	83.30	4553.02	48.06	23.66			1051	0.794	131	533.9	130	11.8	1.04	4.9E-4	22.10	69.4	0.27	0.17	2.39E-8	251.1	1.50	155	0.152				
24.4	17.96	83.31	4550.43	47.91	23.51			1051	0.794	131	537.7	130	11.8	1.05	4.9E-4	22.10	69.4	0.27	0.17	2.39E-8	251.1	1.50	155	0.152				

Experiment Information		Vol	Re	Im	Imag	Re	Im	Imag	Re	Im	Imag		
$f \sim 1053$ Hz		3.53E-4	2.60E-4	-8.5E-4	0.097	7.06E-4	-0.031	-0.030	0.061	7.52	0.050		
L = 58 cm		3.53E-4	2.60E-4	-8.6E-4	0.097	7.06E-4	-0.031	-0.030	0.061	7.44	0.050		
PR ~ 0.9 %		3.53E-4	2.60E-4	-8.6E-4	0.097	7.06E-4	-0.031	-0.030	0.061	7.45	0.050		
					0.097				7.47		5.04		
2.61E-4		2.60E-4	0.080	5.22E-4	-0.014	-0.030	0.031	4.57	0.050	-8.4E-4	5.98E-3		
2.61E-4		2.60E-4	-7.1E-4	0.080	5.22E-4	-0.014	-0.030	0.031	4.55	0.050	-8.4E-4	5.98E-3	
2.61E-4		2.60E-4	-7.1E-4	0.080	5.22E-4	-0.014	-0.030	0.031	4.55	0.050	-8.4E-4	5.98E-3	
					0.080				4.55		5.04		
2.19E-4		2.60E-4	-6.5E-4	0.073	4.39E-4	-0.009	-0.030	0.021	3.77	0.050	-8.4E-4	5.98E-3	
2.19E-4		2.60E-4	-6.5E-4	0.073	4.39E-4	-0.009	-0.030	0.021	3.77	0.050	-8.4E-4	5.98E-3	
2.19E-4		2.60E-4	-6.5E-4	0.073	4.39E-4	-0.009	-0.030	0.021	3.77	0.050	-8.4E-4	5.98E-3	
					0.073				3.77		5.04		
PR ~ 1.1 %		3.34E-4	2.60E-4	-8.3E-4	0.093	6.69E-4	-0.031	-0.030	0.062	7.55	0.050	-8.4E-4	5.05E-3
3.34E-4		2.60E-4	-8.3E-4	0.093	6.69E-4	-0.031	-0.030	0.062	7.55	0.050	-8.4E-4	5.05E-3	
3.34E-4		2.60E-4	-8.3E-4	0.093	6.69E-4	-0.031	-0.030	0.062	7.54	0.050	-8.4E-4	5.05E-3	
					0.093				7.55		5.03		
2.43E-4		2.60E-4	-6.8E-4	0.077	4.87E-4	-0.014	-0.030	0.031	4.54	0.050	-8.4E-4	5.05E-3	
2.43E-4		2.60E-4	-6.8E-4	0.077	4.87E-4	-0.014	-0.030	0.031	4.54	0.050	-8.4E-4	5.05E-3	
2.43E-4		2.60E-4	-6.8E-4	0.077	4.87E-4	-0.014	-0.030	0.031	4.54	0.050	-8.4E-4	5.05E-3	
					0.077				4.54		5.03		
2.00E-4		2.60E-4	-6.1E-4	0.069	3.99E-4	-0.008	-0.030	0.021	3.74	0.050	-8.4E-4	5.05E-3	
2.00E-4		2.60E-4	-6.1E-4	0.069	3.99E-4	-0.008	-0.030	0.021	3.74	0.050	-8.4E-4	5.05E-3	
2.00E-4		2.60E-4	-6.1E-4	0.069	3.99E-4	-0.008	-0.030	0.021	3.74	0.050	-8.4E-4	5.05E-3	
					0.069				3.74		5.03		
PR ~ 1.3 %		3.08E-4	2.60E-4	-7.8E-4	0.088	6.15E-4	-0.029	-0.030	0.062	7.43	0.050	-8.4E-4	4.36E-3
3.08E-4		2.60E-4	-7.8E-4	0.088	6.15E-4	-0.029	-0.030	0.062	7.43	0.050	-8.4E-4	4.36E-3	
3.08E-4		2.60E-4	-7.8E-4	0.088	6.15E-4	-0.029	-0.030	0.062	7.43	0.050	-8.4E-4	4.36E-3	
					0.088				7.38		5.02		
2.23E-4		2.60E-4	-6.4E-4	0.073	4.46E-4	-0.013	-0.030	0.031	4.47	0.050	-8.4E-4	4.37E-3	
2.23E-4		2.60E-4	-6.4E-4	0.073	4.46E-4	-0.013	-0.030	0.031	4.48	0.050	-8.4E-4	4.37E-3	
2.23E-4		2.60E-4	-6.4E-4	0.073	4.46E-4	-0.013	-0.030	0.031	4.48	0.050	-8.4E-4	4.37E-3	
					0.073				4.48		5.02		
1.90E-4		2.60E-4	-5.9E-4	0.067	3.79E-4	-0.008	-0.030	0.021	3.75	0.050	-8.4E-4	4.36E-3	
1.90E-4		2.60E-4	-5.9E-4	0.067	3.79E-4	-0.008	-0.030	0.021	3.75	0.050	-8.4E-4	4.36E-3	
1.90E-4		2.60E-4	-5.9E-4	0.067	3.79E-4	-0.008	-0.030	0.021	3.75	0.050	-8.4E-4	4.36E-3	
					0.067				3.75		5.02		
PR ~ 1.5 %		2.86E-4	2.60E-4	-6.2E-4	0.084	5.73E-4	-0.028	-0.030	0.064	7.62	0.050	-8.4E-4	3.87E-3
2.86E-4		2.60E-4	-6.2E-4	0.084	5.73E-4	-0.028	-0.030	0.064	7.60	0.050	-8.4E-4	3.87E-3	
2.86E-4		2.60E-4	-6.2E-4	0.084	5.73E-4	-0.028	-0.030	0.064	7.60	0.050	-8.4E-4	3.87E-3	
					0.084				7.61		5.02		
2.12E-4		2.60E-4	-6.2E-4	0.071	4.23E-4	-0.012	-0.030	0.031	4.52	0.050	-8.4E-4	3.87E-3	
2.12E-4		2.60E-4	-6.2E-4	0.071	4.23E-4	-0.012	-0.030	0.031	4.52	0.050	-8.4E-4	3.87E-3	
2.12E-4		2.60E-4	-6.2E-4	0.071	4.23E-4	-0.012	-0.030	0.031	4.52	0.050	-8.4E-4	3.87E-3	
					0.071				4.54		5.02		
1.80E-4		2.60E-4	-5.8E-4	0.067	3.79E-4	-0.008	-0.030	0.030	4.91	0.050	-8.4E-4	3.87E-3	
1.80E-4		2.60E-4	-5.8E-4	0.067	3.79E-4	-0.008	-0.030	0.030	4.91	0.050	-8.4E-4	3.87E-3	
1.80E-4		2.60E-4	-5.8E-4	0.067	3.79E-4	-0.008	-0.030	0.030	4.91	0.050	-8.4E-4	3.87E-3	
					0.067				4.91		5.02		



Experiment		Y01		Y02		Y03		Y04		Y05		Y06		Y07		Y08		Y09		Y10	
Y01	Y02	Y03	Y04	Y05	Y06	Y07	Y08	Y09	Y10	Y01	Y02	Y03	Y04	Y05	Y06	Y07	Y08	Y09	Y10		
1 ~ 1053 Hz	2.60E-4	2.60E-4	-7.0E-4	0.079	5.20E-4	-0.026	-0.030	0.063	7.43	0.050	-8.4E-4	3.47E-3	5.01								
L = 58 cm	2.60E-4	2.60E-4	-7.0E-4	0.079	5.20E-4	-0.026	-0.030	0.062	7.33	0.050	-8.4E-4	3.47E-3	5.01								
PR ~ 1.7 %	2.60E-4	2.60E-4	-7.0E-4	0.079	5.20E-4	-0.025	-0.030	0.060	7.18	0.050	-8.4E-4	3.47E-3	5.01								
				0.079					<b>7.31</b>												
1.96E-4	2.60E-4	2.60E-4	-2.8E-3	0.284	3.92E-4	-0.049	-0.030	0.031	<b>6.55</b>	0.050	-8.4E-4	3.47E-3	5.01								
1.96E-4	2.60E-4	2.60E-4	-2.8E-3	0.284	3.92E-4	-0.049	-0.030	0.031	6.53	0.050	-8.4E-4	3.47E-3	5.01								
1.96E-4	2.60E-4	2.60E-4	-2.8E-3	0.284	3.92E-4	-0.049	-0.030	0.030	6.49	0.050	-8.4E-4	3.47E-3	5.01								
									<b>6.62</b>												
1.69E-4	2.60E-4	2.60E-4	-2.4E-3	0.240	3.38E-4	-0.030	-0.030	0.021	4.72	0.050	-8.4E-4	3.47E-3	5.01								
1.69E-4	2.60E-4	2.60E-4	-2.4E-3	0.240	3.38E-4	-0.030	-0.030	0.021	4.71	0.050	-8.4E-4	3.47E-3	5.01								
1.69E-4	2.60E-4	2.60E-4	-2.4E-3	0.241	3.38E-4	-0.030	-0.030	0.021	4.69	0.050	-8.4E-4	3.47E-3	5.01								
				0.241					<b>4.71</b>												
PR ~ 19 %	2.47E-4	2.60E-4	-6.8E-4	0.077	4.94E-4	-0.025	-0.030	0.062	6.29	0.050	-8.4E-4	3.47E-3	5.01								
2.47E-4	2.60E-4	2.60E-4	-6.8E-4	0.077	4.94E-4	-0.025	-0.030	0.061	7.24	0.050	-8.4E-4	3.47E-3	5.01								
2.47E-4	2.60E-4	2.60E-4	-6.8E-4	0.077	4.94E-4	-0.025	-0.030	0.061	7.21	0.050	-8.4E-4	3.47E-3	5.01								
				0.077					<b>7.25</b>												
1.87E-4	2.60E-4	2.60E-4	-2.6E-3	0.266	3.74E-4	-0.047	-0.030	0.031	6.36	0.050	-8.4E-4	3.47E-3	5.01								
1.87E-4	2.60E-4	2.60E-4	-2.6E-3	0.267	3.74E-4	-0.046	-0.030	0.031	6.29	0.050	-8.4E-4	3.47E-3	5.01								
1.87E-4	2.60E-4	2.60E-4	-2.6E-3	0.266	3.74E-4	-0.046	-0.030	0.031	6.33	0.050	-8.4E-4	3.47E-3	5.01								
				0.266					<b>6.33</b>												
1.62E-4	2.60E-4	2.60E-4	-2.2E-3	0.226	3.24E-4	-0.028	-0.030	0.021	4.58	0.050	-8.4E-4	3.47E-3	5.01								
1.62E-4	2.60E-4	2.60E-4	-2.2E-3	0.226	3.24E-4	-0.028	-0.030	0.021	4.58	0.050	-8.4E-4	3.47E-3	5.01								
1.62E-4	2.60E-4	2.60E-4	-2.2E-3	0.226	3.24E-4	-0.028	-0.030	0.020	4.57	0.050	-8.4E-4	3.47E-3	5.01								
				0.226					<b>4.57</b>												
PR ~ 2.1 %	2.40E-4	2.60E-4	-6.6E-4	0.075	4.81E-4	-0.024	-0.030	0.060	7.08	0.050	-8.4E-4	3.47E-3	5.01								
2.40E-4	2.60E-4	2.60E-4	-6.6E-4	0.075	4.81E-4	-0.024	-0.030	0.061	7.19	0.050	-8.4E-4	3.47E-3	5.01								
2.40E-4	2.60E-4	2.60E-4	-6.6E-4	0.075	4.81E-4	-0.024	-0.030	0.060	7.15	0.050	-8.4E-4	3.47E-3	5.01								
				0.075					<b>7.14</b>												
1.82E-4	2.60E-4	2.60E-4	-2.5E-3	0.256	3.65E-4	-0.044	-0.030	0.031	6.17	0.050	-8.4E-4	3.47E-3	5.01								
1.82E-4	2.60E-4	2.60E-4	-2.5E-3	0.256	3.65E-4	-0.044	-0.030	0.031	6.16	0.050	-8.4E-4	3.47E-3	5.01								
1.82E-4	2.60E-4	2.60E-4	-2.5E-3	0.256	3.65E-4	-0.044	-0.030	0.031	6.18	0.050	-8.4E-4	3.47E-3	5.01								
				0.256					<b>6.18</b>												
7.93E-5	2.60E-4	2.60E-4	-2.1E-3	0.215	1.59E-4	-0.026	-0.030	0.021	4.48	0.050	-8.4E-4	3.47E-3	5.01								
7.93E-5	2.60E-4	2.60E-4	-2.1E-3	0.215	1.59E-4	-0.026	-0.030	0.021	4.48	0.050	-8.4E-4	3.47E-3	5.01								
7.93E-5	2.60E-4	2.60E-4	-2.1E-3	0.215	1.59E-4	-0.026	-0.030	0.021	4.48	0.050	-8.4E-4	3.47E-3	5.01								
				0.215					<b>4.48</b>												

Experiment Information	PR Vol (mV)	Wire Volt (mV)	Wire Res (mΩ)	I <sub>s</sub> (mA)	I <sub>sp</sub> (mA)	Cur. (mA)	Vol. (V)	Freq. (Hz)	mCV	Rs (MΩ)	n (MHz)	V <sub>th</sub> (V)	R <sub>a</sub> (mΩ)	R <sub>d</sub> (mΩ)	NxD (mΩ)	X	S (mΩ)	KC (mΩ)	KA (mΩ)	KR (mΩ)	GrD		Rs (mΩ)	PR % SPL (dB)	Power (mW)
																					GrD <sub>1</sub>	GrD <sub>2</sub>			
1 - 564 Hz	22.7	8.147	353.06	4259.95	30.53	7.83	90	360	565	0.478	88	310.9	86	7.1	0.61	2.6E-4	24.68	77.5	0.14	0.09	1.81E-8	227.4	0.90	150	0.029
L = 47 cm	22.8	8.147	353.06	4259.95	30.53	7.73			565	0.478	88	314.9	86	7.1	0.62	2.6E-4	24.68	77.5	0.14	0.09	1.78E-8	227.5	0.90	150	0.029
PR - 0.9 %	22.8	8.147	353.06	4259.95	30.53	7.73			565	0.478	88	314.9	86	7.1	0.62	2.6E-4	24.68	77.5	0.14	0.09	1.78E-8	227.5	0.90	150	0.029
	22.7	12.128	541.96	4392.70	38.47	15.77	130	580	565	0.478	88	352.8	86	7.1	0.69	2.6E-4	24.68	77.5	0.14	0.09	3.64E-8	227.4	0.90	150	0.067
	22.8	12.128	541.97	4392.78	38.48	15.68			565	0.478	88	354.9	86	7.1	0.69	2.6E-4	24.68	77.5	0.14	0.09	3.61E-8	227.5	0.90	150	0.067
	22.8	12.128	541.97	4392.78	38.48	15.68			565	0.478	88	354.9	86	7.1	0.69	2.6E-4	24.68	77.5	0.14	0.09	3.61E-8	227.5	0.90	150	0.067
	22.8	15.117	696.20	4526.82	46.49	23.69	160	730	565	0.477	87	376.0	86	7.1	0.73	2.6E-4	24.63	77.4	0.14	0.09	5.51E-8	226.6	0.90	150	0.107
	22.8	15.117	696.20	4527.12	46.51	23.71			565	0.477	87	376.7	86	7.1	0.73	2.6E-4	24.63	77.4	0.14	0.09	5.51E-8	226.6	0.90	150	0.107
	22.8	15.118	696.19	4526.75	46.49	23.69			565	0.477	87	376.1	86	7.1	0.69	2.6E-4	24.63	77.4	0.14	0.09	5.51E-8	226.6	0.90	150	0.107
PR - 1.1 %	22.8	9.240	400.86	4254.56	30.81	8.01	100	450	565	0.582	130	391.6	128	8.7	0.77	2.6E-4	30.05	94.4	0.14	0.09	8.40E-9	337.3	1.10	152	0.038
	22.9	9.240	400.86	4254.56	30.81	7.91			565	0.582	130	396.5	128	8.7	0.77	2.6E-4	30.06	94.4	0.14	0.09	8.28E-9	337.5	1.10	152	0.038
	23.0	9.240	400.86	4254.56	30.81	7.81			565	0.582	130	401.6	128	8.7	0.78	2.6E-4	30.06	94.4	0.14	0.09	8.17E-9	337.7	1.10	152	0.038
	22.9	13.485	603.15	4396.71	38.71	15.81	140	640	565	0.582	130	435.4	128	8.7	0.95	2.6E-4	30.06	94.4	0.14	0.09	1.68E-8	337.5	1.10	152	0.083
	23.1	13.485	603.15	4396.71	38.71	15.61			565	0.582	130	441.0	128	8.7	0.95	2.6E-4	30.07	94.5	0.14	0.09	1.63E-8	337.9	1.10	152	0.083
	23.2	13.485	603.15	4396.71	38.71	15.51			565	0.582	130	443.9	128	8.7	0.95	2.6E-4	30.07	94.6	0.14	0.09	1.62E-8	338.0	1.10	152	0.083
	23.1	16.857	778.57	4540.16	47.29	24.19	180	820	565	0.581	130	459.2	128	8.6	0.90	2.6E-4	30.01	94.3	0.14	0.09	2.54E-8	336.7	1.10	152	0.134
	23.3	16.857	778.58	4540.27	47.30	24.00			565	0.581	130	462.9	128	8.6	0.90	2.6E-4	30.02	94.3	0.14	0.09	2.52E-8	337.1	1.10	152	0.134
	23.4	16.857	778.58	4540.22	47.30	23.90			565	0.581	130	464.9	128	8.7	0.91	2.6E-4	30.03	94.3	0.14	0.09	2.50E-8	337.2	1.10	152	0.134
PR - 1.3 %	23.4	10.48	455.64	4273.80	31.36	7.96	110	480	566	0.689	183	507.8	180	10.3	0.99	2.6E-4	35.65	112.0	0.14	0.09	2.52E-8	337.0			
	23.5	10.48	455.64	4273.80	31.36	7.86			566	0.689	183	514.3	180	10.3	1.00	2.6E-4	35.66	112.0	0.14	0.09	2.50E-8	337.2			
	23.6	10.48	455.63	4273.71	31.35	7.75			566	0.689	184	521.3	181	10.3	1.02	2.6E-4	35.66	112.0	0.14	0.09	2.48E-8	337.8			
	23.4	14.76	660.74	4400.46	38.94	15.54	160	700	566	0.691	183	531.4	180	10.3	1.04	2.6E-4	35.65	112.0	0.14	0.09	8.19E-9	414.7	1.31	153	0.049
	23.3	14.76	660.73	4400.39	38.93	15.63			566	0.691	183	528.1	180	10.3	1.03	2.6E-4	35.65	112.0	0.14	0.09	8.17E-9	414.5	1.31	153	0.049
	23.2	14.76	660.71	4400.26	38.92	15.72			566	0.691	183	528.0	180	10.3	1.03	2.6E-4	35.64	112.0	0.14	0.09	8.15E-9	414.3	1.31	153	0.049
	23.4	18.39	849.74	4542.11	47.41	24.01	190	890	566	0.690	183	551.0	180	10.3	1.08	2.6E-4	35.66	112.0	0.14	0.09	2.47E-8	414.5	1.30	153	0.159
	23.5	18.41	849.76	4542.16	47.42	23.62			566	0.690	183	560.7	180	10.3	1.10	2.6E-4	35.66	111.9	0.14	0.09	2.45E-8	414.3	1.30	153	0.159
	23.5	18.38	849.77	4542.14	47.47	24.07			566	0.690	183	549.4	180	10.3	1.07	2.6E-4	35.66	111.9	0.14	0.09	2.43E-8	414.1	1.30	153	0.159
	23.4	11.59	504.82	4281.61	31.83	8.43	130	540	566	0.797	244	587.7	180	11.9	1.15	2.6E-4	41.12	129.2	0.14	0.09	2.51E-9	631.6	1.51	155	0.060
	23.5	11.59	504.81	4281.52	31.82	8.32			566	0.797	244	595.2	240	11.9	1.16	2.6E-4	41.13	129.2	0.14	0.09	2.49E-9	632.3	1.51	155	0.060
	23.6	11.59	504.80	4281.44	31.82	8.22			566	0.797	244	602.8	240	11.9	1.18	2.6E-4	41.13	129.2	0.14	0.09	2.47E-9	632.3	1.51	155	0.060
	23.4	16.48	739.93	4413.54	39.72	16.32	180	780	566	0.796	243	632.6	239	11.9	1.24	2.6E-4	41.07	129.0	0.14	0.09	4.89E-9	630.0	1.50	155	0.124
	23.5	16.47	739.90	4416.04	39.87	16.37			566	0.796	243	630.2	239	11.9	1.23	2.6E-4	41.08	129.0	0.14	0.09	4.90E-9	630.3	1.50	155	0.124
	23.5	16.48	739.83	4413.54	39.72	16.22			566	0.796	243	636.5	239	11.9	1.24	2.6E-4	41.08	129.0	0.14	0.09	4.88E-9	630.3	1.50	155	0.124
	23.5	20.10	927.50	4536.47	47.07	23.57	210	970	566	0.796	243	669.6	239	11.9	1.31	2.6E-4	41.08	129.0	0.14	0.09	7.05E-9	630.3	1.50	155	0.190
	23.5	20.10	927.70	4536.96	47.10	23.60			566	0.796	243	668.8	239	11.9	1.31	2.6E-4	41.08	129.0	0.14	0.09	7.06E-9	630.3	1.50	155	0.190
	23.5	20.10	927.70	4536.96	47.10	23.60			566	0.796	243	669.1	239	11.9	1.31	2.6E-4	41.08	129.0	0.14	0.09	7.06E-9	630.3	1.50	155	0.190

normata		normata		normata		normata		normata		normata			
PR	PR	PR	PR	PR	PR	PR	PR	PR	PR	PR	PR		
1 ~ 564 Hz	3.43E-4	2.60E-4	-8.4E-4	0.094	6.86E-4	-0.032	0.030	0.064	7.73	0.050	-8.5E-4	6.04E-3	5.04
$L = 47 \text{ cm}$	3.43E-4	2.60E-4	-8.4E-4	0.094	6.86E-4	-0.032	0.030	0.065	7.82	0.050	-8.4E-4	6.04E-3	5.04
PR - 0.9 %	3.43E-4	2.60E-4	-8.4E-4	0.094	6.86E-4	-0.032	0.030	0.065	7.82	0.050	-8.4E-4	6.04E-3	5.04
2.45E-4	2.60E-4	<b>6.8E-4</b>	<b>0.077</b>	<b>4.89E-4</b>	<b>-0.014</b>	<b>0.030</b>	<b>0.032</b>	<b>4.57</b>	<b>0.050</b>	<b>-8.5E-4</b>	<b>6.04E-3</b>	<b>5.04</b>	
2.45E-4	2.60E-4	<b>6.8E-4</b>	<b>0.077</b>	<b>4.89E-4</b>	<b>-0.014</b>	<b>0.030</b>	<b>0.032</b>	<b>4.59</b>	<b>0.050</b>	<b>-8.4E-4</b>	<b>6.04E-3</b>	<b>5.04</b>	
2.45E-4	2.60E-4	<b>6.8E-4</b>	<b>0.077</b>	<b>4.89E-4</b>	<b>-0.014</b>	<b>0.030</b>	<b>0.032</b>	<b>4.59</b>	<b>0.050</b>	<b>-8.4E-4</b>	<b>6.04E-3</b>	<b>5.04</b>	
2.04E-4	2.60E-4	<b>6.1E-4</b>	<b>0.070</b>	<b>4.07E-4</b>	<b>-0.009</b>	<b>0.030</b>	<b>0.021</b>	<b>3.77</b>	<b>0.050</b>	<b>-8.4E-4</b>	<b>6.05E-3</b>	<b>5.04</b>	
2.04E-4	2.60E-4	<b>6.1E-4</b>	<b>0.070</b>	<b>4.07E-4</b>	<b>-0.009</b>	<b>0.030</b>	<b>0.021</b>	<b>3.77</b>	<b>0.050</b>	<b>-8.4E-4</b>	<b>6.05E-3</b>	<b>5.04</b>	
2.04E-4	2.60E-4	<b>6.1E-4</b>	<b>0.070</b>	<b>4.07E-4</b>	<b>-0.009</b>	<b>0.030</b>	<b>0.021</b>	<b>3.77</b>	<b>0.050</b>	<b>-8.4E-4</b>	<b>6.05E-3</b>	<b>5.04</b>	
PR - 1.1 %	3.09E-4	2.60E-4	<b>7.8E-4</b>	<b>0.098</b>	<b>6.19E-4</b>	<b>-0.029</b>	<b>0.030</b>	<b>0.062</b>	<b>7.71</b>	<b>0.050</b>	<b>-8.4E-4</b>	<b>5.07E-3</b>	<b>5.03</b>
3.09E-4	2.60E-4	<b>7.8E-4</b>	<b>0.098</b>	<b>6.19E-4</b>	<b>-0.029</b>	<b>0.030</b>	<b>0.063</b>	<b>7.59</b>	<b>0.050</b>	<b>-8.4E-4</b>	<b>5.07E-3</b>	<b>5.03</b>	
3.09E-4	2.60E-4	<b>7.8E-4</b>	<b>0.098</b>	<b>6.19E-4</b>	<b>-0.030</b>	<b>0.030</b>	<b>0.064</b>	<b>7.67</b>	<b>0.050</b>	<b>-8.4E-4</b>	<b>5.07E-3</b>	<b>5.03</b>	
2.26E-4	2.60E-4	<b>6.5E-4</b>	<b>0.073</b>	<b>4.52E-4</b>	<b>-0.013</b>	<b>0.030</b>	<b>0.032</b>	<b>4.58</b>	<b>0.050</b>	<b>-8.4E-4</b>	<b>5.07E-3</b>	<b>5.03</b>	
2.26E-4	2.60E-4	<b>6.5E-4</b>	<b>0.073</b>	<b>4.52E-4</b>	<b>-0.013</b>	<b>0.030</b>	<b>0.032</b>	<b>4.58</b>	<b>0.050</b>	<b>-8.4E-4</b>	<b>5.07E-3</b>	<b>5.03</b>	
2.26E-4	2.60E-4	<b>6.5E-4</b>	<b>0.073</b>	<b>4.52E-4</b>	<b>-0.013</b>	<b>0.030</b>	<b>0.032</b>	<b>4.57</b>	<b>0.050</b>	<b>-8.4E-4</b>	<b>5.07E-3</b>	<b>5.03</b>	
1.88E-4	2.60E-4	<b>5.9E-4</b>	<b>0.067</b>	<b>3.77E-4</b>	<b>-0.008</b>	<b>0.030</b>	<b>0.021</b>	<b>3.73</b>	<b>0.050</b>	<b>-8.4E-4</b>	<b>5.08E-3</b>	<b>5.03</b>	
1.88E-4	2.60E-4	<b>5.9E-4</b>	<b>0.067</b>	<b>3.77E-4</b>	<b>-0.008</b>	<b>0.030</b>	<b>0.021</b>	<b>3.74</b>	<b>0.050</b>	<b>-8.4E-4</b>	<b>5.08E-3</b>	<b>5.03</b>	
1.88E-4	2.60E-4	<b>5.9E-4</b>	<b>0.067</b>	<b>3.77E-4</b>	<b>-0.008</b>	<b>0.030</b>	<b>0.021</b>	<b>3.75</b>	<b>0.050</b>	<b>-8.4E-4</b>	<b>5.08E-3</b>	<b>5.03</b>	
PR ~ 1.3 %	2.79E-4	2.60E-4	<b>4.2E-3</b>	<b>0.418</b>	<b>5.59E-4</b>	<b>-0.139</b>	<b>-0.030</b>	<b>0.063</b>	<b>15.51</b>	<b>0.050</b>	<b>-8.4E-4</b>	<b>4.38E-3</b>	<b>5.02</b>
2.79E-4	2.60E-4	<b>4.2E-3</b>	<b>0.418</b>	<b>5.59E-4</b>	<b>-0.140</b>	<b>-0.030</b>	<b>0.064</b>	<b>15.69</b>	<b>0.050</b>	<b>-8.4E-4</b>	<b>4.38E-3</b>	<b>5.02</b>	
2.79E-4	2.60E-4	<b>4.2E-3</b>	<b>0.418</b>	<b>5.59E-4</b>	<b>-0.142</b>	<b>-0.030</b>	<b>0.064</b>	<b>15.69</b>	<b>0.050</b>	<b>-8.4E-4</b>	<b>4.38E-3</b>	<b>5.02</b>	
2.11E-4	2.60E-4	<b>3.1E-3</b>	<b>0.308</b>	<b>4.23E-4</b>	<b>-0.055</b>	<b>-0.030</b>	<b>0.032</b>	<b>7.06</b>	<b>0.050</b>	<b>-8.4E-4</b>	<b>4.38E-3</b>	<b>5.02</b>	
2.11E-4	2.60E-4	<b>3.1E-3</b>	<b>0.308</b>	<b>4.23E-4</b>	<b>-0.056</b>	<b>-0.030</b>	<b>0.032</b>	<b>7.03</b>	<b>0.050</b>	<b>-8.4E-4</b>	<b>4.38E-3</b>	<b>5.02</b>	
2.11E-4	2.60E-4	<b>3.1E-3</b>	<b>0.308</b>	<b>4.23E-4</b>	<b>-0.055</b>	<b>-0.030</b>	<b>0.032</b>	<b>7.00</b>	<b>0.050</b>	<b>-8.4E-4</b>	<b>4.38E-3</b>	<b>5.02</b>	
1.78E-4	2.60E-4	<b>2.5E-3</b>	<b>0.254</b>	<b>3.55E-4</b>	<b>-0.031</b>	<b>-0.030</b>	<b>0.021</b>	<b>4.81</b>	<b>0.050</b>	<b>-8.4E-4</b>	<b>4.37E-3</b>	<b>5.02</b>	
1.78E-4	2.60E-4	<b>2.5E-3</b>	<b>0.255</b>	<b>3.55E-4</b>	<b>-0.031</b>	<b>-0.030</b>	<b>0.021</b>	<b>4.85</b>	<b>0.050</b>	<b>-8.4E-4</b>	<b>4.37E-3</b>	<b>5.02</b>	
1.78E-4	2.60E-4	<b>2.5E-3</b>	<b>0.254</b>	<b>3.55E-4</b>	<b>-0.031</b>	<b>-0.030</b>	<b>0.021</b>	<b>4.82</b>	<b>0.050</b>	<b>-8.4E-4</b>	<b>4.37E-3</b>	<b>5.02</b>	
1.95E-4	2.60E-4	<b>3.8E-3</b>	<b>0.382</b>	<b>5.16E-4</b>	<b>-0.120</b>	<b>-0.030</b>	<b>0.059</b>	<b>13.71</b>	<b>0.050</b>	<b>-8.4E-4</b>	<b>3.86E-3</b>	<b>5.02</b>	
1.95E-4	2.60E-4	<b>3.8E-3</b>	<b>0.382</b>	<b>5.16E-4</b>	<b>-0.121</b>	<b>-0.030</b>	<b>0.060</b>	<b>13.87</b>	<b>0.050</b>	<b>-8.4E-4</b>	<b>3.86E-3</b>	<b>5.02</b>	
1.95E-4	2.60E-4	<b>3.8E-3</b>	<b>0.382</b>	<b>5.16E-4</b>	<b>-0.123</b>	<b>-0.030</b>	<b>0.061</b>	<b>14.03</b>	<b>0.050</b>	<b>-8.4E-4</b>	<b>3.86E-3</b>	<b>5.02</b>	
1.95E-4	2.60E-4	<b>3.8E-3</b>	<b>0.382</b>	<b>5.16E-4</b>	<b>-0.123</b>	<b>-0.030</b>	<b>0.061</b>	<b>13.87</b>	<b>0.050</b>	<b>-8.4E-4</b>	<b>3.86E-3</b>	<b>5.02</b>	
1.68E-4	2.60E-4	<b>2.3E-3</b>	<b>0.236</b>	<b>3.36E-4</b>	<b>-0.030</b>	<b>-0.030</b>	<b>0.021</b>	<b>4.71</b>	<b>0.050</b>	<b>-8.4E-4</b>	<b>3.87E-3</b>	<b>5.02</b>	
1.68E-4	2.60E-4	<b>2.3E-3</b>	<b>0.236</b>	<b>3.36E-4</b>	<b>-0.030</b>	<b>-0.030</b>	<b>0.021</b>	<b>4.71</b>	<b>0.050</b>	<b>-8.4E-4</b>	<b>3.87E-3</b>	<b>5.02</b>	
1.68E-4	2.60E-4	<b>2.3E-3</b>	<b>0.236</b>	<b>3.36E-4</b>	<b>-0.030</b>	<b>-0.030</b>	<b>0.021</b>	<b>4.71</b>	<b>0.050</b>	<b>-8.4E-4</b>	<b>3.87E-3</b>	<b>5.02</b>	

Experiment Information	T <sub>a</sub> (C)	PR Volt (mV)	Wire R <sub>q</sub> (mΩ)	I <sub>q</sub> (mA)	T <sub>g</sub> (C)	T <sub>g</sub> (mV)	Our V <sub>q</sub> (mV)	Freq (Hz)	mic V <sub>q</sub> (mV)	R <sub>q</sub> (Ω)	h (W/m <sup>2</sup> K)	Cor R <sub>q</sub> (mΩ)	KC (mΩ)	KA (mΩ)	KA (mΩ)	S (mΩ)	KC (mΩ)	KA (mΩ)	KA (mΩ)	Grid		PR %	SPL (dB)	Power (W)	
																				R <sub>q</sub> (mΩ)	R <sub>q</sub> (mΩ)	R <sub>q</sub> (mΩ)			
1 ~ 564 Hz	23.6	12.10	526.39	4276.37	31.51	7.91	130	560	866	0.902	313	681.3	308	134	1.33	2.6E-4	46.55	146.3	0.14	0.09	1.43E-9	809.8	1.70	156	0.065
L = 47 cm	23.5	12.10	626.40	4276.46	31.52	8.02	130	560	566	0.902	313	672.4	307	134	1.31	2.6E-4	46.55	146.2	0.14	0.09	1.45E-9	809.4	1.70	156	0.065
PR ~ 1.7%	23.4	12.10	526.40	4276.46	31.52	8.12	130	560	568	0.902	313	684.1	307	134	1.30	2.6E-4	46.54	146.2	0.14	0.09	1.47E-9	808.9	1.70	156	0.065
23.6	17.63	792.22	4417.20	39.94	16.34	180	830	566	0.902	313	723.7	308	134	1.41	2.6E-4	46.55	146.3	0.14	0.09	2.96E-9	809.8	1.70	156	0.142	
23.5	17.64	792.23	4414.75	39.79	16.29	180	830	566	0.902	313	726.2	307	134	1.42	2.6E-4	46.54	146.2	0.14	0.09	2.98E-9	809.4	1.70	156	0.142	
23.4	17.64	792.22	4414.70	39.79	16.39	180	830	566	0.902	313	721.6	307	134	1.41	2.6E-4	46.54	146.2	0.14	0.09	2.98E-9	808.9	1.70	156	0.142	
24.1	21.37	989.72	4552.62	48.04	23.94	220	130	566	0.903	314	747.9	309	135	1.46	2.6E-4	46.64	146.5	0.14	0.09	4.29E-9	813.8	1.71	156	0.215	
24.0	21.36	989.72	4554.75	48.17	24.17	220	130	566	0.903	314	740.6	309	135	1.45	2.6E-4	46.64	146.5	0.14	0.09	4.33E-9	813.4	1.71	156	0.215	
24.0	21.37	989.73	4552.67	48.04	24.04	220	130	566	0.903	314	744.8	309	135	1.46	2.6E-4	46.64	146.5	0.14	0.09	4.31E-9	813.4	1.71	156	0.215	
PR ~ 19 %	23.8	12.786	556.96	4281.96	31.85	8.05	140	590	566	1.009	392	749.0	385	150	1.46	2.6E-4	52.09	163.7	0.14	0.09	9.28E-10	1014.5	1.91	157	0.072
23.7	12.786	556.96	4281.96	31.85	8.15	140	590	566	1.009	391	739.8	385	150	1.45	2.6E-4	52.08	163.6	0.14	0.09	9.41E-10	1013.9	1.91	157	0.072	
23.6	12.785	556.96	4282.30	31.87	8.27	140	590	566	1.009	391	729.0	385	150	1.42	2.6E-4	52.08	163.6	0.14	0.09	9.57E-10	1013.4	1.91	157	0.072	
23.7	18.32	822.62	4413.95	39.74	16.04	190	860	566	1.008	391	795.2	384	150	1.55	2.6E-4	52.08	163.6	0.14	0.09	9.42E-10	1013.9				
23.6	18.31	822.66	4416.57	39.90	16.30	190	860	566	1.008	391	782.3	384	150	1.53	2.6E-4	52.03	163.5	0.14	0.09	1.86E-9	1011.9	1.91	157	0.153	
23.5	18.31	822.61	4416.31	39.88	16.38	190	860	566	1.008	390	778.2	384	150	1.52	2.6E-4	52.02	163.4	0.14	0.09	1.91E-9	1010.8	1.91	157	0.153	
22.7	22.20	1023.50	4531.98	46.80	24.10	230	1070	566	1.011	392	798.0	385	150	1.56	2.6E-4	52.10	163.7	0.14	0.09	2.80E-9	1012.3	1.91	157	0.231	
22.7	22.22	1023.60	4528.35	46.59	23.89	230	1070	566	1.011	392	806.1	385	150	1.53	2.6E-4	52.02	163.4	0.14	0.09	2.78E-9	1012.3	1.91	157	0.231	
22.7	22.23	1023.60	4526.31	46.46	23.76	230	1070	566	1.011	392	804.9	385	150	1.58	2.6E-4	52.10	163.7	0.14	0.09	2.78E-9	1012.3	1.91	157	0.231	
PR ~ 21 %	25.0	13.21	577.75	4299.23	32.88	7.88	140	610	567	1.117	481	819.8	473	167	1.60	2.6E-4	52.10	163.7	0.14	0.09	6.00E-9	1245.4	2.11	158	0.078
24.8	13.21	577.75	4299.23	32.88	8.03	140	610	567	1.117	481	799.5	473	167	1.56	2.6E-4	57.68	181.2	0.14	0.09	6.17E-10	1244.0	2.11	158	0.078	
24.7	13.21	577.74	4299.16	32.88	8.18	140	610	567	1.117	481	790.1	473	167	1.54	2.6E-4	57.66	181.1	0.14	0.09	6.25E-10	1243.0	2.11	158	0.078	
24.8	18.65	840.02	4427.56	40.56	15.66	200	880	567	1.117	481	847.0	473	167	1.65	2.6E-4	57.67	181.2	0.14	0.09	6.14E-10	1244.2				
24.6	18.64	840.01	4429.86	40.70	15.90	200	880	567	1.117	481	833.8	473	167	1.63	2.6E-4	57.66	181.2	0.14	0.09	6.27E-10	1244.7	2.11	158	0.159	
24.8	18.65	840.01	4427.51	40.55	15.75	200	880	567	1.117	481	841.8	473	167	1.64	2.6E-4	57.66	181.2	0.14	0.09	6.20E-9	1244.0	2.11	158	0.159	
24.9	22.94	1064.84	4562.94	48.65	23.65	240	1110	567	1.117	481	874.2	473	167	1.71	2.6E-4	57.68	181.2	0.14	0.09	1.80E-9	1245.4	2.11	158	0.248	
24.9	22.95	1064.90	4561.21	48.55	23.65	240	1110	567	1.117	481	875.6	473	167	1.71	2.6E-4	57.67	181.2	0.14	0.09	1.80E-9	1244.7	2.11	158	0.249	
PR ~ 2.3 %	24.8	13.76	602.04	4300.91	32.98	8.18	150	640	567	1.220	573	857.1	564	182	1.67	2.6E-4	62.98	197.9	0.14	0.09	4.39E-10	1484.0	2.31	158	0.084
24.7	13.76	602.05	4300.98	32.99	8.20	150	640	567	1.220	573	846.3	565	182	1.65	2.6E-4	62.97	197.8	0.14	0.09	4.45E-10	1483.2	2.31	158	0.084	
24.7	13.76	602.04	4300.91	32.98	8.28	150	640	567	1.220	573	846.8	565	182	1.65	2.6E-4	62.97	197.8	0.14	0.09	4.45E-10	1483.5	2.31	158	0.084	
24.7	19.18	883.73	4426.73	40.51	15.81	200	910	567	1.222	575	887.2	566	182	1.73	2.6E-4	63.07	198.2	0.14	0.09	8.43E-10	1484.1	2.31	158	0.169	
24.6	19.18	883.75	4426.83	40.51	15.91	200	910	567	1.222	575	881.3	565	182	1.72	2.6E-4	63.06	198.1	0.14	0.09	8.50E-10	1487.3	2.31	158	0.169	
24.5	19.17	883.73	4429.04	40.65	16.15	200	910	567	1.222	575	866.1	565	182	1.70	2.6E-4	63.05	198.1	0.14	0.09	8.64E-10	1486.4	2.31	158	0.168	
24.6	23.73	1102.20	4565.79	48.83	24.23	250	1150	567	1.221	574	913.9	565	182	1.72	2.6E-4	63.06	198.1	0.14	0.09	8.53E-10	1487.3				
24.6	23.72	1102.19	4567.88	48.94	24.34	250	1150	567	1.221	574	909.3	565	182	1.78	2.6E-4	63.01	198.0	0.14	0.09	1.30E-9	1484.8	2.31	158	0.266	
24.6	23.73	1102.20	4565.79	48.83	24.23	250	1150	567	1.221	574	912.4	565	182	1.78	2.6E-4	63.01	198.0	0.14	0.09	1.30E-9	1484.8	2.31	158	0.266	

Electron Information		Proton Information		Neutron Information		Gamma Information		Hadron Information		Lepton Information		Background Information	
Electron	Proton	Neutron	Gamma	Hadron	Lepton	Background	Electron	Proton	Neutron	Gamma	Hadron	Lepton	Background
1 - 564 Hz	2.50E-4	2.60E-4	0.367	5.00E-4	-0.122	-0.030	0.063	14.10	0.050	-8.4E-4	3.48E-3	5.01	
$I = 47$ cm	2.50E-4	2.60E-4	-3.7E-3	0.367	5.00E-4	-0.121	-0.030	0.062	13.93	0.050	-8.4E-4	3.48E-3	5.01
PR - 17 %	2.50E-4	2.60E-4	-3.7E-3	0.367	5.00E-4	-0.119	-0.030	0.062	13.77	0.050	-8.4E-4	3.48E-3	5.01
1.86E-4	2.60E-4	2.6E-3	0.264	3.72E-4	-0.045	-0.030	0.031	6.24	0.050	-8.4E-4	3.48E-3	5.01	
1.86E-4	2.60E-4	2.6E-3	0.264	3.72E-4	-0.045	-0.030	0.031	6.25	0.050	-8.4E-4	3.48E-3	5.01	
1.86E-4	2.60E-4	2.6E-3	0.264	3.72E-4	-0.045	-0.030	0.031	6.22	0.050	-8.4E-4	3.48E-3	5.01	
1.61E-4	2.60E-4	2.2E-3	0.224	3.22E-4	-0.028	-0.030	0.021	4.59	0.050	-8.4E-4	3.48E-3	5.01	
1.61E-4	2.60E-4	2.2E-3	0.224	3.22E-4	-0.028	-0.030	0.021	4.57	0.050	-8.4E-4	3.48E-3	5.01	
1.61E-4	2.60E-4	2.2E-3	0.224	3.22E-4	-0.028	-0.030	0.021	4.58	0.050	-8.4E-4	3.48E-3	5.01	
PR - 19 %	2.40E-4	2.60E-4	6.6E-4	0.075	4.79E-4	-0.025	-0.030	0.062	7.33	0.050	-8.4E-4	3.18E-3	5.01
2.40E-4	2.60E-4	6.6E-4	0.075	4.79E-4	-0.024	-0.030	0.061	7.25	0.050	-8.4E-4	3.18E-3	5.01	
2.40E-4	2.60E-4	6.6E-4	0.075	4.79E-4	-0.024	-0.030	0.060	7.17	0.050	-8.4E-4	3.18E-3	5.01	
1.82E-4	2.60E-4	2.5E-3	0.255	3.63E-4	-0.045	-0.030	0.031	6.21	0.050	-8.4E-4	3.18E-3	5.01	
1.82E-4	2.60E-4	2.5E-3	0.255	3.63E-4	-0.044	-0.030	0.031	6.14	0.050	-8.4E-4	3.18E-3	5.01	
1.82E-4	2.60E-4	2.5E-3	0.255	3.63E-4	-0.044	-0.030	0.031	6.16	0.050	-8.4E-4	3.18E-3	5.01	
7.95E-5	2.60E-4	2.2E-3	0.217	1.59E-4	-0.027	-0.030	0.021	4.51	0.050	-8.5E-4	3.17E-3	5.01	
7.95E-5	2.60E-4	2.2E-3	0.217	1.59E-4	-0.027	-0.030	0.021	4.53	0.050	-8.5E-4	3.17E-3	5.01	
7.95E-5	2.60E-4	2.1E-3	0.217	1.59E-4	-0.027	-0.030	0.021	4.54	0.050	-8.5E-4	3.17E-3	5.01	
1.79E-4	2.60E-4	2.5E-3	0.251	3.58E-4	-0.045	-0.030	0.032	6.28	0.050	-8.4E-4	2.93E-3	5.01	
1.79E-4	2.60E-4	2.5E-3	0.252	3.58E-4	-0.044	-0.030	0.031	6.22	0.050	-8.4E-4	2.93E-3	5.01	
1.79E-4	2.60E-4	2.5E-3	0.251	3.58E-4	-0.045	-0.030	0.032	6.26	0.050	-8.4E-4	2.93E-3	5.01	
7.88E-5	2.60E-4	2.1E-3	0.211	1.58E-4	-0.026	-0.030	0.021	4.52	0.050	-8.4E-4	2.93E-3	5.01	
7.88E-5	2.60E-4	2.1E-3	0.211	1.58E-4	-0.026	-0.030	0.021	4.53	0.050	-8.4E-4	2.93E-3	5.01	
7.88E-5	2.60E-4	2.1E-3	0.211	1.58E-4	-0.026	-0.030	0.021	4.53	0.050	-8.4E-4	2.93E-3	5.01	
1.76E-4	2.60E-4	3.3E-3	0.328	4.52E-4	-0.106	-0.030	0.061	12.62	0.050	-8.4E-4	2.73E-3	5.01	
1.76E-4	2.60E-4	3.3E-3	0.328	4.52E-4	-0.105	-0.030	0.060	12.47	0.050	-8.4E-4	2.73E-3	5.01	
1.76E-4	2.60E-4	3.3E-3	0.328	4.52E-4	-0.105	-0.030	0.060	12.48	0.050	-8.4E-4	2.73E-3	5.01	
7.81E-5	2.60E-4	2.0E-3	0.205	1.56E-4	-0.025	-0.030	0.021	4.43	0.050	-8.4E-4	2.73E-3	5.01	
7.81E-5	2.60E-4	2.0E-3	0.205	1.56E-4	-0.025	-0.030	0.021	4.42	0.050	-8.4E-4	2.73E-3	5.01	
7.81E-5	2.60E-4	2.0E-3	0.205	1.56E-4	-0.025	-0.030	0.021	4.43	0.050	-8.4E-4	2.73E-3	5.01	



Experiment Information		WFOV Ref. uncert.	PR Ref. uncert.	WFOV uncert. (%)	WFOV Ref. uncert.	WFOV uncert. (%)	WFOV Ref. uncert.	WFOV uncert. (%)	WFOV Ref. uncert.	WFOV uncert. (%)	WFOV Ref. uncert.	WFOV uncert. (%)	
$f \sim 1213$ Hz	9.92E-5	2.60E-4	-5.1E-4	0.058	1.98E-4	-0.022	-0.030	0.062	7.18	0.020	-8.4E-4	6.05E-3	2.09
$L = 84$ cm	9.92E-5	2.60E-4	-5.1E-4	0.058	1.98E-4	-0.022	-0.030	0.062	7.18	0.020	-8.4E-4	6.05E-3	2.09
PR ~ 0.9 %	9.92E-5	2.60E-4	-5.1E-4	0.058	1.98E-4	-0.022	-0.030	0.062	7.18	0.020	-8.4E-4	6.05E-3	2.09
	9.09E-5	2.60E-4	-3.6E-4	0.046	1.82E-4	-0.009	-0.030	0.031	4.42	0.020	-8.4E-4	6.05E-3	2.09
	9.09E-5	2.60E-4	-3.6E-4	0.046	1.82E-4	-0.009	-0.030	0.031	4.42	0.020	-8.4E-4	6.05E-3	2.09
	9.09E-5	2.60E-4	-3.6E-4	0.046	1.82E-4	-0.009	-0.030	0.031	4.42	0.020	-8.4E-4	6.05E-3	2.09
	8.71E-5	2.60E-4	-3.2E-4	0.042	1.74E-4	-0.006	-0.030	0.021	3.70	0.020	-8.4E-4	6.03E-3	2.09
	8.71E-5	2.60E-4	-3.2E-4	0.042	1.74E-4	-0.006	-0.030	0.021	3.71	0.020	-8.4E-4	6.03E-3	2.09
	8.71E-5	2.60E-4	-3.2E-4	0.042	1.74E-4	-0.006	-0.030	0.021	3.71	0.020	-8.4E-4	6.03E-3	2.09
									3.70				
PR ~ 1.1 %	9.47E-5	2.60E-4	-4.8E-4	0.056	1.89E-4	-0.022	-0.030	0.064	7.42	0.020	-8.4E-4	5.05E-3	2.06
	9.47E-5	2.60E-4	-4.8E-4	0.056	1.89E-4	-0.022	-0.030	0.064	7.43	0.020	-8.4E-4	5.05E-3	2.06
	9.47E-5	2.60E-4	-4.8E-4	0.056	1.89E-4	-0.022	-0.030	0.064	7.43	0.020	-8.4E-4	5.05E-3	2.06
									7.42				
	8.77E-5	2.60E-4	-3.2E-4	0.042	1.75E-4	-0.008	-0.030	0.032	4.47	0.020	-8.5E-4	5.05E-3	2.06
	8.77E-5	2.60E-4	-3.2E-4	0.042	1.75E-4	-0.008	-0.030	0.032	4.45	0.020	-8.5E-4	5.05E-3	2.06
	8.77E-5	2.60E-4	-3.2E-4	0.042	1.75E-4	-0.008	-0.030	0.032	4.45	0.020	-8.5E-4	5.05E-3	2.06
									4.45				
	3.38E-4	2.60E-4	-2.7E-4	0.050	6.76E-4	-0.007	-0.030	0.021	3.73	0.020	-8.5E-4	5.06E-3	2.06
	3.38E-4	2.60E-4	-2.7E-4	0.050	6.76E-4	-0.007	-0.030	0.021	3.73	0.020	-8.5E-4	5.06E-3	2.06
	3.38E-4	2.60E-4	-2.7E-4	0.050	6.76E-4	-0.007	-0.030	0.021	3.73	0.020	-8.5E-4	5.06E-3	2.06
									3.73				
PR ~ 1.3 %	9.00E-5	2.60E-4	-3.4E-4	0.044	1.80E-4	-0.016	-0.030	0.059	6.79	0.020	-8.5E-4	4.37E-3	2.05
	9.00E-5	2.60E-4	-3.4E-4	0.044	1.80E-4	-0.016	-0.030	0.060	6.87	0.020	-8.5E-4	4.37E-3	2.05
	9.00E-5	2.60E-4	-3.4E-4	0.044	1.80E-4	-0.016	-0.030	0.065	6.80	0.020	-8.5E-4	4.37E-3	2.05
									6.82				
	3.51E-4	2.60E-4	-2.1E-3	0.215	7.01E-4	-0.042	-0.030	0.031	6.01	0.020	-8.5E-4	4.36E-3	2.05
	3.51E-4	2.60E-4	-2.1E-3	0.215	7.01E-4	-0.041	-0.030	0.030	5.96	0.020	-8.5E-4	4.36E-3	2.05
	3.51E-4	2.60E-4	-2.1E-3	0.215	7.01E-4	-0.042	-0.030	0.031	5.99	0.020	-8.5E-4	4.36E-3	2.05
									5.98				
	2.97E-4	2.60E-4	-1.8E-3	0.181	5.93E-4	-0.025	-0.030	0.021	4.41	0.020	-8.5E-4	4.37E-3	2.05
	2.97E-4	2.60E-4	-1.8E-3	0.181	5.93E-4	-0.025	-0.030	0.021	4.40	0.020	-8.5E-4	4.37E-3	2.05
	2.97E-4	2.60E-4	-1.8E-3	0.181	5.93E-4	-0.025	-0.030	0.021	4.41	0.020	-8.5E-4	4.37E-3	2.05

Experiment Information	T <sub>a</sub> (C)	PR Volt (mV)	Wire Volt (mV)	Wire Resist (mΩ)	T <sub>b</sub> (C)	T <sub>c</sub> (C)	Cur (mA)	Vol (V)	Freq (Hz)	mic V (mV)	R <sub>5</sub> (Ω)	h (mm)	W/m <sup>2</sup> K	Corr	R <sub>D</sub> (Ω)	N <sub>D</sub> (D)	X	e	KC (m)	A (mm)	B (2ΔA, A) (mm)	Grid		SPL %	Power (W)			
																						R <sub>1</sub>	R <sub>2</sub>	R <sub>3</sub>	R <sub>4</sub>			
f = 1213 Hz	23.5	39.51	270.65	673.37	31.85	8.35	410	340	1213	0.795	113	433.6	113	29.6	2.12	0.001	7.66	24.1	1.93	1.23	1.74E-7	81.5	1.50	155	0.109			
L = 64 cm	23.5	39.46	270.28	673.30	31.82	8.32	413	340	1213	0.795	113	434.0	113	29.6	2.12	0.001	7.66	24.1	1.93	1.23	1.74E-7	81.5	1.50	155	0.108			
PR = 1.5 %	23.5	39.43	270.10	673.37	31.85	8.35	413	340	1213	0.795	113	431.9	113	29.6	2.11	0.001	7.66	24.1	1.93	1.23	1.74E-7	81.5	1.50	155	0.108			
												433.2	113	29.6	2.12	0.001	7.66	24.1	1.93	1.23	1.74E-7	81.5						
	23.7	52.59	369.76	691.15	39.60	15.90	540	460	1213	0.796	114	414.0	114	29.6	2.02	0.001	7.67	24.1	1.93	1.23	3.30E-7	81.8	1.50	155	0.198			
	23.7	52.60	369.74	690.98	39.53	15.83	410	340	1213	0.796	114	416.0	114	29.6	2.03	0.001	7.67	24.1	1.93	1.23	3.28E-7	81.8	1.50	155	0.198			
	23.7	52.59	369.74	691.11	39.59	15.89	410	340	1213	0.796	114	414.8	114	29.6	2.03	0.001	7.67	24.1	1.93	1.23	3.29E-7	81.8	1.50	155	0.198			
	23.8	63.66	459.70	708.84	47.76	23.96	650	560	1213	0.792	113	413.6	113	29.5	2.02	0.001	7.63	24.0	1.93	1.23	5.06E-7	81.0	1.50	155	0.298			
	23.8	63.65	459.73	710.00	47.83	24.03	650	560	1213	0.792	113	412.4	113	29.5	2.01	0.001	7.63	24.0	1.93	1.23	5.08E-7	81.0	1.50	155	0.298			
	23.8	63.59	459.64	710.53	48.06	24.26	650	560	1213	0.792	113	408.0	113	29.5	1.99	0.001	7.63	24.0	1.93	1.23	5.13E-7	81.0	1.50	155	0.297			
	PR = 1.7 %	24.3	41.09	282.02	674.68	32.42	8.12	430	350	1215	0.901	146	483.1	146	33.6	2.36	0.001	8.68	27.3	1.94	1.23	1.02E-7	104.7	1.70	156	0.118		
		24.3	41.09	282.01	674.66	32.41	8.11	430	350	1215	0.901	146	483.7	146	33.6	2.36	0.001	8.68	27.3	1.94	1.23	1.02E-7	104.7	1.70	156	0.118		
		24.3	41.09	282.01	674.66	32.41	8.11	430	350	1215	0.901	146	483.7	146	33.6	2.36	0.001	8.68	27.3	1.94	1.23	1.02E-7	104.7	1.70	156	0.118		
	24.4	56.69	398.57	692.85	40.35	15.95	580	490	1215	0.800	145	481.0	145	33.6	2.35	0.001	8.67	27.2	1.94	1.23	2.01E-7	104.7	1.70	156	0.230			
	24.4	56.67	398.57	693.10	40.45	16.05	580	490	1215	0.900	145	477.6	145	33.6	2.33	0.001	8.67	27.2	1.94	1.23	2.03E-7	104.5	1.70	156	0.230			
	24.4	56.68	398.57	692.97	40.40	16.00	580	490	1215	0.900	145	479.3	145	33.6	2.34	0.001	8.67	27.2	1.94	1.23	2.02E-7	104.5	1.70	156	0.230			
	24.4	68.14	492.77	710.88	48.21	23.81	700	600	1215	0.899	145	477.5	145	33.5	2.33	0.001	8.66	27.2	1.94	1.23	2.01E-7	104.3	1.70	156	0.342			
	24.4	68.13	492.72	710.91	48.22	23.82	700	600	1215	0.898	145	477.1	145	33.5	2.33	0.001	8.66	27.2	1.94	1.23	2.03E-7	104.3	1.70	156	0.341			
	24.4	68.09	492.67	711.26	48.37	23.97	700	600	1215	0.899	145	476.2	145	33.5	2.33	0.001	8.66	27.2	1.94	1.23	2.04E-7	104.3	1.70	156	0.341			
	24.4	68.09	492.67	711.26	48.37	23.97	700	600	1215	0.899	145	476.2	145	33.5	2.33	0.001	8.66	27.2	1.94	1.23	2.02E-7	104.3	1.70	156	0.341			
	24.4	68.09	492.67	711.26	48.37	23.97	700	600	1215	0.899	145	476.2	145	33.5	2.33	0.001	8.66	27.2	1.94	1.23	2.03E-7	104.3	1.70	156	0.341			
	24.4	68.09	492.67	711.26	48.37	23.97	700	600	1215	0.899	145	476.2	145	33.5	2.33	0.001	8.66	27.2	1.94	1.23	2.04E-7	104.3	1.70	156	0.341			
	24.4	68.09	492.67	711.26	48.37	23.97	700	600	1215	0.899	145	476.2	145	33.5	2.33	0.001	8.66	27.2	1.94	1.23	2.02E-7	104.3	1.70	156	0.341			
	24.4	68.09	492.67	711.26	48.37	23.97	700	600	1215	0.899	145	476.2	145	33.5	2.33	0.001	8.66	27.2	1.94	1.23	2.03E-7	104.3	1.70	156	0.341			
	24.4	68.09	492.67	711.26	48.37	23.97	700	600	1215	0.899	145	476.2	145	33.5	2.33	0.001	8.66	27.2	1.94	1.23	2.04E-7	104.3	1.70	156	0.341			
	24.4	68.09	492.67	711.26	48.37	23.97	700	600	1215	0.899	145	476.2	145	33.5	2.33	0.001	8.66	27.2	1.94	1.23	2.02E-7	104.3	1.70	156	0.341			
	24.4	68.09	492.67	711.26	48.37	23.97	700	600	1215	0.899	145	476.2	145	33.5	2.33	0.001	8.66	27.2	1.94	1.23	2.03E-7	104.3	1.70	156	0.341			
	24.4	68.09	492.67	711.26	48.37	23.97	700	600	1215	0.899	145	476.2	145	33.5	2.33	0.001	8.66	27.2	1.94	1.23	2.04E-7	104.3	1.70	156	0.341			
	24.4	68.09	492.67	711.26	48.37	23.97	700	600	1215	0.899	145	476.2	145	33.5	2.33	0.001	8.66	27.2	1.94	1.23	2.02E-7	104.3	1.70	156	0.341			
	24.4	68.09	492.67	711.26	48.37	23.97	700	600	1215	0.899	145	476.2	145	33.5	2.33	0.001	8.66	27.2	1.94	1.23	2.03E-7	104.3	1.70	156	0.341			
	24.4	68.09	492.67	711.26	48.37	23.97	700	600	1215	0.899	145	476.2	145	33.5	2.33	0.001	8.66	27.2	1.94	1.23	2.04E-7	104.3	1.70	156	0.341			
	24.4	68.09	492.67	711.26	48.37	23.97	700	600	1215	0.899	145	476.2	145	33.5	2.33	0.001	8.66	27.2	1.94	1.23	2.02E-7	104.3	1.70	156	0.341			
	24.4	68.09	492.67	711.26	48.37	23.97	700	600	1215	0.899	145	476.2	145	33.5	2.33	0.001	8.66	27.2	1.94	1.23	2.03E-7	104.3	1.70	156	0.341			
	24.4	68.09	492.67	711.26	48.37	23.97	700	600	1215	0.899	145	476.2	145	33.5	2.33	0.001	8.66	27.2	1.94	1.23	2.04E-7	104.3	1.70	156	0.341			
	24.4	68.09	492.67	711.26	48.37	23.97	700	600	1215	0.899	145	476.2	145	33.5	2.33	0.001	8.66	27.2	1.94	1.23	2.02E-7	104.3	1.70	156	0.341			
	24.4	68.09	492.67	711.26	48.37	23.97	700	600	1215	0.899	145	476.2	145	33.5	2.33	0.001	8.66	27.2	1.94	1.23	2.03E-7	104.3	1.70	156	0.341			
	24.4	68.09	492.67	711.26	48.37	23.97	700	600	1215	0.899	145	476.2	145	33.5	2.33	0.001	8.66	27.2	1.94	1.23	2.04E-7	104.3	1.70	156	0.341			
	24.4	68.09	492.67	711.26	48.37	23.97	700	600	1215	0.899	145	476.2	145	33.5	2.33	0.001	8.66	27.2	1.94	1.23	2.02E-7	104.3	1.70	156	0.341			
	24.4	68.09	492.67	711.26	48.37	23.97	700	600	1215	0.899	145	476.2	145	33.5	2.33	0.001	8.66	27.2	1.94	1.23	2.03E-7	104.3	1.70	156	0.341			
	24.4	68.09	492.67	711.26	48.37	23.97	700	600	1215	0.899	145	476.2	145	33.5	2.33	0.001	8.66	27.2	1.94	1.23	2.04E-7	104.3	1.70	156	0.341			
</td																												



Experiment Information	PR	Wires	Wires	Cur.	Freq.	m/s	Re	Cor.	Re(D)	Nu(D)	X	G(I)		Re	PR %	SPL (dB)	Power (W)							
												T <sub>c</sub> (K)	h	Re	Re(D)	h	δ							
T = 1213 Hz L = 64 cm PR - 2.1 %	22.6 22.6 22.6	36.665 36.665 36.665	250.4 250.6 250.5	671.33 671.87 671.60	30.96 31.20 31.08	8.36 8.60 8.48	380 320 320	1212 1212 1212	1.115 1.115 1.115	222 222 222	41.5 41.5 41.5	1.62 1.77 1.79	0.001 0.001 0.001	10.73 10.73 10.73	33.7 33.7 33.7	1.93 1.93 1.93	1.23 1.23 1.23	4.54E-8 4.67E-8 4.61E-8	160.0 160.0 160.0	2.11 2.11 2.11	158 158 158	0.093 0.093 0.093		
22.4 22.4 22.4	49.580 49.580 49.580	347.4 347.6 347.5	688.77 689.17 688.87	16.17 16.34 16.26	38.57 38.74 38.56	16.17 16.34 16.26	510 510 510	430 430 430	1212 1212 1212	1.116 1.116 1.116	223 223 223	41.5 41.5 41.5	1.76 1.74 1.75	0.001 0.001 0.001	10.74 10.74 10.74	33.7 33.7 33.7	1.93 1.93 1.93	1.23 1.23 1.23	8.77E-8 8.82E-8 8.82E-8	160.2 160.2 160.2	2.11 2.11 2.11	158 158 158	0.175 0.175 0.175	
22.2 22.2 22.2	59.646 59.646 59.646	429.3 430.2 438.9	707.51 708.99 706.85	46.74 47.39 46.45	24.54 25.19 24.25	610 610 610	530 530 530	1212 1212 1212	1.114 1.114 1.114	222 222 222	41.4 41.4 41.4	1.73 1.69 1.74	0.001 0.001 0.001	10.71 10.71 10.71	33.7 33.7 33.7	1.93 1.93 1.93	1.23 1.23 1.23	1.34E-7 1.38E-7 1.35E-7	159.5 159.5 159.5	2.11 2.11 2.11	158 158 158	0.260 0.260 0.260		
PR - 2.3 % 21.6 21.6 21.6	36.320 36.320 36.320	247.2 246.9 247.0	669.05 668.23 668.50	29.97 29.61 29.73	8.37 8.01 8.13	380 380 380	310 310 310	1210 1210 1210	1.222 1.222 1.222	267 267 267	363.4 359.0 353.7	267 267 267	45.4 45.4 45.4	1.78 1.85 1.83	0.001 0.001 0.001	11.76 11.76 11.76	36.9 36.9 36.9	1.93 1.93 1.93	1.23 1.23 1.23	3.17E-8 3.04E-8 3.08E-8	192.1 192.1 192.1	2.31 2.31 2.31	158 158 158	0.091 0.091 0.091
21.3 21.3 21.3	49.247 49.247 49.247	343.5 343.8 343.2	685.65 686.25 685.05	37.20 37.47 36.94	15.90 16.17 15.64	510 510 510	430 430 430	1210 1210 1210	1.223 1.223 1.223	267 267 267	360.1 354.6 355.8	267 267 267	45.4 45.4 45.4	1.72 1.73 1.76	0.001 0.001 0.001	11.74 11.74 11.76	37.0 37.0 37.0	1.93 1.93 1.93	1.23 1.23 1.23	6.03E-8 6.13E-8 5.93E-8	192.2 192.2 192.2	2.31 2.31 2.31	158 158 158	0.172 0.172 0.172
21.1 21.1 21.1	59.127 59.127 59.127	423.6 422.6 423.8	704.24 702.58 704.58	45.32 44.59 45.46	24.22 24.39 24.36	610 610 610	520 520 520	1210 1210 1210	1.221 1.221 1.221	266 266 266	350.2 345.3 345.3	266 266 266	45.3 45.3 45.3	1.71 1.76 1.72	0.001 0.001 0.001	11.74 11.74 11.74	36.9 36.9 36.9	1.93 1.93 1.93	1.23 1.23 1.23	9.26E-8 8.99E-8 9.32E-8	191.4 191.4 191.4	2.31 2.31 2.31	158 158 158	0.254 0.254 0.254
PR - 2.5 % 21.2 21.2 21.2	37.657 37.657 37.657	255.6 255.8 255.9	667.22 667.74 668.00	29.17 29.40 29.51	7.97 8.20 8.31	390 390 390	320 320 320	1210 1210 1210	1.324 1.324 1.324	313 313 313	409.0 388.0 382.7	313 313 313	49.1 49.1 49.1	1.94 1.92 1.92	0.001 0.001 0.001	12.73 12.73 12.73	40.0 40.0 40.0	1.93 1.93 1.93	1.23 1.23 1.23	2.20E-8 2.26E-8 2.30E-8	225.1 225.1 225.1	2.50 2.50 2.50	159 159 159	0.098 0.098 0.098
21.4 21.4 21.4	44.201 44.201 44.201	304.3 303.9 304.3	676.74 675.85 676.74	33.32 32.93 33.32	11.92 11.63 11.32	460 460 460	380 380 380	1210 1210 1210	1.324 1.324 1.324	313 313 313	392.0 394.4 382.0	313 313 313	49.1 49.1 49.1	1.87 1.87 1.87	0.001 0.001 0.001	12.74 12.74 12.74	40.0 40.0 40.0	1.93 1.93 1.93	1.23 1.23 1.23	3.29E-8 3.18E-8 3.29E-8	225.3 225.3 225.3	2.50 2.50 2.50	159 159 159	0.137 0.137 0.137
21.5 21.5 21.5	50.408 50.408 50.408	351.3 351.5 351.2	685.07 685.46 684.87	36.95 37.12 36.87	15.45 15.62 15.37	520 520 520	430 430 430	1210 1210 1210	1.325 1.325 1.325	313 313 313	368.1 364.1 390.1	313 313 313	49.2 49.2 49.2	1.90 1.88 1.91	0.001 0.001 0.001	12.75 12.75 12.75	40.1 40.1 40.1	1.93 1.93 1.93	1.23 1.23 1.23	4.24E-8 4.29E-8 4.22E-8	225.7 225.7 225.7	2.50 2.50 2.50	159 159 159	0.180 0.180 0.180
21.6	50.408	351.2	684.87	36.87	15.37	387.4	387.4	1210	1.325	313	392.0	313	49.2	1.88	0.001	12.75	40.1	1.93	1.23	4.25E-8	225.7	2.50	159	0.180

Experiment Information	Wavelength	PR Res.	PR Uncert.	WFR		WFR		WFR		WFR		WFR		WFR	
				Vol.	uncert.	Vol.	uncert.	Vol.	uncert.	Vol.	uncert.	Vol.	uncert.	Vol.	uncert.
1 - 1213 Hz	9.00E-5	2.60E-4	4.6E-4	0.054	1.80E-4	0.019	-0.030	6.96	0.020	-8.5E-4	2.95E-3	2.02			
L = 64 cm	9.00E-5	2.60E-4	4.6E-4	0.054	1.80E-4	0.019	-0.030	6.81	0.020	-8.5E-4	2.93E-3	2.02			
PR - 2.1 %	9.00E-5	2.60E-4	4.6E-4	0.054	1.80E-4	0.019	-0.030	6.68	0.020	-8.5E-4	2.93E-3	2.02			
8.44E-5	2.60E-4	4.3E-4	0.051	1.69E-4	0.010	-0.030	0.031	4.42	0.020	-8.5E-4	2.93E-3	2.02			
8.44E-5	2.60E-4	4.3E-4	0.051	1.69E-4	0.010	-0.030	0.031	4.40	0.020	-8.5E-4	2.93E-3	2.02			
8.44E-5	2.60E-4	4.3E-4	0.051	1.69E-4	0.010	-0.030	0.031	4.41	0.020	-8.5E-4	2.93E-3	2.02			
8.16E-5	2.60E-4	4.2E-4	0.050	1.63E-4	-0.007	-0.030	0.020	3.69	0.020	-8.5E-4	2.93E-3	2.02			
8.16E-5	2.60E-4	4.2E-4	0.050	1.63E-4	-0.007	-0.030	0.020	3.66	0.020	-8.5E-4	2.93E-3	2.02			
8.17E-5	2.60E-4	4.2E-4	0.050	1.63E-4	-0.007	-0.030	0.021	3.70	0.020	-8.5E-4	2.93E-3	2.02			
PR - 2.3 %	9.03E-5	2.60E-4	4.6E-4	0.054	1.80E-4	-0.019	-0.030	0.060	6.96	0.020	-8.5E-4	2.73E-3	2.02		
9.03E-5	2.60E-4	4.6E-4	0.054	1.81E-4	-0.020	-0.030	0.062	7.21	0.020	-8.5E-4	2.73E-3	2.02			
9.02E-5	2.60E-4	4.6E-4	0.054	1.80E-4	-0.020	-0.030	0.062	7.12	0.020	-8.5E-4	2.73E-3	2.02			
8.46E-5	2.60E-4	4.3E-4	0.051	1.69E-4	-0.010	-0.030	0.031	4.46	0.020	-8.5E-4	2.73E-3	2.02			
8.45E-5	2.60E-4	4.3E-4	0.051	1.68E-4	-0.010	-0.030	0.031	4.42	0.020	-8.5E-4	2.73E-3	2.02			
8.46E-5	2.60E-4	4.3E-4	0.051	1.69E-4	-0.010	-0.030	0.032	4.50	0.020	-8.5E-4	2.73E-3	2.02			
8.18E-5	2.60E-4	4.2E-4	0.050	1.64E-4	-0.007	-0.030	0.021	3.71	0.020	-8.5E-4	2.73E-3	2.02			
8.18E-5	2.60E-4	4.2E-4	0.050	1.64E-4	-0.007	-0.030	0.021	3.74	0.020	-8.5E-4	2.73E-3	2.02			
8.18E-5	2.60E-4	4.2E-4	0.050	1.64E-4	-0.007	-0.030	0.021	3.70	0.020	-8.5E-4	2.73E-3	2.02			
PR - 2.5 %	8.96E-5	2.60E-4	4.6E-4	0.053	1.79E-4	-0.020	-0.030	0.063	7.24	0.020	-8.5E-4	2.56E-3	2.02		
8.95E-5	2.60E-4	4.6E-4	0.053	1.79E-4	-0.019	-0.030	0.061	7.07	0.020	-8.5E-4	2.56E-3	2.02			
8.95E-5	2.60E-4	4.6E-4	0.053	1.79E-4	-0.019	-0.030	0.060	6.99	0.020	-8.5E-4	2.56E-3	2.02			
8.64E-5	2.60E-4	4.4E-4	0.052	1.73E-4	-0.013	-0.030	0.042	5.33	0.020	-8.5E-4	2.56E-3	2.02			
8.65E-5	2.60E-4	4.4E-4	0.052	1.73E-4	-0.014	-0.030	0.043	5.45	0.020	-8.5E-4	2.56E-3	2.02			
8.64E-5	2.60E-4	4.4E-4	0.052	1.73E-4	-0.013	-0.030	0.042	5.33	0.020	-8.5E-4	2.56E-3	2.02			
8.42E-5	2.60E-4	4.3E-4	0.051	1.68E-4	-0.010	-0.030	0.032	4.53	0.020	-8.5E-4	2.56E-3	2.02			
8.42E-5	2.60E-4	4.3E-4	0.051	1.68E-4	-0.010	-0.030	0.032	4.51	0.020	-8.5E-4	2.56E-3	2.02			
8.42E-5	2.60E-4	4.3E-4	0.051	1.68E-4	-0.010	-0.030	0.033	4.55	0.020	-8.5E-4	2.56E-3	2.02			

Experiment Information	PR (mV)	Wire Volt (mV)	Wire Res (mΩ)	T <sub>a</sub> (C)	T <sub>b</sub> (mV)	T <sub>c</sub> (mV)	Cur (mA)	Vol (mV)	f <sub>RFQ</sub> (Hz)	mic Y	R <sub>a</sub> (mΩ)	h (W/m <sup>2</sup> K)	Cor (m)	K <sub>C</sub> (N/m)	K <sub>A</sub> (N/m)	G <sub>RD</sub> (2A/m)	R <sub>s</sub> (mΩ)	R <sub>sRs</sub> (A)	R <sub>s</sub> (mΩ)	PR %	SPL (dB)	Power (W)			
1- 1053 Hz L = 58 cm PR ~ 0.9 %	20.2	25.7579	174.206	664.82	28.12	7.92	270	230	1045	0.479	47	191.8	47	17.7	0.94	0.001	5.33	16.7	1.67	1.66	9.81E-7	36.3	0.91	150	0.046
	20.2	25.7563	174.204	664.86	28.14	7.94			1045	0.479	47	191.4	47	17.7	0.93	0.001	5.33	16.7	1.67	1.66	9.83E-7	36.3	0.91	150	0.046
	20.2	25.7558	174.189	664.81	28.12	7.92			1045	0.479	47	191.8	47	17.7	0.94	0.001	5.33	16.7	1.67	1.66	9.81E-7	36.3	0.91	150	0.046
20.2	35.124	244.101	683.15	36.12	15.92	360	310	1045	0.479	47	182.4	47	17.7	0.89	0.001	5.33	16.7	1.67	1.66	1.97E-6	36.3	0.91	150	0.087	
	20.2	35.122	244.064	683.17	36.13	15.93			1045	0.479	47	182.3	47	17.7	0.89	0.001	5.33	16.7	1.67	1.66	1.97E-6	36.3	0.91	150	0.087
	20.2	35.121	244.088	683.18	36.13	15.93			1045	0.479	47	182.2	47	17.7	0.89	0.001	5.33	16.7	1.67	1.66	1.97E-6	36.3	0.91	150	0.087
20.2	42.061	299.842	700.76	43.79	23.59	430	370	1045	0.480	47	181.0	47	17.8	0.88	0.001	5.34	16.8	1.67	1.66	2.90E-6	36.4	0.91	150	0.128	
	20.2	42.060	299.837	700.76	43.80	23.60			1045	0.480	47	181.0	47	17.8	0.88	0.001	5.34	16.8	1.67	1.66	2.90E-6	36.4	0.91	150	0.128
	20.2	42.059	299.825	700.75	43.79	23.59			1045	0.480	47	181.0	47	17.8	0.88	0.001	5.34	16.8	1.67	1.66	2.90E-6	36.4	0.91	150	0.128
PR ~ 1.1 %	20.0	31.634	213.82	664.43	27.95	7.95	330	270	1045	0.583	70	289.1	69	21.6	1.41	0.001	6.48	20.4	1.67	1.66	4.50E-7	53.6	1.10	152	0.069
	20.0	31.628	213.79	664.46	27.97	7.97			1045	0.583	70	287.4	69	21.6	1.40	0.001	6.48	20.4	1.67	1.66	4.51E-7	53.6	1.10	152	0.069
	20.0	31.628	213.79	664.46	27.97	7.97			1045	0.583	70	287.4	69	21.6	1.41	0.001	6.48	20.4	1.67	1.66	4.51E-7	53.6	1.10	152	0.069
20.0	42.760	286.99	682.74	35.94	15.94	440	370	1045	0.584	70	259.8	69	21.6	1.32	0.001	6.49	20.4	1.67	1.66	8.96E-7	53.8	1.10	152	0.129	
	20.0	42.759	286.98	682.74	35.94	15.94			1045	0.584	70	269.8	69	21.6	1.32	0.001	6.49	20.4	1.67	1.66	8.96E-7	53.8	1.10	152	0.129
	20.0	42.759	286.98	682.74	35.94	15.94			1045	0.584	70	269.8	69	21.6	1.32	0.001	6.49	20.4	1.67	1.66	8.96E-7	53.8	1.10	152	0.129
20.0	51.208	325.20	701.05	43.92	23.92	530	450	1045	0.584	70	264.7	69	21.6	1.29	0.001	6.49	20.4	1.67	1.66	1.35E-6	53.8	1.10	152	0.190	
	20.0	51.198	325.14	701.07	43.93	23.93			1045	0.584	70	264.5	69	21.6	1.29	0.001	6.49	20.4	1.67	1.66	1.35E-6	53.8	1.10	152	0.190
	20.0	51.192	325.09	701.05	43.92	23.92			1045	0.584	70	264.6	69	21.6	1.29	0.001	6.49	20.4	1.67	1.66	1.35E-6	53.8	1.10	152	0.190
PR ~ 1.3 %	20.2	36.803	249.323	665.94	28.61	8.41	380	320	1045	0.690	98	365.5	97	25.6	1.80	0.001	7.67	24.1	1.67	1.66	2.42E-7	75.2	1.30	153	0.093
	20.2	36.798	249.284	665.96	28.62	8.42			1045	0.690	98	365.5	97	25.5	1.80	0.001	7.67	24.1	1.67	1.66	2.42E-7	75.2	1.30	153	0.093
	20.2	36.794	249.282	665.99	28.63	8.43			1045	0.690	98	365.3	97	25.5	1.80	0.001	7.67	24.1	1.67	1.66	2.42E-7	75.2	1.30	153	0.093
20.4	49.32	343.27	684.17	36.56	16.16	510	430	1045	0.690	98	354.7	97	25.6	1.73	0.001	7.67	24.1	1.67	1.66	4.63E-7	75.3	1.30	153	0.172	
	20.4	49.31	343.33	684.43	36.58	16.28			1045	0.690	98	352.2	97	25.6	1.72	0.001	7.67	24.1	1.67	1.66	4.63E-7	75.3	1.30	153	0.172
	20.4	49.31	343.30	684.37	36.65	16.25			1045	0.690	98	352.8	97	25.6	1.72	0.001	7.67	24.1	1.67	1.66	4.63E-7	75.3	1.30	153	0.172
20.4	59.67	426.22	702.15	44.40	24.00	610	520	1045	0.690	98	358.8	97	25.6	1.75	0.001	7.67	24.1	1.67	1.66	6.88E-7	75.3	1.30	153	0.259	
	20.4	59.72	426.25	701.61	44.47	23.77			1045	0.690	98	359.0	97	25.6	1.75	0.001	7.67	24.1	1.67	1.66	6.88E-7	75.3	1.30	153	0.259
	20.4	59.72	426.25	702.12	44.39	23.99			1045	0.690	98	352.6	97	25.6	1.77	0.001	7.67	24.1	1.67	1.66	6.88E-7	75.3	1.30	153	0.259
PR ~ 1.5 %	23.3	38.99	266.39	671.61	31.08	7.78	400	340	1051	0.799	132	451.8	131	29.7	2.19	0.001	8.88	27.9	1.67	1.67	1.23E-7	101.0	1.51	155	0.106
	23.3	38.97	266.30	671.73	31.14	7.84			1051	0.799	132	448.5	131	29.7	2.19	0.001	8.88	27.9	1.67	1.67	1.23E-7	101.0	1.51	155	0.106
	23.3	38.95	266.23	671.90	31.21	7.91			1051	0.799	132	444.0	131	29.7	2.17	0.001	8.88	27.9	1.67	1.67	1.23E-7	101.0	1.51	155	0.106
23.0	53.84	377.56	689.34	38.82	15.82	560	470	1051	0.801	133	435.2	131	29.8	2.13	0.001	8.90	27.9	1.67	1.67	2.47E-7	101.2	1.51	155	0.207	
	23.0	53.83	377.51	689.38	38.83	15.83			1051	0.801	133	434.6	131	29.8	2.12	0.001	8.90	27.9	1.67	1.67	2.47E-7	101.2	1.51	155	0.207
	23.0	53.85	377.66	689.40	38.84	15.84			1051	0.801	133	434.7	131	29.8	2.12	0.001	8.90	27.9	1.67	1.67	2.47E-7	101.2	1.51	155	0.207
22.6	64.88	467.04	707.61	46.79	24.19	670	570	1050	0.801	132	420.8	131	29.8	2.12	0.001	8.90	28.0	1.67	1.67	3.81E-7	101.3	1.51	155	0.308	
	22.6	64.84	467.03	708.04	46.97	24.37			1050	0.801	132	419.7	131	29.8	2.05	0.001	8.90	28.0	1.67	1.67	3.82E-7	101.3	1.51	155	0.308
	22.6	64.83	467.05	708.18	47.03	24.43			1050	0.801	132	419.6	131	29.8	2.06	0.001	8.90	28.0	1.67	1.67	3.81E-7	101.3	1.51	155	0.308

Experiment	Wire Information	Vox uncert.	IPR		Wire Vol. uncert.		Wire Vol. uncert.		Wire Vol. uncert.		Wire Vol. uncert.		Wire Vol. uncert.	
			Res. uncert.	Res. uncert.	Vol. uncert. (%)	Vol. uncert. (%)								
I ~ 1053 Hz I = 58 cm PR ~ 0.9 %	9.87E-5	2.60E-4	-5.1E-4	0.058	1.97E-4	-0.022	-0.030	0.063	7.32	0.020	-8.5E-4	6.03E-3	2.09	
	9.87E-5	2.60E-4	-5.1E-4	0.058	1.97E-4	-0.022	-0.030	0.063	7.30	0.020	-8.5E-4	6.03E-3	2.09	
	9.87E-5	2.60E-4	-5.1E-4	0.058	1.97E-4	-0.022	-0.030	0.063	7.32	0.020	-8.5E-4	6.03E-3	2.09	
	9.05E-5	2.60E-4	-3.5E-4	0.045	1.81E-4	-0.009	-0.030	0.031	4.43	0.020	-8.5E-4	6.03E-3	2.09	
PR ~ 1.1 %	9.05E-5	2.60E-4	-3.5E-4	0.045	1.81E-4	-0.009	-0.030	0.031	4.43	0.020	-8.5E-4	6.03E-3	2.09	
	8.67E-5	2.60E-4	-3.1E-4	0.041	1.73E-4	-0.006	-0.030	0.021	3.72	0.020	-8.5E-4	6.02E-3	2.09	
	8.67E-5	2.60E-4	-3.1E-4	0.041	1.73E-4	-0.006	-0.030	0.021	3.72	0.020	-8.5E-4	6.02E-3	2.09	
	8.67E-5	2.60E-4	-3.1E-4	0.041	1.73E-4	-0.006	-0.030	0.021	3.72	0.020	-8.5E-4	6.02E-3	2.09	
PR ~ 1.1 %	1.17E-4	2.60E-4	-3.9E-4	0.048	2.34E-4	-0.018	-0.030	0.063	7.20	0.020	-8.5E-4	5.06E-3	2.06	
	1.17E-4	2.60E-4	-3.9E-4	0.048	2.34E-4	-0.018	-0.030	0.063	7.18	0.020	-8.5E-4	5.06E-3	2.06	
	1.17E-4	2.60E-4	-3.9E-4	0.048	2.34E-4	-0.018	-0.030	0.063	7.18	0.020	-8.5E-4	5.06E-3	2.06	
	1.04E-4	2.60E-4	-3.0E-4	0.041	2.07E-4	-0.008	-0.030	0.031	4.42	0.020	-8.5E-4	5.05E-3	2.06	
PR ~ 1.3 %	1.04E-4	2.60E-4	-3.0E-4	0.041	2.07E-4	-0.008	-0.030	0.031	4.42	0.020	-8.5E-4	5.05E-3	2.06	
	3.34E-4	2.60E-4	-2.7E-4	0.050	6.68E-4	-0.007	-0.030	0.021	3.72	0.020	-8.5E-4	5.05E-3	2.06	
	3.34E-4	2.60E-4	-2.7E-4	0.050	6.68E-4	-0.007	-0.030	0.021	3.72	0.020	-8.5E-4	5.05E-3	2.06	
	3.34E-4	2.60E-4	-2.7E-4	0.050	6.68E-4	-0.007	-0.030	0.021	3.72	0.020	-8.5E-4	5.05E-3	2.06	
PR ~ 1.3 %	9.01E-5	2.60E-4	-3.4E-4	0.044	1.80E-4	-0.016	-0.030	0.059	6.84	0.020	-8.5E-4	5.05E-3	2.06	
	9.01E-5	2.60E-4	-3.4E-4	0.044	1.80E-4	-0.016	-0.030	0.059	6.83	0.020	-8.5E-4	5.05E-3	2.06	
	9.01E-5	2.60E-4	-3.4E-4	0.044	1.80E-4	-0.016	-0.030	0.059	6.82	0.020	-8.5E-4	5.05E-3	2.06	
	3.51E-4	2.60E-4	-2.1E-3	0.044	0.050	-0.007	-0.030	0.031	3.72	0.020	-8.5E-4	5.05E-3	2.06	
PR ~ 1.5 %	3.51E-4	2.60E-4	-2.1E-3	0.044	0.050	-0.007	-0.030	0.031	3.72	0.020	-8.5E-4	5.05E-3	2.06	
	2.95E-4	2.60E-4	-1.7E-3	0.179	5.88E-4	-0.042	-0.030	0.031	6.00	0.020	-8.5E-4	4.37E-3	2.05	
	2.95E-4	2.60E-4	-1.7E-3	0.179	5.88E-4	-0.042	-0.030	0.031	5.97	0.020	-8.5E-4	4.37E-3	2.05	
	2.95E-4	2.60E-4	-1.7E-3	0.179	5.88E-4	-0.042	-0.030	0.031	5.96	0.020	-8.5E-4	4.37E-3	2.05	
PR ~ 1.5 %	1.08E-4	2.60E-4	-2.6E-3	0.265	2.18E-4	-0.102	-0.030	0.064	12.45	0.020	-8.4E-4	3.85E-3	2.05	
	1.08E-4	2.60E-4	-2.6E-3	0.265	2.18E-4	-0.102	-0.030	0.064	12.38	0.020	-8.4E-4	3.85E-3	2.04	
	1.08E-4	2.60E-4	-2.6E-3	0.265	2.18E-4	-0.101	-0.030	0.063	12.28	0.020	-8.4E-4	3.85E-3	2.04	
	3.25E-4	2.60E-4	-1.9E-3	0.197	6.50E-4	-0.039	-0.030	0.032	5.88	0.020	-8.4E-4	3.85E-3	2.04	
PR ~ 1.5 %	3.25E-4	2.60E-4	-1.9E-3	0.197	6.50E-4	-0.039	-0.030	0.032	5.87	0.020	-8.4E-4	3.85E-3	2.04	
	3.25E-4	2.60E-4	-1.9E-3	0.197	6.50E-4	-0.039	-0.030	0.032	5.88	0.020	-8.4E-4	3.85E-3	2.04	
	2.74E-4	2.60E-4	-1.6E-3	0.166	5.48E-4	-0.023	-0.030	0.021	4.30	0.020	-8.5E-4	3.85E-3	2.04	
	2.74E-4	2.60E-4	-1.6E-3	0.166	5.48E-4	-0.023	-0.030	0.021	4.28	0.020	-8.5E-4	3.85E-3	2.04	
PR ~ 1.5 %	2.74E-4	2.60E-4	-1.6E-3	0.166	5.48E-4	-0.023	-0.030	0.020	4.28	0.020	-8.5E-4	3.85E-3	2.04	
	2.74E-4	2.60E-4	-1.6E-3	0.166	5.48E-4	-0.023	-0.030	0.020	4.28	0.020	-8.5E-4	3.85E-3	2.04	

Experiment Information	T <sub>a</sub> (C)	PR Volt (mV)	W <sub>res</sub> Res (mΩ)	W <sub>res</sub> Volt (mV)	I <sub>B</sub> (mA)	I <sub>T, A</sub> (mA)	Cur. Volt (mA)	Freq (Hz)	micV (mV)	R <sub>S</sub> (mΩ)	I <sub>Rs</sub> (mA)	W <sub>102K</sub> (mV)	Con. (mV)	R <sub>1</sub> (2.0V <sub>1</sub> )	KC (mA)	MA (mA)	E (mA)	Gr(D)	Rs/R <sub>S</sub>	PR %	SPL (dB)	Power (W)			
f = 1053 Hz	22.6	42.26	288.48	671.03	30.83	8.23	440	360	1049	0.901	168	501.7	166	33.5	2.45	0.001	10.02	3.15	1.67	1.06	7.98E-8	128.6	1.70	156	0.124
L = 58 cm	22.6	42.25	288.46	671.14	30.88	8.28	440	360	1049	0.901	168	498.5	166	33.5	2.44	0.001	10.02	3.15	1.67	1.06	8.04E-8	128.6	1.70	156	0.124
PR ~ 1 %	22.6	42.24	288.49	671.37	30.96	8.38	440	360	1049	0.901	168	492.5	166	33.5	2.41	0.001	10.02	3.15	1.67	1.06	8.14E-8	128.6	1.70	156	0.124
	22.6	56.25	364.04	688.61	38.50	15.90	580	490	1049	0.986	167	472.1	165	33.4	2.31	0.001	9.99	3.14	1.67	1.06	1.57E-7	127.8	1.70	156	0.225
	22.6	56.25	364.01	688.55	38.47	15.87	580	490	1049	0.986	167	472.8	165	33.4	2.32	0.001	9.99	3.14	1.67	1.06	1.56E-7	127.8	1.70	156	0.226
	22.6	56.26	364.02	688.45	38.43	15.83	580	490	1049	0.986	167	474.3	165	33.4	2.31	0.001	9.99	3.14	1.67	1.06	1.56E-7	127.8	1.70	156	0.226
PR ~ 1.9 %	20.8	36.255	245.8	686.45	28.83	8.03	380	310	1046	1.008	209	375.6	207	37.4	1.83	0.001	11.21	35.2	1.67	1.06	2.4E-7	126.6	1.69	156	0.344
	20.8	36.255	245.9	686.72	28.95	8.15	380	310	1046	1.008	209	370.3	207	37.4	1.81	0.001	11.21	35.2	1.67	1.06	2.4E-7	126.6	1.69	156	0.343
	20.8	36.255	246.0	686.99	29.07	8.27	380	310	1046	1.008	209	365.2	207	37.4	1.78	0.001	11.21	35.2	1.67	1.06	2.4E-7	126.6	1.69	156	0.344
PR ~ 2.1 %	20.9	49.349	343.9	685.03	36.93	16.03	510	430	1046	1.005	208	358.4	206	37.3	1.75	0.001	11.18	35.1	1.67	1.06	2.4E-7	126.6	1.69	156	0.344
	20.9	49.349	344.1	685.42	37.11	16.21	510	430	1046	1.005	208	354.8	206	37.3	1.73	0.001	11.18	35.1	1.67	1.06	2.4E-7	126.6	1.69	156	0.344
	20.9	49.349	344.2	685.62	37.19	16.29	510	430	1046	1.005	208	353.0	206	37.3	1.72	0.001	11.18	35.1	1.67	1.06	2.4E-7	126.6	1.69	156	0.344
PR ~ 2.1 %	21.1	60.108	429.3	702.10	44.38	23.28	620	530	1046	1.006	209	375.3	207	37.3	1.83	0.001	11.19	35.2	1.67	1.06	1.4E-7	160.4	1.90	157	0.173
	21.1	60.106	430.5	704.06	45.23	24.13	620	530	1046	1.006	209	363.0	207	37.3	1.77	0.001	11.19	35.2	1.67	1.06	1.5E-7	160.4	1.90	157	0.173
	21.1	60.106	429.9	703.08	44.81	23.71	620	530	1046	1.006	209	369.1	207	37.3	1.80	0.001	11.18	35.2	1.67	1.06	1.4E-7	160.4	1.90	157	0.173
PR ~ 2.1 %	21.6	34.953	237.6	668.21	29.60	8.00	360	300	1048	1.117	257	356.1	207	37.3	1.80	0.001	11.19	35.2	1.67	1.06	1.0E-7	159.8	1.67	157	0.262
	21.6	34.953	237.9	669.06	29.97	8.37	360	300	1048	1.117	257	356.4	206	37.3	1.74	0.001	11.18	35.1	1.67	1.06	1.0E-7	159.8	1.67	157	0.263
	21.6	34.953	238.0	669.34	30.09	8.49	360	300	1048	1.117	257	357.1	207	37.3	1.70	0.001	11.18	35.1	1.67	1.06	1.0E-7	159.8	1.67	157	0.263
PR ~ 2.3 %	22.1	36.275	247.0	689.33	30.09	7.99	370	320	1049	1.221	308	379.7	304	45.4	1.85	0.001	13.57	42.6	1.67	1.06	1.0E-7	159.8	1.67	157	0.084
	22.1	36.275	247.5	670.69	30.68	8.58	370	320	1049	1.221	308	354.2	304	45.4	1.73	0.001	13.57	42.6	1.67	1.06	2.32E-8	197.5	2.11	158	0.085
	22.1	36.275	247.8	671.50	31.04	8.94	370	320	1049	1.221	308	346.6	304	45.4	1.66	0.001	13.57	42.6	1.67	1.06	2.32E-8	197.5	2.11	158	0.085
PR ~ 2.3 %	22.2	41.509	286.3	678.00	33.87	11.67	430	360	1049	1.220	307	344.8	304	45.3	1.68	0.001	13.56	42.6	1.67	1.06	3.40E-8	235.2	2.31	158	0.091
	22.2	41.509	285.8	676.82	33.36	11.16	430	360	1049	1.220	307	360.1	304	45.3	1.76	0.001	13.56	42.6	1.67	1.06	3.24E-8	235.2	2.31	158	0.091
	22.2	41.509	286.0	677.29	33.56	11.36	430	360	1049	1.220	307	357.8	304	45.3	1.73	0.001	13.56	42.6	1.67	1.06	3.31E-8	235.2	2.31	158	0.091
PR ~ 2.3 %	22.1	47.216	330.4	687.87	38.17	16.07	490	410	1049	1.221	308	324.6	304	45.4	1.61	0.001	13.57	42.6	1.67	1.06	4.61E-8	235.4	2.31	158	0.159
	22.1	47.216	330.3	687.66	38.08	15.98	490	410	1049	1.221	308	330.4	304	45.4	1.61	0.001	13.57	42.6	1.67	1.06	4.64E-8	235.4	2.31	158	0.159
	22.1	47.216	329.6	686.20	37.45	16.35	490	410	1049	1.221	308	344.4	304	45.4	1.68	0.001	13.57	42.6	1.67	1.06	4.46E-8	235.4	2.31	158	0.158
	22.1	47.216	329.6	686.20	37.45	16.35	490	410	1049	1.221	308	334.1	304	45.4	1.63	0.001	13.57	42.6	1.67	1.06	4.59E-8	235.4	2.31	158	0.158



Experiment Information	T <sub>a</sub> (C)	PR Volt (mV)	Wire Res (mΩ)	T <sub>b</sub> (mK)	T <sub>c</sub> (K)	T <sub>d</sub> (K)	V <sub>c</sub> (mV)	I <sub>c</sub> (mA)	Freq (Hz)	mic. V (V)	R <sub>s</sub> (Ω)	h (W/m <sup>2</sup> K)	W <sub>IR</sub> (K)	X	e (eV)	KC (eV)	ΔΔΔ (eV)	R <sub>s</sub> (Ω)	PR %	SPL (dB)	Power (W)				
Gr(D)	R <sub>s</sub> (Ω)	R <sub>s</sub> (Ω)																							
I - 864 Hz	20.8	31.261	211.923	666.39	28.81	8.01	330	270	563	0.481	89	280.2	87	17.8	1.37	0.001	9.94	31.2	0.90	0.57	2.83E-7	92.0	0.91	150	0.067
L = 47 cm	20.8	31.259	211.909	666.39	28.81	8.01	330	270	563	0.481	89	280.1	87	17.8	1.37	0.001	9.94	31.2	0.90	0.57	2.83E-7	92.0	0.91	150	0.067
PR - 0.9 %	20.8	31.259	211.906	666.38	28.80	8.00	330	270	563	0.481	85	280.3	87	17.8	1.37	0.001	9.94	31.2	0.90	0.57	2.83E-7	92.0	0.91	150	0.067
20.8	42.231	294.129	684.64	36.76	15.56	440	370	563	0.479	88	263.5	86	17.8	1.29	0.001	9.89	31.1	0.90	0.57	5.78E-7	91.3	0.91	150	0.126	
20.8	42.229	294.120	684.65	36.77	15.57	563	0.479	88	263.4	86	17.8	1.29	0.001	9.89	31.1	0.90	0.57	5.78E-7	91.3	0.91	150	0.126			
20.8	42.231	294.122	684.64	36.77	15.57	563	0.479	88	263.4	86	17.8	1.29	0.001	9.89	31.1	0.90	0.57	5.78E-7	91.3	0.91	150	0.126			
20.6	50.703	362.98	703.72	45.09	24.49	620	450	563	0.479	88	254.5	86	17.7	1.24	0.001	9.89	31.1	0.90	0.57	8.89E-7	91.2	0.91	150	0.187	
20.6	50.698	362.98	703.79	45.12	24.52	563	0.479	88	254.5	86	17.7	1.24	0.001	9.89	31.1	0.90	0.57	8.87E-7	91.2	0.91	150	0.187			
20.6	50.693	362.85	703.61	45.04	24.44	563	0.479	88	254.5	86	17.7	1.24	0.001	9.89	31.1	0.90	0.57	8.88E-7	91.2	0.91	150	0.187			
PR ~ 1.1 %	20.8	36.902	250.369	666.99	29.07	8.27	360	320	563	0.584	131	378.4	129	21.6	1.85	0.001	12.06	37.9	0.90	0.57	2.62E-7	135.7	1.10	152	0.094
20.8	36.904	250.356	666.97	29.06	8.26	360	320	563	0.584	131	378.5	129	21.6	1.85	0.001	12.06	37.9	0.90	0.57	2.63E-7	135.7	1.10	152	0.094	
20.8	36.894	250.371	667.09	29.11	8.31	360	320	563	0.584	131	376.4	129	21.6	1.85	0.001	12.06	37.9	0.90	0.57	1.36E-7	135.7	1.10	152	0.094	
20.7	48.92	340.72	684.64	36.77	16.07	510	420	563	0.585	131	349.1	129	21.7	1.72	0.001	12.08	38.0	0.90	0.57	2.61E-7	136.1	1.11	152	0.170	
20.7	48.91	340.76	684.66	36.86	16.16	563	0.585	131	351.8	129	21.7	1.72	0.001	12.08	38.0	0.90	0.57	2.62E-7	136.1	1.11	152	0.170			
20.7	48.92	340.74	684.65	36.74	16.04	563	0.585	131	351.8	129	21.7	1.71	0.001	12.06	37.9	0.90	0.57	3.99E-7	135.7	1.10	152	0.170			
20.8	59.16	423.64	703.92	45.17	24.37	610	520	563	0.584	131	348.2	129	21.6	1.70	0.001	12.06	37.9	0.90	0.57	3.99E-7	135.7	1.10	152	0.255	
20.8	59.16	423.62	703.89	45.16	24.36	563	0.584	131	348.4	129	21.6	1.70	0.001	12.06	37.9	0.90	0.57	3.99E-7	135.7	1.10	152	0.255			
20.8	59.17	423.65	703.82	45.13	24.33	563	0.584	131	348.9	129	21.6	1.70	0.001	12.06	37.9	0.90	0.57	3.98E-7	135.7	1.10	152	0.255			
20.8	59.16	423.64	703.92	45.17	24.37	610	520	563	0.585	131	348.5	129	21.6	1.70	0.001	12.06	37.9	0.90	0.57	3.98E-7	135.7	1.10	152	0.255	
20.8	59.17	423.62	703.89	45.16	24.36	563	0.585	131	348.6	129	21.6	1.70	0.001	12.06	37.9	0.90	0.57	3.98E-7	135.7	1.10	152	0.255			
20.8	59.17	423.65	703.82	45.13	24.33	563	0.585	131	348.5	129	21.6	1.70	0.001	12.06	37.9	0.90	0.57	3.98E-7	135.7	1.10	152	0.255			
20.8	59.16	423.64	703.92	45.17	24.37	610	520	563	0.584	131	345.5	129	21.6	1.70	0.001	12.06	37.9	0.90	0.57	3.98E-7	135.7	1.10	152	0.255	
20.8	59.17	423.62	703.89	45.16	24.36	563	0.584	131	345.6	129	21.6	1.70	0.001	12.06	37.9	0.90	0.57	3.98E-7	135.7	1.10	152	0.255			
20.8	59.17	423.65	703.82	45.13	24.33	563	0.584	131	345.7	129	21.6	1.70	0.001	12.06	37.9	0.90	0.57	3.98E-7	135.7	1.10	152	0.255			
21.7	53.54	374.33	687.27	30.50	8.40	410	340	565	0.690	192	435.5	179	25.6	2.13	0.001	14.23	44.7	0.90	0.57	7.04E-8	188.9	1.30	153	0.110	
22.1	39.79	271.38	687.07	30.56	8.46	565	0.690	182	432.1	179	25.6	2.11	0.001	14.23	44.7	0.90	0.57	7.09E-8	188.9	1.30	153	0.110			
22.1	39.79	271.37	687.04	30.56	8.46	565	0.690	182	433.2	179	25.6	2.12	0.001	14.23	44.7	0.90	0.57	7.07E-8	188.9	1.30	153	0.110			
21.7	53.54	374.33	687.27	30.50	8.41	410	340	565	0.690	182	418.5	178	25.6	2.04	0.001	14.20	44.6	0.90	0.57	1.37E-7	187.9	1.30	153	0.204	
21.7	53.56	374.36	687.07	30.53	8.41	565	0.690	182	421.0	178	25.6	2.06	0.001	14.20	44.6	0.90	0.57	1.37E-7	187.9	1.30	153	0.204			
21.7	53.56	374.35	687.05	30.54	8.41	565	0.690	182	421.2	178	25.6	2.06	0.001	14.20	44.6	0.90	0.57	1.37E-7	187.9	1.30	153	0.204			
20.9	63.53	454.47	702.65	44.62	23.87	650	560	565	0.668	181	412.5	177	25.5	2.01	0.001	14.16	44.5	0.90	0.57	2.05E-7	186.5	1.30	153	0.294	
20.9	63.53	454.47	702.65	44.62	23.87	565	0.668	181	409.5	177	25.5	2.00	0.001	14.16	44.5	0.90	0.57	2.05E-7	186.5	1.30	153	0.294			
20.9	63.53	454.47	702.65	44.62	23.87	565	0.668	181	411.5	177	25.5	2.01	0.001	14.16	44.5	0.90	0.57	2.05E-7	186.5	1.30	153	0.294			
PR ~ 1.5 %	20.1	42.31	286.21	664.96	28.18	8.08	440	360	562	0.795	242	507.3	239	29.5	2.48	0.001	16.45	51.7	0.90	0.57	3.84E-8	252.3	1.50	155	0.123
20.1	42.31	286.18	664.89	28.15	8.05	562	0.795	242	509.1	239	29.5	2.49	0.001	16.45	51.7	0.90	0.57	3.83E-8	252.3	1.50	155	0.123			
20.1	42.30	286.21	665.12	28.25	8.15	562	0.795	242	507.9	239	29.5	2.46	0.001	16.45	51.7	0.90	0.57	3.88E-8	252.3	1.50	155	0.123			
20.2	56.68	393.42	682.31	35.75	15.55	580	490	562	0.795	242	485.6	238	29.4	2.37	0.001	16.43	51.6	0.90	0.57	7.42E-8	251.8	1.50	155	0.227	
20.2	56.65	393.48	682.77	35.95	15.75	562	0.795	242	479.2	238	29.4	2.34	0.001	16.43	51.6	0.90	0.57	7.52E-8	251.8	1.50	155	0.227			
20.2	56.64	393.49	682.81	35.97	15.77	562	0.795	242	478.6	238	29.4	2.34	0.001	16.43	51.6	0.90	0.57	7.52E-8	251.8	1.50	155	0.227			
20.2	69.17	494.55	702.82	44.70	24.50	710	600	562	0.795	242	474.0	238	29.4	2.32	0.001	16.43	51.6	0.90	0.57	1.17E-7	251.8	1.50	155	0.348	
20.2	69.17	494.45	702.68	44.63	24.43	562	0.795	242	474.3	238	29.4	2.32	0.001	16.43	51.6	0.90	0.57	1.16E-7	251.8	1.50	155	0.348			
20.2	69.17	494.42	702.64	44.62	24.42	562	0.795	242	473.7	238	29.4	2.31	0.001	16.43	51.6	0.90	0.57	1.17E-7	251.8	1.50	155	0.348			



Experiment Information	PR	Wire Volt (mV)	Wire Resist (mΩ)	Ts (s)	T <sub>s</sub> -T <sub>h</sub> (s)	Cur (mA)	Vol (V)	Freq (Hz)	Inductance (mH)	Ra (V)	R <sub>g</sub> (Ω)	N <sub>g</sub> (2MAA)	Cor (N <sub>g</sub> )	R <sub>ed</sub> (Ω)	N <sub>ed</sub> (2MAA)	X (s)	KC (mA)	A <sub>1</sub> (mA)	G(D)	R <sub>s</sub> (Ω)	R <sub>s</sub> (Ω)	SPL (%)	Power (W)		
1 - 564 Hz	20.4	44.14	286.03	665.94	28.61	8.21	460	380	663	0.902	311	544.3	306	33.4	2.68	0.001	18.62	58.5	0.90	0.57	2.36E-8	323.0	1.70	156	0.134
L = 47 cm	20.4	44.13	295.01	666.05	28.66	8.26	563	0.902	311	541.1	306	33.4	2.64	0.001	18.62	58.5	0.90	0.57	2.39E-8	323.0	1.70	156	0.134		
PR - 1.7 %	20.4	44.14	288.99	665.85	28.57	8.17	563	0.902	311	546.8	306	33.4	2.68	0.001	18.62	58.5	0.90	0.57	2.38E-8	323.0	1.70	156	0.134		
20.3	58.78	408.94	683.89	36.44	16.14	610	490	563	0.902	311	504.4	306	33.4	2.46	0.001	18.62	58.5	0.90	0.57	4.60E-8	322.8	1.70	156	0.245	
20.3	58.78	408.87	683.77	36.39	16.09	563	0.902	311	506.9	306	33.4	2.47	0.001	18.62	58.5	0.90	0.57	4.60E-8	322.8	1.70	156	0.244			
20.3	58.78	408.85	683.74	36.37	16.07	563	0.902	311	505.5	306	33.4	2.47	0.001	18.62	58.5	0.90	0.57	4.67E-8	322.8	1.70	156	0.244			
20.4	70.42	503.49	702.83	44.70	24.30	720	620	563	0.902	311	494.1	306	33.4	2.41	0.001	18.62	58.5	0.90	0.57	7.03E-8	323.0	1.70	156	0.361	
20.4	70.43	503.67	702.98	44.76	24.36	563	0.902	311	493.0	306	33.4	2.42	0.001	18.62	58.5	0.90	0.57	7.03E-8	323.0	1.70	156	0.361			
20.4	70.42	503.40	702.70	44.64	24.24	563	0.902	311	495.1	306	33.4	2.41	0.001	18.62	58.5	0.90	0.57	7.03E-8	323.0	1.70	156	0.361			
PR - 1.9 %	20.4	45.00	304.64	665.47	28.41	8.01	480	380	562	1.009	390	579.9	384	37.4	2.83	0.001	20.87	65.6	0.90	0.57	1.47E-8	406.1	1.91	157	0.139
20.4	45.00	304.63	665.45	28.40	8.00	562	1.009	390	580.5	384	37.4	2.84	0.001	20.87	65.6	0.90	0.57	1.47E-8	406.1	1.91	157	0.139			
20.4	45.00	304.62	665.43	28.39	7.99	562	1.009	390	581.2	384	37.4	2.84	0.001	20.87	65.6	0.90	0.57	1.46E-8	406.1	1.91	157	0.139			
20.4	60.29	419.12	683.36	36.21	15.81	620	520	562	1.009	390	541.3	384	37.4	2.64	0.001	20.87	65.6	0.90	0.57	2.90E-8	406.1	1.91	157	0.257	
20.4	60.31	419.06	683.03	36.06	15.66	562	1.009	390	540.5	384	37.4	2.67	0.001	20.87	65.6	0.90	0.57	2.87E-8	406.1	1.91	157	0.257			
20.4	60.28	419.08	683.40	36.23	15.83	562	1.009	390	542.7	384	37.4	2.65	0.001	20.87	65.6	0.90	0.57	2.90E-8	406.1	1.91	157	0.257			
20.4	72.23	515.37	701.38	44.07	23.67	740	630	562	1.009	390	532.6	384	37.4	2.60	0.001	20.87	65.6	0.90	0.57	4.34E-8	406.1	1.91	157	0.379	
20.4	72.22	515.38	701.49	44.12	23.72	562	1.009	390	531.4	384	37.4	2.60	0.001	20.87	65.6	0.90	0.57	4.35E-8	406.1	1.91	157	0.379			
20.4	72.24	515.38	701.30	44.03	23.63	562	1.009	390	533.5	384	37.4	2.61	0.001	20.87	65.6	0.90	0.57	4.33E-8	406.1	1.91	157	0.379			
PR - 2.1 %	22.5	46.046	314.40	670.33	30.53	8.03	480	390	564	1.112	475	609.9	384	37.4	2.60	0.001	20.87	65.6	0.90	0.57	4.34E-8	406.1	1.91	157	0.147
22.5	46.046	314.40	670.33	30.53	8.03	564	1.112	475	609.9	384	37.4	2.60	0.001	20.87	65.6	0.90	0.57	4.34E-8	406.1	1.91	157	0.147			
22.5	46.046	314.40	670.33	30.53	8.03	564	1.112	475	609.9	384	37.4	2.60	0.001	20.87	65.6	0.90	0.57	4.34E-8	406.1	1.91	157	0.147			
22.6	61.997	434.0	688.13	38.29	15.69	640	530	564	1.112	475	580.7	469	41.3	2.84	0.001	23.00	72.3	0.90	0.57	1.92E-8	494.4	2.10	158	0.274	
22.6	61.997	434.2	688.45	38.43	15.83	564	1.112	475	575.9	469	41.3	2.61	0.001	23.00	72.3	0.90	0.57	1.94E-8	494.4	2.10	158	0.274			
22.6	61.997	434.3	688.61	38.50	15.90	564	1.112	475	576.7	469	41.3	2.82	0.001	23.00	72.3	0.90	0.57	1.93E-8	494.4	2.10	158	0.274			
22.6	74.595	536.9	707.52	46.74	24.14	760	650	564	1.112	475	561.7	469	41.3	2.74	0.001	23.00	72.3	0.90	0.57	2.95E-8	494.4	2.10	158	0.407	
22.6	74.595	536.8	707.39	46.69	24.09	564	1.112	475	562.9	469	41.3	2.75	0.001	23.00	72.3	0.90	0.57	2.95E-8	494.4	2.10	158	0.407			
22.6	74.595	536.6	707.12	46.57	23.97	564	1.112	475	563.4	469	41.3	2.76	0.001	23.00	72.3	0.90	0.57	2.95E-8	494.4	2.10	158	0.407			
PR - 2.3 %	22.9	41.876	286.1	671.59	31.08	8.18	430	380	565	1.219	571	542.6	562	45.3	2.65	0.001	25.18	79.1	0.90	0.57	6.95E-9	592.2	2.30	158	0.122
22.9	41.876	286.4	669.95	30.36	7.46	565	1.219	571	521.6	562	45.3	2.55	0.001	25.18	79.1	0.90	0.57	6.34E-9	592.2	2.30	158	0.122			
22.9	41.876	286.7	670.65	30.67	7.77	565	1.219	571	520.1	562	45.3	2.54	0.001	25.18	79.1	0.90	0.57	6.60E-9	592.2	2.30	158	0.122			
22.9	50.373	348.0	679.10	34.35	11.45	520	430	565	1.220	572	518.4	563	45.4	2.53	0.001	25.20	79.2	0.90	0.57	7.90E-9	593.2	2.31	158	0.178	
22.9	50.373	348.8	680.66	35.03	12.13	565	1.220	572	590.4	563	45.4	2.40	0.001	25.20	79.2	0.90	0.57	1.03E-8	593.2	2.31	158	0.178			
22.9	50.373	347.8	678.71	34.18	11.28	565	1.220	572	525.9	563	45.4	2.57	0.001	25.20	79.2	0.90	0.57	9.56E-9	593.2	2.31	158	0.178			
23.0	62.000	435.6	690.64	39.38	16.38	640	540	565	1.219	571	558.3	562	45.3	2.73	0.001	25.18	79.1	0.90	0.57	1.39E-8	592.5	2.30	158	0.275	
23.0	62.000	434.9	689.53	38.90	15.90	565	1.219	571	534.8	562	45.3	2.81	0.001	25.18	79.1	0.90	0.57	1.46E-8	592.5	2.30	158	0.275			
23.0	62.000	436.7	692.38	40.14	17.14	565	1.219	571	555.8	562	45.3	2.71	0.001	25.18	79.1	0.90	0.57	1.40E-8	592.5	2.30	158	0.275			





## LIST OF REFERENCES

1. Garrett, S. L., Adeff, J. A., Hofler, T. J., Thermoacoustic Refrigerator for Space Applications, *Journal Thermophysics and Heat Transfer*, Vol. 7, No. 4, 1993, pp. 595-599.
2. Lee, B. H., Richardson, P. D., Effect of Sound on Heat Transfer from a Horizontal Circular Cylinder at Large Wavelengths, *Journal of Mechanical Engineering Science*, Vol. 7, No. 2 1965, pp. 127-130.
3. Swift, G. W., Thermoacoustic Engines and Refrigerators, *Physics Today*, July 1995, pp. 22-28.
4. A. D. Little, Inc., Energy Efficient Alternatives to Chlorofluorocarbons, Revised Final Report - Ref. 66384 (US Dept. of Energy, ER-33, GTW), April 1992.
5. Garrett, S. L., Hofler, T. J., Perkins, D. K., Thermoacoustic Refrigeration, Greenpeace Ozone-Safe Cooling Conference, 1993.
6. Gebhart, B., Jaluria, Y., Mahajan, R. L., Sammakia, B., *Buoyancy Induced Flows and Transport*, Hemisphere: New York, 1988.
7. Fand, R. M., Cheng, P., The Influence of Sound on Heat Transfer from a Cylinder in Crossflow, *International Journal of Heat and Mass Transfer*, Vol. 6, 1963, pp. 571-596.
8. Fand, R. M., Kaye, J., Acoustic Streaming near a Heated Cylinder, *The Journal of the Acoustical Society of America*, Vol. 32, No. 5, May 1960, pp. 579-584.
9. Fand, R. M., Kaye, J., The Influence of Sound on Free Convection from a Horizontal Cylinder, *Journal of Heat Transfer*, May 1961, pp. 133-148.
10. Fand, R. M., Mechanism of Interaction between Vibrations and Heat Transfer, *Journal of the Acoustical Society of America*, Vol. 34, No. 12, December 1962, pp. 1887-1894.
11. Morse, P. M., Ingard, K. U., *Theoretical Acoustics*, McGraw-Hill: New York, 1968.
12. Stuart, J. T., Double Boundary Layers in Oscillatory Viscous Flow, *Journal of Fluid Mechanics*, Vol. 24, 1966, pp. 673-685.

13. Honji, H., Streaked Flow Around an Oscillating Circular Cylinder, *Journal of Fluid Mechanics*, Vol. 107, 1981, pp. 509-520.
14. Williamson, C. H. K., Sinusoidal Flow Relative to Circular Cylinders, *Journal of Fluid Mechanics*, Vol. 155, 1985, pp. 141-174.
15. Faltinsen, O. M., *Sea Loads on Ships and Offshore Structures*, Cambridge University Press, 1990.
16. Sarpkaya, T., Force on a Circular Cylinder in Viscous Oscillatory Flow at Low Keulegan-Carpenter Numbers, *Journal of Fluid Mechanics*, Vol. 165, 1986, pp. 61-71.
17. Harder, D., Convective Heat Transfer From a Cylinder in a Strong Acoustic Field, Masters Thesis, Naval Postgraduate School, 1995.
18. Mozerkewich, G., Heat Transfer from a Cylinder in an Acoustic Standing Wave, *Journal of the Acoustical Society of America*, Vol. 98, No. 4, October 1995, pp. 2209-2216.
19. Richardson, P. D., Effects of Sound and Vibrations on Heat Transfer, *Applied Mechanics Reviews*, Vol. 20, No. 3, March 1967, pp. 201-217.
20. Beckwith, T. G., Marangoni, R. D., Lienhard, J. H., *Mechanical Measurements*, 5th ed., Addison-Wesley: New York, 1993.

## **INITIAL DISTRIBUTION LIST**

1. Defense Technical Information Center.....2  
8725 John J. Kingman Rd., STE 0944  
Ft. Belvoir, VA 22060-6218
2. Dudley Knox Library.....2  
Naval Postgraduate School  
411 Dyer Rd.  
Monterey, CA 93943-5101
3. Naval/Mechanical Engineering Curriculum.....1  
Code 34  
Naval Postgraduate School  
700 Dyer Road, Room 115  
Monterey, CA 93943-5107
4. Professor A. Gopinath.....2  
Code ME/GK  
Naval Postgraduate School  
700 Dyer Road, Room 333  
Monterey, CA 93943
5. Mr. Don P. Bridenstine.....1  
831 Lightstreet Road  
Bloomsburg, PA 17815
6. Mark Bridenstine.....1  
20 Beaver Dam Road  
South Berwick, ME 03908